

NEA NUCLEAR SCIENCE COMMITTEE
NEA COMMITTEE ON SAFETY OF NUCLEAR INSTALLATIONS

PRESSURISED WATER REACTOR MAIN STEAM LINE BREAK (MSLB) BENCHMARK

Volume II: Summary Results of Phase I (Point Kinetics)

by

T. Beam, K. Ivanov, B. Taylor and A. Baretta
Nuclear Engineering Program
The Pennsylvania State University
University Park, PA 16802, USA

December 2000

**US Nuclear Regulatory Commission
OECD Nuclear Energy Agency**

ORGANISATION FOR ECONOMIC CO-OPERATION AND DEVELOPMENT

Pursuant to Article 1 of the Convention signed in Paris on 14th December 1960, and which came into force on 30th September 1961, the Organisation for Economic Co-operation and Development (OECD) shall promote policies designed:

to achieve the highest sustainable economic growth and employment and a rising standard of living in Member countries, while maintaining financial stability, and thus to contribute to the development of the world economy;

to contribute to sound economic expansion in Member as well as non-member countries in the process of economic development; and

to contribute to the expansion of world trade on a multilateral, non-discriminatory basis in accordance with international obligations.

The original Member countries of the OECD are Austria, Belgium, Canada, Denmark, France, Germany, Greece, Iceland, Ireland, Italy, Luxembourg, the Netherlands, Norway, Portugal, Spain, Sweden, Switzerland, Turkey, the United Kingdom and the United States. The following countries became Members subsequently through accession at the dates indicated hereafter: Japan (28th April 1964), Finland (28th January 1969), Australia (7th June 1971), New Zealand (29th May 1973), Mexico (18th May 1994), the Czech Republic (21st December 1995), Hungary (7th May 1996), Poland (22nd November 1996) and the Republic of Korea (12th December 1996). The Commission of the European Communities takes part in the work of the OECD (Article 13 of the OECD Convention).

NUCLEAR ENERGY AGENCY

The OECD Nuclear Energy Agency (NEA) was established on 1st February 1958 under the name of the OEEC European Nuclear Energy Agency. It received its present designation on 20th April 1972, when Japan became its first non-European full Member. NEA membership today consists of 27 OECD Member countries: Australia, Austria, Belgium, Canada, Czech Republic, Denmark, Finland, France, Germany, Greece, Hungary, Iceland, Ireland, Italy, Japan, Luxembourg, Mexico, the Netherlands, Norway, Portugal, Republic of Korea, Spain, Sweden, Switzerland, Turkey, the United Kingdom and the United States. The Commission of the European Communities also takes part in the work of the Agency.

The mission of the NEA is:

- to assist its Member countries in maintaining and further developing, through international co-operation, the scientific, technological and legal bases required for a safe, environmentally friendly and economical use of nuclear energy for peaceful purposes, as well as
- to provide authoritative assessments and to forge common understandings on key issues, as input to government decisions on nuclear energy policy and to broader OECD policy analyses in areas such as energy and sustainable development.

Specific areas of competence of the NEA include safety and regulation of nuclear activities, radioactive waste management, radiological protection, nuclear science, economic and technical analyses of the nuclear fuel cycle, nuclear law and liability, and public information. The NEA Data Bank provides nuclear data and computer program services for participating countries.

In these and related tasks, the NEA works in close collaboration with the International Atomic Energy Agency in Vienna, with which it has a Co-operation Agreement, as well as with other international organisations in the nuclear field.

© OECD 2000

Permission to reproduce a portion of this work for non-commercial purposes or classroom use should be obtained through the Centre français d'exploitation du droit de copie (CCF), 20, rue des Grands-Augustins, 75006 Paris, France, Tel. (33-1) 44 07 47 70, Fax (33-1) 46 34 67 19, for every country except the United States. In the United States permission should be obtained through the Copyright Clearance Center, Customer Service, (508)750-8400, 222 Rosewood Drive, Danvers, MA 01923, USA, or CCC Online: <http://www.copyright.com/>. All other applications for permission to reproduce or translate all or part of this book should be made to OECD Publications, 2, rue André-Pascal, 75775 Paris Cedex 16, France.

FOREWORD

Since the beginning of the pressurised water reactor (PWR) main steam line break (MSLB) benchmark activities, four benchmark workshops have taken place. The first was held in Washington DC, USA (April 1997), the second in Madrid, Spain (June 1998), the third in Garching near Munich, Germany (March 1999) and the fourth in Paris, France (January 2000). It was agreed that in performing this series of exercises participants were working at the edge of present developments in the coupling of neutronics and thermal hydraulics, and that this benchmark would lead to a common background understanding of the key issues. It was also agreed that the PWR MSLB Benchmark would be published in four volumes.

Volume 1 of the *PWR MSLB Benchmark: Final Specifications*, was issued by the OECD/NEA in April 1999 [NEA/NSC/DOC(99)8]. A small team at Pennsylvania State University (PSU) was responsible for authoring the final specifications, co-ordinating the benchmark activities, answering questions, analysing the solutions submitted by benchmark participants and providing reports summarising the results for each phase. In performing these tasks the PSU team collaborated with Adi Irani and Nick Trikouros of GPU Nuclear, Inc.

Volume 2 summarises the results of Phase I on point kinetics. The report is supplemented by brief descriptions of the system codes used, as provided by the participants. In addition, detailed descriptions (including graphs where useful) of the models used are given. These are presented as answers to the questionnaire for the first exercise, so that compliance with the specifications can be verified. The list of deviations from the specifications, if any, is provided, and any specific assumptions are stated. Based on the information provided, the benchmark co-ordinators and report reviewers decided whether the models used in the solutions provided by the participants complied sufficiently with the system model's specifications. Solutions that deviated in the modelling in ways not compatible with the specifications were not included in the statistical evaluation procedure.

Acknowledgements

This report is dedicated to the students of Penn State University, the next generation of nuclear engineers, who are the reason why we are here.

The authors would like to thank Dr. H. Finnemann of Siemens, Dr. S. Langenbuch from the Gesellschaft für Reaktorsicherheit (GRS), and Professor J. Aragoes from Universidad Politécnica Madrid (UPM), whose support and encouragement in establishing and carrying out this benchmark were invaluable.

This report is the sum of many efforts, by the participants, the sponsoring agencies – the US Nuclear Regulatory Commission and the OECD Nuclear Energy Agency – and their staff. Special appreciation goes to the report reviewers: Adi Irani from GPU Nuclear Inc., Dr. S. Langenbuch from GRS, and Dr. A. Knoll from Siemens. Their comments and suggestions were very valuable and significantly improved the quality of this report. We would like to thank them for the effort and time involved.

Particularly noteworthy were the efforts of Farouk Eltawila assisted by David Ebert, both of the US Nuclear Regulatory Commission. With their help, funding was secured, enabling this project to proceed. We also thank them for their excellent technical advice and assistance.

The authors wish to express their sincere appreciation for the outstanding support offered by Dr. Enrico Sartori, who not only provided efficient administration, organisation and valuable technical recommendations, but most importantly provided friendly counsel and advice.

Finally, we are grateful to Nadejda Todorova and Amanda Costa for having devoted their competence and skills to the final editing of this report.

TABLE OF CONTENTS

FOREWORD.....	3
<i>Acknowledgements</i>	4
Chapter 1. INTRODUCTION.....	9
Chapter 2. DESCRIPTION OF FIRST BENCHMARK EXERCISE	11
Description of MSLB transient.....	11
Simulated transient scenario	12
Initial steady state conditions.....	13
Reactor point kinetics parameters	13
Analysis assumptions.....	16
Chapter 3. STATISTICAL METHODOLOGY.....	21
Standard techniques for comparison of results	21
Time history data	21
Reference results.....	22
Chapter 4. RESULTS AND DISCUSSION	25
Break flow rate.....	25
Pressure	26
Temperatures	27
Reactor power	30
Reactivity	33
Steam generator mass	33
Sequence of events.....	35
Chapter 5. CONCLUSIONS	65

REFERENCES	69
APPENDIX A – <i>Description of computer codes used for analysis in the first phase of the PWR MSLB benchmark</i>	71
APPENDIX B – <i>Sequence of events for the first phase of the PWR MSLB benchmark</i>	77
APPENDIX C – <i>Questionnaire for the first phase of the PWR MSLB benchmark</i>	83

List of figures

Figure 2.1. EOC HFP assembly relative radial power distribution (quarter core symmetry)	16
Figure 2.2. EOC HFP core average power relative power distribution.....	16
Figure 2.3. Steam line nodalisation	17
Figure 4.1. Total break flow rate	37
Figure 4.2. Break flow rate – 24 inch.....	38
Figure 4.3. Break flow rate – 8 inch.....	39
Figure 4.4. Average pressure.....	40
Figure 4.5. Broken loop pressure	41
Figure 4.6. Intact loop pressure	42
Figure 4.7. Pressuriser pressure.....	43
Figure 4.8. Broken steam line pressure	44
Figure 4.9. Intact steam line pressure	45
Figure 4.10. Average coolant temperature	46
Figure 4.11. Broken hot leg temperature.....	47
Figure 4.12. Intact hot leg temperature	48
Figure 4.13. Broken cold leg temperature.....	49
Figure 4.14. Intact cold leg temperature.....	50
Figure 4.15. Fuel temperature	51
Figure 4.16. Fission power	52
Figure 4.17. Total power	53

Figure 4.18. Decay power	54
Figure 4.19. Total reactivity	55
Figure 4.20. Moderator reactivity.....	56
Figure 4.21. Doppler reactivity	57
Figure 4.22. Scram reactivity	58
Figure 4.23. Broken steam generator mass.....	59
Figure 4.24. Intact steam generator mass	60
Figure 4.25. Heat transfer: broken steam generator	61
Figure 4.26. Heat transfer: intact steam generator.....	62
Figure 4.27. Integrated leakage: vapour mass	63
Figure 4.27. Integrated leakage: liquid mass.....	64

List of tables

Table 1.1. List of participants in the first phase of the PWR MSLB benchmark.....	10
Table 2.1. Initial conditions for TMI-1 at 2 772 MW _t	13
Table 2.2. Summary of point kinetics analysis input values	15
Table 2.3. Delay constants and fractions of delayed neutrons	15
Table 2.4. Rod worth versus time after trip (Versions 1 and 2)	15
Table 2.5. MSLB analysis assumptions	17
Table 2.6. Description of MSSVs per OTSG	18
Table 2.7. Main feedwater flow boundary conditions to broken SG.....	18
Table 2.8. Main feedwater flow boundary conditions to intact steam generator.....	18
Table 2.9. HPI flow versus pressure.....	19
Table 4.1. Deviations: total break flow rate, 24 inch break flow rate and 8 inch break flow rate at end of transient	26
Table 4.2. Deviations: average pressure, pressure in the broken loop and pressure in the intact loop	27

Table 4.3. Deviations: broken steam line pressure, intact steam line pressure and pressuriser pressure	28
Table 4.4. Deviations: broken loop hot and cold leg temperatures at the end of transient.....	29
Table 4.5. Deviations: intact loop hot and cold leg temperatures at the end of transient.....	29
Table 4.6. Deviations: average moderator temperature and fuel temperature at the end of the transient	30
Table 4.7. Deviations: time of reactor trip (initial peak) and time of highest power after trip (second peak).....	31
Table 4.8. Deviations: percentage of initial power at time of reactor trip (initial peak), time of highest power after trip (second peak) and end of transient for total power.....	32
Table 4.9. Deviations: percentage of initial power at time of reactor trip (initial peak), time of highest power after trip (second peak) and end of transient for fission power	32
Table 4.10. Deviations: total reactivity at time of highest power after reactor trip and at end of transient	34
Table 4.11. Deviations: moderator reactivity, Doppler reactivity and scram reactivity at end of transient	34

Chapter 1

INTRODUCTION

Incorporation of a full three-dimensional (3-D) reactor core model into system transient codes allows “best-estimate” simulations of interactions between reactor core behaviour and plant dynamics. Until recently, few system transient codes incorporated full 3-D modelling of the reactor core; however, recent progress in computer technology made the development of such coupled code systems feasible. Unfortunately, there is limited experience using this technology. One way to verify the performance of these computer codes is to develop plant transient benchmarks for which a 3-D neutronics core model can be used and verified. The Nuclear Energy Agency Nuclear Science Committee (NEA NSC) has developed such a series of benchmarks.

Over the past eight years, the NEA NSC has developed a series of benchmark problems to study the accuracy of the computer codes used to obtain solutions for coupled space-time kinetics/thermal-hydraulic problems in nuclear reactors. These benchmarks, based on well-defined problems with a complete set of input data, are used to verify the data exchange and test the neutronics coupling to the fuel-rod-heat conduction solution methodology [1]. This series of benchmarks studies 3-D core transient calculations for light water reactors (LWR), boiling water reactors (BWR) and pressurised water reactors (PWR). A recent addition to this series, sponsored by the Organisation for Economic Co-operation and Development (OECD), United States Nuclear Regulatory Commission (US NRC), and the Pennsylvania State University (PSU), is the PWR Main Steam Line Break (MSLB) benchmark problem [2].

The PWR MSLB benchmark problem uses a three-dimensional neutronics core model to further verify the capability of coupled codes to analyse complex transients with coupled core-plant interactions and to fully test the thermal-hydraulic coupling. It is based on real plant design and operational data for the Three Mile Island Unit 1 nuclear power plant (TMI-1 NPP). The purpose of this benchmark is threefold: to verify the capability of system codes to analyse complex transients with coupled core-plant interactions; to fully test the 3-D neutronics/thermal-hydraulic coupling; and to evaluate discrepancies between the predictions of coupled codes in best-estimate transient simulations.

The purposes of this benchmark are met via the use of three exercises that are briefly described below [3]:

1. A *point kinetics plant simulation*, which models the primary and secondary systems. The purpose of this exercise is to test the thermal-hydraulic system response. The participants are provided with compatible point kinetics model inputs that preserve axial and radial power distribution, and scram reactivity obtained using a 3-D core neutronics model and a complete system description.
2. A *coupled 3-D neutronics thermal-hydraulics evaluation of core response*. The purpose of this phase is to test the neutronics response to imposed thermal-hydraulic conditions. The participants are provided with transient boundary conditions (radial distribution of mass

flow rates and liquid temperatures at the core inlet, and radial averaged pressure versus time at both the core inlet and outlet), the initial axial liquid velocities, the initial axial distribution of liquid temperatures and a complete core description.

3. A *best-estimate coupled core-plant transient model*. This exercise simulates the entire transient and combines the first two exercises, fully testing the thermal-hydraulic/neutronic coupling.

A small benchmark team at PSU is responsible for authoring the final specification for the PWR MSLB benchmark problem, answering questions, analysing the solutions submitted by benchmark participants and providing reports summarising the results for each phase.

The purpose of this report is to present the final results for the first exercise of the PWR MSLB benchmark problem, the point kinetics exercise. This report is representative of results received from fourteen participants representing nineteen organisations and eight countries. A list of participants who have submitted information to the PSU benchmark team for the first exercise, along with the code used to perform the analysis, is found in Table 1.1. A more detailed description of each code is presented in Appendix A. Chapter 2 contains an updated description of the transient, while a discussion of the statistical methodology employed in this comparative analysis is presented in Chapter 3. Chapter 4 provides a detailed analysis of the final results for the first exercise, and a summary of the sequence of events for each participant is found in Appendix B. Chapter 5 provides a brief summary of the conclusions drawn from this exercise.

Table 1.1. List of participants in the first phase of the PWR MSLB benchmark

Participant number	Company name	Country	Code
1	VTT-1	Finland	SMABRE
2	GRS	Germany	ATHLET
3	F ZR	Germany	ATHLET
4	GPUN/CSA/EPRI	USA	RETRAN-3D
5	Universities of Pisa and Zagreb	Italy/Croatia	RELAP5/MOD 3.2
6	BE	United Kingdom	RELAP5
7	IPSN/CEA	France	CATHARE 2
8	FZK/SKWU	Germany	RELAP5/MOD3.2
9	NETCorp	USA	DNP/3D
10	Iberdrola	Spain	RETRAN-3D
11	UPV	Spain	TRAC-PF1/MOD3
12	VTT-2	Finland	APROS
13	Purdue/NRC	USA	RELAP5/MOD3
14	PSU	USA	TRAC -PF1/MOD2

Chapter 2

DESCRIPTION OF FIRST BENCHMARK EXERCISE

The transient chosen for this benchmark is a simulated main steam line break (MSLB) transient in a pressurised water reactor (PWR). The PWR in this case is modelled after real plant design and operational data for the Three Mile Island Unit 1 nuclear power plant (TMI-1 NPP). Traditionally, this problem has been modelled using the point kinetics approach. Unfortunately, the point kinetics approach requires the use of extremely conservative assumptions in order to account for the asymmetry in the core region that takes place during the transient. These conservative assumptions unnecessarily limit the ability of the plant to undergo power upgrades or extended fuel cycles. Using the 3-D kinetics approach for this transient may provide a margin to re-criticality over the point kinetics, thus allowing for the improvement of both operational flexibility and nuclear power plant performance. The purpose of this chapter is to provide a detailed description of the simulated main steam line break transient specified for this benchmark problem.

Description of MSLB transient

Significant space-time effects in the core caused by asymmetric cooling and an assumed stuck-out control rod during reactor trip characterise the MSLB transient. The asymmetry in the reactor core, both neutronic and thermal-hydraulically, is caused by the expected power tilt, and makes this transient difficult to analyse. Realistic simulation requires evaluation of core response using a coupled 3-D neutronics/core thermal-hydraulics code supplemented by a 1-D simulation of the remainder of the reactor coolant system (RCS). The limiting MSLB for TMI-1 is at hot full power (HFP) because the steam generator liquid inventory increases with increasing power level. The worst case overcooling occurs at the maximum power level, which corresponds to the maximum liquid inventory in the steam generator (SG).

As mentioned previously, the reference problem for this benchmark is a simulated MSLB resulting from the double-ended rupture of one steam line upstream of the cross-connect. The steam line break results in the loss of secondary coolant, and the broken SG depressurises, while the intact SG is isolated when the turbine stop valves slam shut. As a result of the break in the steam line the steam flow rate in the broken SG increases, thus improving heat transfer and lowering the average reactor coolant temperature. As the average reactor coolant temperature decreases, the power begins to increase. Unfortunately, the loop with the break sees a great deal of cooling, while the intact loop sees little, if any, cooling throughout the transient. Because of the difference in temperatures between the two loops, one would expect to see a power tilt within the core to the cooler side.

The power tilt within the core region is expected because of the negative moderator temperature coefficient. A reactor trip occurs due to either low reactor coolant pressure or high neutron flux. Following the reactor trip, the turbine trips and the turbine stop valves and feedwater control valves close. Low steam line pressure initiates automatic feedwater isolation, which causes the steam generator associated with the rupture to blow dry. While not modelled for this exercise, continued RCS cool-down and decay heat removal would be achieved by emergency feedwater (EFW) flow to

the intact SG with steam flow through the turbine bypass valve. The high-pressure injection (HPI) system may be activated due to low RCS pressure during the cool-down period following a large area steam line break.

One of the major concerns for the MSLB transient is the return to power and criticality in the latter half of the transient. Because of this concern, the MSLB scenario is based on assumptions that conservatively maximise the consequences for a return to power. These assumptions, along with a detailed description of the reference problem, can be found in the following paragraphs.

Simulated transient scenario

The double-ended rupture of one steam line is assumed to occur upstream of the MSIVs at the cross-connect. The rupture of the 24 inch (60.96 cm) outer diameter main steam line (this is the largest possible break) results in the highest break flow and maximises the RCS cool-down. The worst single failure is the mechanical failure in the open position of the feedwater regulating valve associated with the affected SG. This failure causes feedwater to cross the common header from the intact to the broken steam generator, thus maximising feedwater flow to the broken steam generator. Closing the feedwater block valve 30 seconds after the break occurs terminates the feedwater flow to the broken SG. This is a conservative assumption and helps to maximise RCS cool-down.

Following break initiation and reactor scram, the steam line turbine stop valves slam shut, effectively isolating the intact steam generator. The 8 inch (20.32 cm) cross-connect between the two steam lines of the broken SG remains open.

Since maximising the primary to secondary heat transfer results in maximum RCS cool-down, all four RCS pumps are assumed to operate during the event. No credit is taken for pressuriser heater operation. This conservative assumption enhances the RCS depressurisation.

The reactor trip is modelled to occur when the neutron power reaches 114% of 2 772 MW_t, or when the primary system pressure at the hot leg pressure tap reaches 1 945 psia (13.41 MPa). A trip delay of 0.4 seconds is used for the high neutron flux trip, while the low RCS pressure trip delay is 0.5 seconds. These values bound the actual delays for TMI-1 and represent the delay from the time the trip condition is reached until the time the control rods are free to fall.

The high-pressure injection (HPI) system initiates with a 25 second delay when the primary system pressure drops to 1 645 psia (11.34 MPa). HPI is expected to activate because of the large overcooling which occurs during this simulated MSLB transient. No credit is taken for the negative reactivity insertion from the addition of boron, and no other emergency core coolant system (ECCS) action is expected.

Since the primary-to-secondary heat transfer is the driving force behind the RCS cool-down and depressurisation, the choice of initial steam generator inventory is important to provide the adequate cool-down capability. An initial steam generator inventory of 57 320 lbm (26 000 kg) is assumed. In addition, the mass of the feedwater between the feedwater isolation valve and the affected steam generator, calculated to be 35 500 lbm (16 103 kg), is modelled as part of the feedwater function and contributes to the overcooling and depressurisation of the RCS.

Vessel mixing is based on test data from Duke Power Company's Oconee Plant, also a B&W design plant. These tests define the amount of mixing that occurs within the vessel as a ratio of the

difference in hot leg temperatures to the difference in cold leg temperatures. There is 20% mixing in the lower plenum and 80% in the upper plenum, and the ratio (dT_{hot}/dT_{cold}) is chosen to be 0.5, a conservative estimate.

Initial steady state conditions

The initial steady state problem places the reactor at 650 effective full power days (EFPD), end of cycle (EOC), with a boron concentration of 5 ppm, average core exposure of 24.58 GWD/MT, and equilibrium Xe and Sm concentrations. The initial operating conditions are as follows: the initial RCS pressure is 2 170 psia (the normal operating value), the initial pressuriser liquid level is set to 220 temperature compensated inches (a typical HFP level) and the initial cold leg temperature is at the normal value of 557°F, which compensates for instrument error. Table 2.1 gives a detailed description of the initial steady state conditions for this transient.

Table 2.1. Initial conditions for TMI-1 at 2 772 MW_t

Parameter	Value
Core power	2 772.0 MW _t
RCS cold leg temperature	555°F, 563.76°K
RCS hot leg temperature	605°F, 591.43°K
Lower plenum pressure	2 228.5 psia, 15.36 MPa
Outlet plenum pressure	2 199.7 psia, 15.17 MPa
RCS pressure	2 170.00 psia, 14.96 MPa
Total RCS flow rate	38 806.2 lb/sec, 17 602.2 kg/sec
Core flow rate	35 389.5 lb/sec, 16 052.4 kg/sec
Bypass flow rate	3 416.7 lb/sec, 1 549.8 kg/sec
Pressuriser level	220 inches, 558.8 cm
Feedwater/steam flow per OTSG	1 679 lb/sec, 761.59 kg/sec
OTSG outlet pressure	930.00 psia, 6.41 MPa
OTSG outlet temperature	571°F, 572.63°K
OTSG superheat	35°F, 19.67°K
Initial SG inventory	57 320 lbm, 26 000 kg
Feedwater temperature	460°F, 510.93°K

Reactor point kinetics parameters

Traditionally, this transient has been modelled using a point kinetics approach. Unfortunately, point kinetics can not consider spatial changes of power density, and is not able to model directly the asymmetrical nature of this transient. In order to overcome this deficiency, the reactivity feedback components that make up the total reactivity must be spatially weighted in both the axial and radial direction. Weighting the reactivity feedback components allows one to take the initial axial power distribution and the power tilt during the transient into consideration; however, it also requires extremely conservative, and limiting, assumptions. For this benchmark, the reactivity feedback is

weighted axially by the core average relative axial power distribution calculated using the 3-D nodal code. Radially, the reactivity feedback is weighted by the assembly relative radial power distribution (quarter core symmetry) calculated using the 3-D nodal code. In each case, the distributions are taken using EOC, HFP conditions.

In order to make the point kinetics and 3-D simulations compatible, one must specify point kinetics model inputs, which preserve axial and radial core power distributions, as well as scram reactivity obtained with the 3-D nodal core model. The following parameters for the point kinetics model and the 3-D neutronic transient core model should be consistent:

- Tripped rod worth.
- Radial power distribution.
- Axial power distribution.
- Moderator temperature coefficient.
- Doppler coefficient.
- Kinetics parameters.

In addition to the parameters specified above, all initial and boundary conditions must be identical between the two cases. The scram worth and maximum stuck rod worth at control rod position N12 are calculated using the 3-D nodal core model. These values are calculated at EOC, hot zero power (HZP) for the conditions shown below:

- Power level equal to 2 772 MW_t, full flow and operating pressure.
- Boron concentration of 5 ppm.
- All control rods in except Group 8 (axial power shape rods – APSR).
- Xe distribution fixed at HFP conditions.
- Moderator temperature of 532°F (551°K).

An estimated value for the tripped rod worth (TRW) was calculated for use as an input parameter in the point kinetics simulation based on the calculated values for the scram and maximum stuck rod worth, and including a 10% rod worth uncertainty at HZP. This scenario is the basic scenario, called Version 1 (V1), and it is used in the current licensing practice. The second scenario version was defined – Version 2 (V2), for the purposes of the second and third exercises in order to better test the neutronics/thermal-hydraulic coupling. The difference is in the calculated TRW value; the minimum value estimated with the 3-D nodal code is used. A summary of the input values for the point kinetics analysis is shown in Table 2.2. Table 2.3 shows the time constants and fractions of delayed neutrons for the six delayed neutron groups used for neutron modelling. EOC, HFP radial and axial relative power distributions (based on 24 equal nodes with an axial height of 14.88 cm) are shown in Figures 2.1 and 2.2, respectively. A scram reactivity table is provided in Table 2.4.

Table 2.2. Summary of point kinetics analysis input values

Parameter	Value
HFP EOC MTC	-34.64 pcm/°F, -62.35 pcm/°K
HFP EOC DTC	-1.43 pcm/°F, -2.57 pcm/°K
HFP EOC delayed neutron fraction (β_{eff})	0.5211E-02
HFP EOC prompt neutron lifetime	0.18445E-04
EOC TRW – V1	4.526% dk/k
EOC TRW – V2	3.040% dk/k

Table 2.3. Decay constants and fractions of delayed neutrons

Group	Decay constant (s ⁻¹)	Relative fraction of delayed neutrons (%)
1	0.012818	0.0153
2	0.03143	0.1086
3	0.125062	0.0965
4	0.329776	0.2019
5	1.414748	0.0791
6	3.822362	0.0197

Total fraction of delayed neutrons: 0.5211%.

Table 2.4. Rod worth versus time after trip (Versions 1 and 2)

Time after reactor trip (seconds)	Per cent of reactivity insertion (%)	Rod worth inserted* (% dk/k)	Rod worth inserted** (% dk/k)
0.0	0.0	0.000	0.000
0.2	0.58	-0.026	-0.018
0.3	0.99	-0.045	-0.030
0.4	1.83	-0.083	-0.056
0.6	5.29	-0.239	-0.161
0.8	12.33	-0.558	-0.375
1.0	21.41	-0.969	-0.651
1.2	33.09	-1.498	-0.101
1.4	50.75	-2.297	-1.428
1.6	72.96	-3.302	-2.218
1.8	91.30	-4.132	-2.776
2.0	99.26	-4.493	-3.018
2.2	99.99	-4.526	-3.040
2.3	100.00	-4.526	-3.040
10 ⁶	100.00	-4.526	-3.040

* Based on 4.526% dk/k TRW – Version 1

** Based on 3.040% dk/k TRW – Version 2

Figure 2.1. EOC HFP assembly relative radial power distribution (quarter core symmetry)

Core centre

0.918	1.253	1.057	1.285	1.031	1.248	0.805	0.439
1.253	1.023	1.270	1.051	1.278	1.048	1.124	0.496
1.057	1.270	1.039	1.278	1.022	1.254	1.051	0.476
1.285	1.053	1.278	1.048	1.273	0.952	0.767	
1.031	1.282	1.022	1.271	1.035	1.093	0.580	
1.248	1.043	1.254	0.952	1.093	0.740		
0.805	1.121	1.051	0.767	0.580			
0.439	0.493	0.475					

Core reflector/boundary

Figure 2.2. EOC HFP core average power relative power distribution

Bottom

0.8008	0.9718	1.05563	1.06437	1.05347	1.03940	1.0245	1.01800	1.00775	1.00160	0.99907	0.99798
0.99785	0.99857	1.0041	1.00391	1.00980	1.01896	1.03230	1.05048	1.05834	1.03893	0.94526	0.79778

Top

Analysis assumptions

There are three primary assumptions, which maximise the likelihood of a return to power. These assumptions are described below:

1. The transient is assumed to take place at HFP, end of cycle (EOC) to ensure the worst possible case scenario. TMI-1 is a Babcox and Wilcox (B&W) designed PWR, and has a once-through steam generator (OTSG). This type of steam generator is unlike a U-tube steam generator, in which the inventory decreases with increasing power, in that its inventory increases with increasing power. The amount of RCS cool-down following a steam line break accident is a function of SG water inventory available for cooling; therefore, the worst case overcooling occurs at the maximum power level, which corresponds to the maximum liquid inventory in the SG. The moderator temperature coefficient is most negative at EOC; therefore, this also is a limiting assumption because it increases the likelihood for a return to power and criticality.
2. The second conservative assumption is the use of a minimal shutdown margin. This leads to a greater chance of a return to power, as well as a larger increase in the power if the system returns to criticality. For this transient, the lowest allowable margin of 1% dk/k is used.
3. The final conservative assumption is that the control rod with the highest worth is stuck out during the transient. This is limiting because it reduces the available scram worth even further and increases the likelihood of a return to power and criticality.

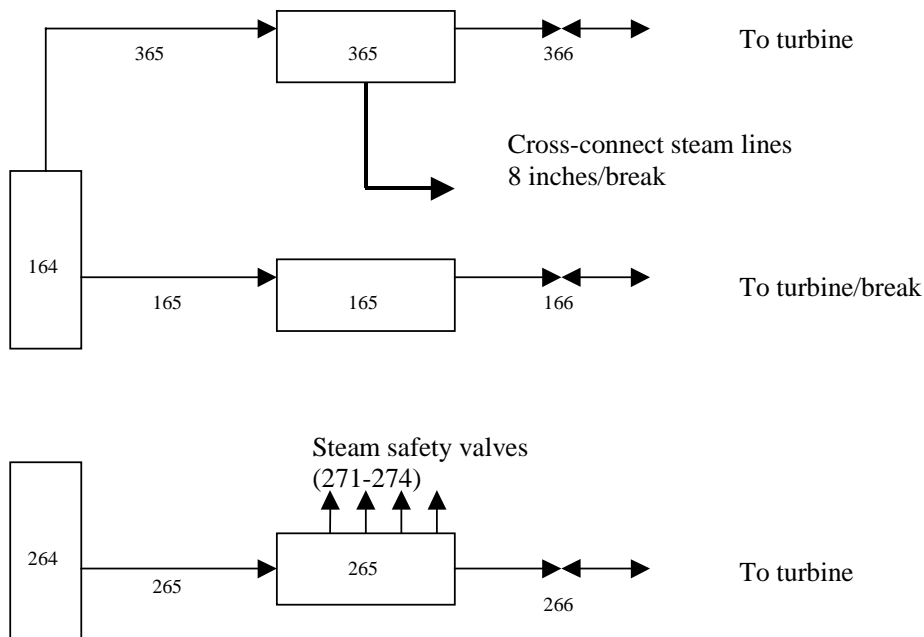
The key assumptions for performing the MSLB analysis are summarised in Table 2.5. Those assumptions that require a more detailed explanation are described below.

Table 2.5. MSLB analysis assumptions

Parameter	Value
Vessel mixing	$dT_{hot}/dT_{cold} = 0.5$
Boron injection	No credit taken
Steam line break 1	24 inch rupture (60.96 cm)
Steam line break 2	8 inch rupture (20.32 cm)
Critical flow model	Moody, cont. coeff. = 1.0
Decay heat multiplier	1.0
High flux trip set point	114%
High flux trip delay time	0.4 sec
Main feedwater flow	Flow vs. time
Emergency feedwater flow	No credit taken
High pressure injection flow	Flow vs. pressure
Low pressure trip set-point	1 945 psia, 13.41 MPa
Low pressure trip delay time	0.5 sec
High pressure trip set-point	2 370 psia, 16.34 MPa
High pressure trip delay time	0.6 sec
Turbine stop valve closure time	0.5 sec

- Break modelling.* For the purposes of this benchmark, a double-ended rupture of one steam line is assumed to occur upstream of the cross-connect. The break is a double-ended break of a 24 inch (60.96 cm) outer diameter main steam line. However, the limiting break area for one end of the break is an 8 inch (20.32 cm) diameter cross-connect area. These assumptions result in the highest break flow assumption and maximise the RCS cool-down. The main steam line piping length of approximately 146.98 ft (44.8 m) is included in the steam line model. The steam line nodalisation, numbered according to the RETRAN model [4], is shown in Figure 2.3. This break model represents a simplistic way of modelling the break flow by modelling a 24 inch and an 8 inch break.

Figure 2.3. Steam line nodalisation



- *Steam safety relief valves.* The steam safety relief valves are modelled on only the intact steam line for this benchmark. See Figure 2.3, along with the data provided in Table 2.6, for more information about the steam safety relief valves.

Table 2.6. Description of MSSVs per OTSG

Description of safety valves	Open set-point (psia/bar)	Close set-point (psia/bar)	Rated flow per valve at 3% accumulation (lbm/hr/kg/hr)
Small safety (1 valve)	1 055.0/72.73	1 012.5/69.8	194 900/88 407
Safety bank 1 (1 valve)	1 065.0/73.42	1 022.0/70.46	824 265/373 887
Safety bank 2 (2 valves)	1 065.0/73.42	1 022.0/70.46	792 610/359 528
Safety bank 3 (2 valves)	1 075.0/74.11	1 031.5/71.12	799 990/362 875

- *Main feedwater and emergency feedwater flows.* For this benchmark, it is assumed that the feedwater regulating valve associated with the broken SG experiences a mechanical failure in the open position. Feedwater (FW) flow to the broken SG is terminated by the closure of the feedwater block valve, which is assumed to close 30 seconds after the break occurs. This conservative assumption maximises feedwater flow to the broken SG, and thus helps to maximise the cool-down, as shown in Table 2.7. After 30 seconds an extended boundary condition models the additional feedwater between the feedwater isolation valve and the downcomer of the broken SG. The mass of feedwater between the isolation valve and the broken SG is approximated as a constant flow over 12 seconds. The main FW flow to the intact SG is held constant until the reactor trip, at which time it is ramped to zero in 10 seconds, as shown in Table 2.8. For the purpose of this benchmark, it is anticipated that 100 seconds of transient time will be sufficient for a return to power to be seen, if it occurs. The liquid levels in the broken SG reach the 10 inch (25.4 cm) actuation set point for the emergency feedwater (EFW) flow just prior to 100 seconds; therefore, there is no need to model the EFW flow.

Table 2.7. Main feedwater flow boundary conditions to broken SG

Time (sec)	Flow (lb/sec, kg/sec)
0	1 679.0/761.59
10	4 000.0/1 814.4
30	3 000.0/1 360.8
42	3 000.0/1 360.8
45	0.0/0.0

Table 2.8. Main feedwater flow boundary conditions to intact steam generator

Time (sec)	Flow (lb/sec, kg/sec)
0	1 679.0, 761.59
Reactor trip	1 679.0, 761.59
Ten seconds after reactor trip	0.0000, 0.0000
100	0.0000, 0.0000

- *Reactor trip.* The reactor is assumed to scram as a result of high neutron flux when the power reaches 114% of 2 772 MW_i (with a 0.4 second delay), or at a low RCS pressure of 1 945 psia (13.41 MPa), with a 0.5 second delay. Subsequent to the reactor trip signal, the most reactive control rod is assumed stuck in its fully withdrawn position.

- *High-pressure injection.* The high-pressure injection (HPI) system is assumed to activate when the primary system pressure drops to 1 645 psia (11.34 MPa), with a 25 second delay. For this benchmark problem, the HPI system is modelled taking credit for two of the four RCS pumps, while no credit is taken for the negative reactivity insertion from the boron addition. The total HPI flow as it varies with reactor coolant system pressure is shown in Table 2.9.

Table 2.9. HPI flow versus pressure

Flow		Pressure	
gpm	kg/s	psia	MPa
470.0	28.43	15	0.103
455.2	27.53	615	4.24
390.0	23.59	1 215	8.38
360.0	21.77	1 515	10.45
345.0	20.87	1 615	11.14
315.0	19.05	1 815	12.51
190.0	11.49	2 415	16.65

- *SG conductors.* The secondary side heat conductors on the SG, downcomer and steam annulus should be given both zero thickness and zero heat transfer coefficient. These two assumptions increase the degree of cool-down for this event, and thus conservatively maximise the chance for a return to power in the second half of the transient.
- *Containment modelling.* The containment response is not modelled and is assumed to stay at atmospheric pressure throughout the transient.
- *Mixing.* As mentioned previously, the simulated main steam line break transient results in asymmetric power and temperature distributions within the core region. As a result of this asymmetry, assuming 100% mixing within the core leads to both non-conservative and non-realistic results. In order to determine the appropriate mixing percentage to use when modelling such a transient, several tests were performed at the Oconee plant, which has a vessel identical to TMI-1. These tests were used to determine the amount of loop flow mixing that occurs within the reactor vessel when there is a large difference in the cold leg temperature behaviour. The tests defined the amount of mixing that occurs within the reactor vessel as:

$$\text{Ratio} = \frac{T_{\text{hot}}(\text{int act}) - T_{\text{hot}}(\text{broken})}{T_{\text{cold}}(\text{int act}) - T_{\text{cold}}(\text{broken})}$$

where a value of 0.0 means 100% mixing, and a value of 1.0 means 0% mixing. For this benchmark problem, a ratio of $R = 0.5$ was chosen to bound the analysis at an upper value. In addition, the mixing was found to be 20% in the lower plenum and 80% in the upper plenum.

Chapter 3

STATISTICAL METHODOLOGY

Standard techniques for comparison of results

The end result of the benchmark exercises should be a comprehensive comparison of all sets of results to the specified problem, as provided by the various participants and their preferred system codes. Such a comparison must necessarily include a figure of merit or similar means to quantify the degree of agreement, or disagreement, among the participants. This goal is, in the present instance, complicated by two circumstances. First, experimental data is not available for a PWR MSLB transient scenario, rendering traditional code-to-data comparison methods inapplicable. Second, several participants have submitted results from multiple versions of the same code. Consequently, not all of the sets of results are completely independent of each other, and simple averaging techniques may not provide an accurate statistical representation of the data.

To resolve these issues, the reference solution for all parameters is based upon a statistical mean value of all submitted values, corrected to account for the interdependence of some results [5]. Comparisons are accomplished by a similarly amended standard deviation. The comparisons to follow are thus properly called code-to-code comparisons, rather than code-to-data comparisons. While perhaps not ideal, this method provides the strongest basis from which to complete a statistical analysis and comparison of the results for this exercise.

Time history data

In this exercise, various parameters such as power, temperature and pressure are plotted as a function of time; these plots are denoted as time histories. Points of interest are isolated and submitted to a basic statistical analysis as described below.

- *Step 1: Isolate points of interest.* Such points include time of highest return to power, highest power before and after trip, and values at the end of transient (EOT) for all parameters. These points are identified for all time-series data sets, and the values of all participants are collected. For Exercise One, most of the parameters are evaluated at EOT, with a few also being evaluated at the power peaks before or after reactor scram.
- *Step 2: Calculate mean values and standard deviations.* This calculation is completed in two stages to account for the multiple versions of some codes. First, the results of all dependent code versions are averaged to provide a single mean value for that code. As discussed previously, the code versions, which are dependent on one another, are those which differ only by perturbations of the calculation or boundary models. In the second stage, these averaged values and the results from single version codes are averaged again to provide the overall mean value, which will serve as the reference solution for that parameter.

In both stages, the averaging process obeys the formula for statistical mean value:

$$\bar{x} = \frac{\sum_{i=1}^N x_i}{N} \quad (3.1)$$

The standard deviation is calculated for the final average and obeys the equation:

$$\sigma = \pm \sqrt{\frac{\sum_{i=1}^N (x_i - \bar{x})^2}{N-1}} \quad (3.2)$$

where \bar{x} represents the final mean value and x_i is the averaged result for those codes with multiple versions or the single value for independent codes. These mean and standard deviation values are calculated at each of the points defined in Step 1 above, to be used in the remaining steps that follow.

- *Step 3: Identify outliers and recalculate mean, if necessary.* It has been noted that for certain parameters, some of the results submitted by one or more participants lie far outside the mean range. To avoid extreme skewing of the mean solution by these outliers, a rudimentary outlier analysis is performed. If any result lays more than three standard deviations above or below the mean solution, it is excluded from the averaging process and the mean and standard deviations are recalculated. Such results are the NETCorp results, which are not included in Tables 4.1-4.11 of Chapter 4. The only other results lying outside of the three-sigma tolerance are the IPSN/CEA predictions of break flow rates and these are denoted with (*) in Table 4.1. This process is repeated until no points lie beyond this three-sigma range.
- *Step 4: Determine and report the deviation and figure of merit for each participant's value.* The deviation, e , which is merely the difference between the participant's value and the mean as determined in Step 2, is calculated according to:

$$e_i = (x_i - \bar{x}) \quad (3.3)$$

After calculating the deviation, the figure of merit can be determined according to the formula:

$$\Phi = \frac{e}{\sigma} \quad (3.4)$$

This figure of merit provides a means for comparison that is more easily interpreted than raw deviations by relating the participant's deviation to the overall standard deviation. The deviations and figures of merit for all codes will be tabulated in the final report for this exercise.

Reference results

The reference results for Phase I of the PWR MSLB benchmark – point kinetics exercise – are based upon a statistical mean value of all submitted results. The reference results are shown at the beginning of Tables 4.1-4.11 of Chapter 4. Fifteen time histories are compared at the EOT. Of particular

interest are total power, fission power and reactivity time histories. For them three points are isolated: highest power before and after trip, and values at the EOT. At each of these isolated points mean values and standard deviations are obtained, according to the methods described above.

Chapter 4

RESULTS AND DISCUSSION

The plots and tables in this section provide a comparison of the participants' results for the parameters that have the greatest effect on the MSLB transient. These parameters include power, temperature, pressure, reactivity, break flow rate and steam generator mass. In each case, the tables (Tables 4.1-4.8) show values for the absolute and relative difference between the mean solution and each participant's results for the given parameter, while the figures (Figures 4.1-4.28) graphically illustrate the agreement or disagreement of participants' predictions. Statistical evaluation is employed for the parameters in the tables in an attempt to make a quantitative comparison. The star in Table 4.1 signifies that the marked result was not included in the generation of mean value and standard deviation for the specified parameter. The NETCorp results are presented only in the plots. The tables and figures for each parameter are discussed in more detail below. Note that the two sets of VTT, Finland results are produced with two different codes – SMABRE (VTT 1) and APROS (VTT 2) while the two sets of the University of Valencia results are produced with the same code (TRAC-PF1) using different vessel models. Valencia 1 results are calculated with the 3-D TRAC vessel model in cylindrical geometry (similar to the PSU model) and the Valencia 2 results are calculated using a channel model.

A remark must be made regarding the comparison of parameters at EOT. When looking at the time of second power peak (Table 4.7), one can see a discrepancy of about 18 seconds between the fastest predictions (Iberdrola and PSU) and the slowest one (IPSN/CEA). Other solutions are placed between these two extremes in terms of chronology. The differences in the predicted transient chronology have consequences for some parameters at EOT (break flow rate, secondary pressure and fuel temperature). For example, if the return to power occurs later, the fuel temperature at EOT is higher, the break flow rate is higher and the broken SG may not be dry yet.

Break flow rate

Figures 4.1, 4.2 and 4.3 provide a comparison for the behaviour of the total, 24 inch and 8 inch break flow rates, respectively. The MSLB transient is initiated at 0.001 seconds by a double-ended break of the Loop A steam line upstream of the MSIVs. As expected, there is an initial peak in the flow out of breaks when the transient is initiated. The second peak occurs 30 seconds into the transients and coincides with the feedwater in the broken SG being ramped to zero. After this second peak, the flow rate of breaks goes to zero as the SG blows dry. In each case, the participants' results are in reasonable agreement concerning the behaviour of this parameter, but there are a number of local deviations throughout the transient. These local deviations are caused by modelling differences in the steam line, break, break flow rate and various other modelling assumptions and code correlations. For example, the differences in the steam-liquid interface friction in the SG influences the liquid entrainment into the steam line and to the break during the blow-down.

A summary of the deviation from the reference results for the break flow rates at the end of the transient are presented in Table 4.1. The values are relatively small, with IPSN/CEA having the largest

Table 4.1. Deviations: total break flow rate, 24 inch break flow rate and 8 inch break flow rate at end of transient

BREAK FLOW RATES	Total Mean = 4.858 kg/s $\sigma = 7.85$ kg/s		24 inch break Mean = 4.392 kg/s $\sigma = 7.11$ kg/s		8 inch break Mean = 0.655 kg/s $\sigma = 0.79$ kg/s	
Participant	Total break flow rate		24 inch break flow rate		8 inch break flow rate	
	e	Φ	e	Φ	e	Φ
British Energy	-4.56	-0.58	-4.09	-0.58	-0.66	-0.83
CSA/GPUN/EPRI	3.74	0.48	2.61	0.37	0.95	1.20
GRS	-4.86	-0.62	-4.39	-0.62	-0.66	-0.83
Iberdrola	-4.36	-0.56	-4.09	-0.58	-0.46	-0.58
IPSN/CEA	115.24*	14.68*	97.41*	13.69*	17.65*	22.44*
Pisa/Zagreb	7.24	0.92	6.51	0.91	0.95	1.20
PSU	21.74	2.77	20.01	2.81	1.56	1.98
Purdue/NRC	-4.06	-0.52	-3.79	-0.53	-0.46	-0.58
Rosendorf	-0.36	-0.05	-0.39	-0.06	-0.16	-0.20
Siemens/FZK	-1.96	-0.25	-2.79	-0.39	0.60	0.76
Valencia 1	-3.06	-0.39	-2.69	-0.38	-0.56	-0.71
Valencia 2	-4.86	-0.62	-2.69	-0.38	-0.46	-0.58
VTT 2	-2.01	-0.26	-1.91	-0.27	-0.29	-0.37
VTT 1	-4.66	-0.59	-4.19	-0.59	-0.66	-0.83

deviation for the total, 24 inch and 8 inch break flow rates. The differences in participants' results for the flow at the end of the break can be attributed primarily to differences in modelling assumptions and/or minor differences in the SG and steam-line nodalisation models.

Pressure

Figures 4.4-4.9 show comparisons for the average, broken and intact loop, broken and intact steam line and pressuriser pressures throughout the transient. In each case, the participants are in reasonable agreement concerning the behaviour of the parameter, and the results form a single cluster. Any local deviations in the pressure behaviour throughout the transient are caused by modelling differences in the reactor coolant system and steam lines, modelling assumptions and code correlations.

The depressurisation of the broken SG results in overcooling of the reactor coolant system (RCS) fluid, which results in a lower average temperature in the core region. As the RCS fluid cools down, it shrinks, resulting in a rapid decrease in the RCS pressure. The HPI low pressure signal is received and HPI is activated with a 25 second delay. As a result of injecting cold water into the core region, the power begins to increase and the RCS pressure begins to even out. Table 4.2 provides a summary of the deviations from the reference (mean) solution for the average pressure and the broken and intact loop pressures at the end of the transient for each participant. The two results of the University of Valencia and the British Energy result show the largest deviation for the average pressure. The deviation for University of Valencia is explained by the fact that this participant's code calculates a larger pressure drop after the initial break as compared, for example, with PSU. Since PSU and the University of Valencia are using the same code to calculate the data submitted for this benchmark, this deviation can be attributed to the differences in modelling assumptions and the nodalisation used for the TMI-1 model. The British Energy large positive deviation is a result of over-calculating the pressure in the broken and intact loops throughout the second half of the transient.

Table 4.2. Deviations: average pressure, pressure in the broken loop and pressure in the intact loop

PRESSURE	Average: Mean = 5.33E+06 Pa σ = 7.3E+05 Pa		Broken loop: Mean = 5.29E+06 Pa σ = 6.8E+05 Pa		Intact loop: Mean = 5.28E+06 Pa σ = 6.5E+05 Pa	
Participant	Average pressure		Broken loop pressure		Intact loop pressure	
	e	Φ	e	Φ	e	Φ
British Energy	1.42E+06	1.95	1.58E+06	2.33	1.59E+06	2.45
CSA/GPUN/EPRI	-7.42E+05	-1.02	–	–	–	–
GRS	-6.62E+05	-0.91	-7.29E+05	-1.08	-6.90E+05	-1.06
Iberdrola	-3.32E+05	-0.45	-4.69E+05	-0.69	-4.60E+05	-0.71
IPSN/CEA	1.85E+04	0.03	2.01E+05	0.30	1.90E+05	0.29
Pisa/Zagreb	8.85E+04	0.12	-2.69E+05	-0.40	-2.60E+05	-0.40
PSU	4.98E+05	0.68	-7.92E+04	-0.12	-4.10E+05	-0.63
Purdue/NRC	4.98E+05	0.68	3.91E+05	0.58	4.00E+05	0.62
Rosendorf	-1.62E+05	-0.22	-1.19E+05	-0.18	-1.20E+05	-0.18
Siemens/FZK	7.38E+05	1.01	7.81E+05	1.15	7.90E+05	1.22
Valencia 1	-1.01E+06	-1.39	-1.11E+06	-1.64	-6.70E+05	-1.03
Valencia 2	-9.22E+05	-1.26	-2.49E+05	-0.37	-4.90E+05	-0.75
VTT 2	4.34E+05	0.59	3.16E+05	0.46	3.25E+05	0.50
VTT 1	5.68E+05	0.78	2.11E+05	0.31	2.60E+05	0.40

As expected, the broken steam line pressure decreases rapidly following the break as a result of the depressurisation in the broken SG. This large drop in steam line pressure is followed by a slow depressurisation throughout the remainder of the transient as the broken SG blows dry. The intact steam line sees a constant pressure until the turbine stop valve to the intact SG is closed, following the reactor trip signal, thus effectively isolating the intact SG. The pressure in the intact steam line increases slightly after the turbine stop valve. As a result of this increase the safety relief valves on the intact steam line start opening. Later into the transient these valves are closing. Following the closure of the safety relief valves, the intact steam line sees a slight depressurisation throughout the remainder of the transient. Table 4.3 provides the deviations from the reference solution for the broken and intact steam line pressures and the pressuriser pressure at the end of the transient. IPSN/CEA sees the largest deviation for the broken steam line. This deviation results from the prediction of largest break flow rate at the end of transient. The Universities of Pisa and Zagreb see the largest deviation for the intact steam line. This is a consequence of modelling assumptions applied by the code user. As can be seen in Appendix C of this report, the participant uses full mixing in the reactor pressure vessel, resulting in a higher energy transfer from the intact half to the broken half. British Energy sees the greatest deviation for the pressuriser pressure due to an over-calculation of the pressure throughout the second half of the transient. While some local deviations exist, overall, these parameters show good agreement with the reference data.

Temperatures

Comparisons of the coolant core average, hot leg (broken and intact loop), cold leg (broken and intact loop) and fuel temperatures (core-averaged) calculated by each code throughout the transient are shown in Figures 4.9-4.15. In each case, the behaviour of the parameter during the transient forms a single cluster. Any local deviations in the temperature behaviour throughout the transient are caused by modelling differences in the reactor coolant system, modelling assumptions and code correlations.

Table 4.3. Deviations: broken steam line pressure, intact steam line pressure and pressuriser pressure

PRESSURE	Broken steam line: Mean = 1.41E+05 Pa σ = 1.2E+04 Pa		Intact steam line: Mean = 4.82E+06 Pa σ = 4.8E+05 Pa		Pressuriser: Mean = 5.59E+06 Pa σ = 7.2E+05 Pa	
Participant	Broken steam line pressure		Intact steam line pressure		Pressuriser pressure	
	e	Φ	e	Φ	e	Φ
British Energy	-4.03E+04	-0.35	4.26E+05	0.90	9.75E+05	1.36
CSA/GPUN/EPRI	-1.39E+05	-1.20	-3.34E+05	-0.70	–	–
GRS	-3.83E+04	-0.33	-1.04E+05	-0.22	–	–
Iberdrola	-2.03E+04	-0.18	-4.24E+05	-0.89	–	–
IPSN/CEA	2.65E+05	2.29	-1.54E+05	-0.32	-5.65E+05	-0.79
Pisa/Zagreb	-4.19E+04	-0.36	-1.21E+06	-2.55	–	–
PSU	-2.73E+04	-0.24	5.16E+05	1.08	-5.05E+05	-0.71
Purdue/NRC	-4.03E+04	-0.35	5.16E+05	1.08	9.50E+04	0.13
Rosendorf	-3.93E+04	-0.34	-2.34E+05	-0.49	–	–
Siemens/FZK	2.40E+05	2.07	6.64E+04	0.14	–	–
Valencia 1	-3.83E+04	-0.33	1.96E+05	0.41	–	–
Valencia 2	-3.76E+04	-0.31	1.06E+05	0.22	–	–
VTT 2	-4.11E+04	-0.34	-1.22E+05	-0.25	–	–
VTT 1	-4.03E+04	-0.35	5.36E+05	1.13	–	–

When the steam line break occurs, the pressure in the broken SG decreases rapidly, which causes the flow rate within the SG to increase. The increased flow rate results in an increase in the heat transfer and overcooling of the RCS fluid. The cold leg temperature plots show an immediate temperature decrease as a result of the broken SG depressurisation; however, the hot leg temperature plots show a more graduate decline. The reason is that the decreasing RCS temperature results in an increase in the core power, which initially offsets the broken SG's cooling effect. Following the initial decrease, the intact cold leg temperature sees a slight increase in temperature as a result of the turbine stop valve closure, which isolates the intact SG. In the second half of the transient, there is an increase in the core power, and the overcooling effect from the broken SG becomes secondary. In addition to the increase in power, the broken SG loses its cooling capacity throughout the transient as it blows dry. The broken loop sees an increase in RCS temperature as a result of this power increase, while the intact loop see the temperature approaching a constant value in the later half of the transient. The deviations for the broken loop are fairly low for both the hot and cold legs, with VTT (Smabre) showing the largest deviation in each case (see Table 4.4). This difference is caused by under-cooling in the broken SG and may be the result of different code correlations. As with the broken loop temperatures, there are small deviations in the intact hot and cold leg temperatures, with the Universities of Pisa and Zagreb seeing the largest deviation (see Table 4.5). This difference is explained by overcooling of the intact cold leg, which is a result of mixing assumptions.

Table 4.6 provides a summary of the deviations for the average moderator and fuel temperatures at the end of the transient. The Universities of Pisa and Zagreb show the largest deviation for the average moderator temperature because of a slight under-cooling in the intact loop throughout the second half of the transient. As expected the fuel temperature time evolution follows the behaviour of the reactor power throughout the transient. IPSN/CEA shows the largest deviation for the fuel temperature as a consequence of the predicted transient behaviour. IPSN/CEA predicts lower break flow rates in the first half of the transient, which results in higher reactor coolant temperatures and

Table 4.4. Deviations: broken loop hot and cold leg temperatures at the end of the transient

TEMPERATURE	Broken loop hot leg: Mean = 526.5 K $\sigma = 5.2$ K		Broken loop cold leg: Mean = 522.6 K $\sigma = 7.0$ K	
Participant	Broken hot leg temp.		Broken cold leg temp.	
	e	Φ	e	Φ
British Energy	4.50	0.87	5.36	0.77
CSA/GPUN/EPRI	3.50	0.68	4.36	0.62
GRS	-1.50	-0.29	-1.64	-0.24
Iberdrola	4.50	0.87	7.36	1.05
IPSN/CEA	-5.50	-1.07	-9.64	-1.38
Pisa/Zagreb	-7.50	-1.45	-6.64	-0.95
PSU	4.50	0.87	5.36	0.77
Purdue/NRC	-4.50	-0.87	-3.64	-0.52
Rosendorf	-2.50	-0.48	-3.64	-0.52
Siemens/FZK	0.50	0.10	0.36	0.05
Valencia 1	0.50	0.10	2.36	0.34
Valencia 2	3.59	0.69	5.80	0.84
VTT 2	-5.92	-1.13	-6.62	-0.95
VTT 1	8.50	1.65	9.36	1.34

Table 4.5. Deviations: Intact loop hot and cold leg temperatures at the end of the transient

TEMPERATURE	Intact loop hot leg: Mean = 532.6 K $\sigma = 6.4$ K		Intact loop cold leg: Mean = 532.9 K $\sigma = 6.8$ K	
Participant	Intact hot leg temp.		Intact cold leg temp.	
	e	Φ	e	Φ
British Energy	7.43	1.16	7.14	1.05
CSA/GPUN/EPRI	-1.57	-0.24	-1.86	-0.27
GRS	-2.57	-0.40	-0.86	-0.13
Iberdrola	-1.57	-0.24	-2.86	-0.42
IPSN/CEA	-1.57	-0.24	-1.86	-0.27
Pisa/Zagreb	-13.57	-2.11	-15.86	-2.33
PSU	7.43	1.16	8.14	1.20
Purdue/NRC	7.43	1.16	8.14	1.20
Rosendorf	-2.57	-0.40	-0.86	-0.13
Siemens/FZK	2.43	0.38	2.14	0.31
Valencia 1	-5.57	-0.87	-6.86	-1.01
Valencia 2	-2.57	-0.40	-4.10	-0.60
VTT 2	-1.34	-0.21	-0.10	-0.01
VTT 1	10.43	1.62	9.14	1.34

Table 4.6. Deviations: average moderator temperature and fuel temperature at the end of the transient

TEMPERATURE	Moderator: Mean = 528.7 K $\sigma = 5.8$ K		Fuel: Mean = 546.8 K $\sigma = 10.0$ K	
Participant	Moderator temperature		Fuel temperature	
	e	Φ	e	Φ
British Energy	6.33	1.10	0.17	0.02
CSA/GPUN/EPRI	–	–	-2.83	-0.28
GRS	-0.67	-0.12	0.17	0.02
Iberdrola	2.33	0.40	-2.83	-0.28
IPSN/CEA	-4.67	-0.81	24.83	2.49
Pisa/Zagreb	-10.67	-1.85	15.17	1.52
PSU	6.33	1.10	8.17	0.82
Purdue/NRC	1.33	0.23	1.17	0.12
Rosendorf	-2.67	-0.46	–	–
Siemens/FZK	1.33	0.23	1.17	0.12
Valencia 1	-1.67	-0.29	-0.83	-0.08
Valencia 2	0.90	0.16	3.50	0.35
VTT 2	-3.07	-0.53	2.24	0.22
VTT 1	9.33	1.62	11.17	1.12

later return to power. At the end of the transient ($t = 100$ s) the IPSN/CEA calculation shows higher reactor power than other participants' results. In summary the fuel temperature deviations reflect the power deviations. Those reflect more or less the deviations in the break flow rates. In addition the differences in fuel temperature predictions at the same power predictions and same coolant temperature predictions can be attributed to the heat structure modelling assumptions as the number of radial zones for the fuel rod.

Reactor power

A comparison of the fission, total and decay power calculated by each code throughout the transient is shown in Figures 4.16-4.18. The power response and the magnitude of the return to power during the transient as predicted by different codes are functions of the total reactivity time evolution. When the break is initiated, the core sees a gradual rise in power in response to the temperature changes within the core region. A rapid power rise occurs when the overcooled liquid from the broken loop reaches the core. The power rise continues until the reactor trips. After the trip, a sharp decrease in power results from the negative reactivity inserted into the core when the reactor scrams. The broken SG continues to overcool the RCS fluid together with the cold water injected from the HPI system, and the reactor sees an increase in power later into the transient. This rise in power quickly decreases because the broken SG loses its cooling capability as its mass and pressure go to zero.

In general, the results follow the above-described behaviour. NETCorp shows the largest deviation because the code has extremely conservative correlations and calculates an increase in power more quickly than the other codes. Twelve of the fifteen participants see a more pronounced return to power in the second half of the transient. The three participants – the Universities of Pisa and Zagreb, GRS and GPU/CSA/EPRI – see a slight rise in power around the same time the other participants experience a higher return-to-power. While there is general agreement about the behaviour of the power

throughout the transient, there is a great deal of disagreement about the size of the return to power. This disagreement is explained below while discussing the differences in the total reactivity time evolution prediction.

Table 4.7 shows the deviation from the reference results for the time of reactor trip (initial peak) and the time of highest power after the trip (second peak). The values vary, with the Universities of Pisa and Zagreb showing the largest deviation for the initial peak (at reactor scram) and IPSN/CEA showing the largest deviation for the second peak.

Table 4.7. Deviations: time of reactor trip (initial peak) and time of highest power after trip (second peak)

TIME	Initial peak: Mean = 5.64 sec $\sigma = 0.79$ sec		Second peak: Mean = 70.2 sec $\sigma = 15.0$ sec	
Participant	Initial peak		Second peak	
	e	Φ	E	Φ
British Energy	-0.54	-0.68	-2.90	-0.19
CSA/GPUN/EPRI	-0.14	-0.18	-6.21	-0.41
GRS	0.86	1.08	6.79	0.45
Iberdrola	-0.64	-0.81	-9.21	-0.61
IPSN/CEA	0.39	0.50	12.58	0.84
Pisa/Zagreb	1.86	2.34	4.79	0.32
PSU	0.36	0.45	-9.21	-0.61
Purdue/NRC	-1.14	-1.44	4.79	0.32
Rosendorf	-0.94	-1.19	11.40	0.76
Siemens/FZK	-0.14	-0.18	3.79	0.25
Valencia 1	0.56	0.71	-4.64	-0.31
Valencia 2	0.56	0.71	-4.31	-0.29
VTT 2	0.56	0.71	11.60	0.77
VTT 1	0.36	0.45	-4.21	-0.28

Tables 4.8 and 4.9 provide deviations from the reference solution for the ratio of the total and fission power to the initial power level (as calculated by each participant at $t = 0.0$ seconds) at the first and second peaks and at the end of the transient. The deviations at the first peak are relatively small, with IPSN/CEA having the largest deviation for both the fission and total powers. One reason is that the IPSN/CEA high flux trip delay time (0.46 seconds) is slightly greater than specified. Another observation is that all participants start at approximately same initial total power level while the initial fission power level varies, depending on the decay heat model used. The effective decay heat energy fraction of the total thermal power (the relative contribution in the steady state) is specified to be equal to 0.07143, which assumes approximately 2 574 MW as initial fission power level. For example IPSN/CEA starts at an initial fission power level of 2 616 MW. The greatest deviations at the end of the transient are calculated by IPSN/CEA for both fission and total powers. In each case, the difference is explained by the prediction of a late return to power in the second half of the transient.

The deviations for the total and fission power at the second peak are quite large, with NETCorp having the greatest value in each case. The results submitted by NETCorp predict a much larger return to power than the other participants' results and the reference results for this parameter. It was determined, after consultation with NETCorp, that this difference can be explained by examining Figures 4.25 and 4.26. From these plots is obvious that NETCorp is calculating a greater amount of

Table 4.8. Deviations: percentage of initial power at time of reactor trip (initial peak), time of highest power after trip (second peak) and end of transient for total power

POWER	Initial peak: Mean = 1.176 $\sigma = 0.039$		Second peak: Mean = 0.190 $\sigma = 0.075$		End of transient: Mean = 0.0628 $\sigma = 0.0320$	
Participant	Total power, initial		Total power, second		Total power, EOT	
	E	Φ	e	Φ	e	Φ
British Energy	0.01	0.18	0.10	1.40	-0.0010	-0.03
CSA/GPUN/EPRI	-0.01	-0.16	-0.09	-1.19	-0.0096	-0.30
GRS	–	–	–	–	–	–
Iberdrola	-0.03	-0.67	-0.01	-0.08	-0.0573	-1.79
IPSN/CEA	0.07	1.69	0.04	0.44	0.0792	2.47
Pisa/Zagreb	-0.03	-0.67	-0.09	-1.20	0.0025	0.08
PSU	-0.01	-0.16	0.05	0.62	0.0061	0.19
Purdue/NRC	-0.04	-0.93	0.02	0.23	0.0043	0.13
Rosendorf	0.04	1.10	0.09	1.27	0.0075	0.23
Siemens/FZK	-0.01	-0.16	0.01	0.18	0.0050	0.16
Valencia 1	0.01	0.14	0.03	0.40	0.0040	0.12
Valencia 2	0.00	0.00	0.05	0.68	0.0100	0.31
VTT 2	0.01	0.16	0.02	0.32	0.0180	0.56
VTT 1	-0.01	-0.16	0.05	0.64	0.0173	0.54

Table 4.9. Deviations: percentage of initial power at time of reactor trip (initial peak), time of highest power after trip (second peak) and end of transient for fission power

POWER	Initial peak: Mean = 1.193 $\sigma = 0.026$		Second peak: Mean = 0.170 $\sigma = 0.074$		End of transient: Mean = 0.0403 $\sigma = 0.0189$	
Participant	Fission power, initial		Fission power, second		Fission power, EOT	
	E	Φ	e	Φ	e	Φ
British Energy	0.01	0.23	0.10	1.36	-0.0144	-0.76
CSA/GPUN/EPRI	–	–	–	–	–	–
GRS	-0.01	-0.57	-0.11	-1.45	-0.0163	-0.86
Iberdrola	-0.02	-0.97	-0.01	-0.18	-0.0170	-0.90
IPSN/CEA	0.06	2.35	0.00	0.00	0.0463	2.45
Pisa/Zagreb	-0.01	-0.57	-0.11	-1.46	-0.0131	-0.69
PSU	0.01	0.23	0.04	0.51	-0.0066	-0.35
Purdue/NRC	-0.02	-0.97	0.01	0.11	-0.0092	-0.49
Rosendorf	0.04	1.68	0.09	1.24	-0.0018	-0.09
Siemens/FZK	0.01	0.23	0.00	0.05	-0.0083	-0.44
Valencia 1	0.01	0.21	0.00	0.01	-0.0053	-0.28
Valencia 2	0.00	0.00	0.04	0.56	-0.0031	-0.16
VTT 2	–	–	–	–	–	–
VTT 1	0.02	0.63	0.04	0.55	0.0070	0.37

overcooling for the broken steam generator than the other participants. It was determined that this additional overcooling is the result of the correlations used to calculate the heat transfer in the SG model. The correlations used by DNP-3D are more conservative than those found in other best-estimate

codes. As a result, there is additional heat transfer in the broken SG, which results in both an earlier and a greater degree of overcooling of the reactor core. These conservative correlations account for the early reactor trip and the large return-to-power in the second half of the transient.

All of the participants except for PSU and the University of Valencia (Valencia 1) use a channel model. PSU and Valencia 1 results are calculated using the 3-D TRAC-PF1 vessel model in cylindrical geometry. In order to evaluate the differences between channel and 3-D vessel modelling for the simulated MSLB transient a detailed comparative analysis was performed for both sets of the University of Valencia's results produced with the same code TRAC-PF1. However, the Valencia 2 results are calculated using a channel model. The impact on the transient simulation can be summarised as follows: the channel model produces a slightly higher return to power at almost the same time with most of the other predicted parameters in very good agreement.

Reactivity

Figures 4.19-4.22 show comparisons for the behaviour of the total, moderator, Doppler and scram reactivity throughout the transient. The scram reactivity is plotted to show that it follows the table provided in the specification. As expected, its value remains at zero until the reactor trips, at which time it drops to a value of -4.526% dk/k and remains at this value through the remainder of the transient. Since the inserted negative tripped rod reactivity is specified, the differences in the total reactivity time evolution arise from the predictions of moderator feedback and Doppler feedback reactivity components. The moderator reactivity component follows the cold leg temperature. The discrepancies in the cold leg temperature predictions are due mostly to differences in modelling the secondary side. It was observed that the major factors affecting the dynamics of the transient are break flow modelling (critical flow model), liquid entrainment, modelling of the aspirator flow and nodalisation of the SG down comer. In addition the disagreement can be attributed to differences in the SG heat transfer correlations used within each participant's code. The Doppler feedback reactivity predictions are sensitive to the relation used for Doppler fuel temperature as well as to the radial and axial nodalisation of the heat structure used (fuel rod).

Table 4.10 provides a summary of deviations from the reference results for the total reactivity at the second peak and the end of the transient. British Energy shows the largest deviation for the second peak, and IPSN/CEA shows the largest deviation at the end of transient. Five participants – NETCorp, British Energy, IPSN/CEA, Rossendorf and Purdue/NRC see return to criticality.

Table 4.11 provides deviations from the reference solution for the moderator, Doppler and scram reactivity values at the end of the transient. The deviations for the moderator reactivity are the result of different code models since none of the participants over-calculate or under-calculate this parameter throughout the transient. The deviations are relatively small for the Doppler reactivity due to the reasons discussed above. The exceptions are the NETCorp results, as can be seen in Figures 4.20 and 4.21. The scram reactivity throughout the transient is provided in the specification and, as one would expect, no disagreement exists for this parameter at the end of the transient.

Steam generator mass

Figures 4.23 and 4.24 provide a comparison for the behaviour of the intact and broken steam generator masses throughout the transient. As expected, the mass in the broken SG decreases throughout the transient, until it eventually blows dry. The intact SG mass initially increases as a result of the closure of the turbine isolation valve for the intact SG at the turbine trip. This mass eventually decreases

Table 4.10. Deviations: total reactivity at time of highest power after reactor trip and at end of transient

REACTIVITY	Total (second peak): Mean = -1.02E-03 $\sigma = 1.41E-03$		Total (end of transient): Mean = -5.09E-03 $\sigma = 2.03E-03$	
Participant	Total reactivity (second peak)		Total reactivity (end of transient)	
	e	Φ	e	Φ
British Energy	1.96E-03	1.39	-2.03E-03	-1.00
CSA/GPUN/EPRI	-1.95E-03	-1.38	-2.91E-03	-1.43
GRS	-1.33E-03	-0.94	-7.22E-04	-0.35
Iberdrola	1.00E-03	0.71	-1.52E-03	-0.75
IPSN/CEA	1.16E-03	0.82	2.93E-03	1.44
Pisa/Zagreb	1.50E-04	0.11	1.45E-03	0.71
PSU	-9.70E-04	-0.69	-2.19E-03	-1.08
Purdue/NRC	1.12E-03	0.80	6.50E-04	0.33
Rosendorf	1.52E-03	1.08	1.91E-03	0.94
Siemens/FZK	9.90E-04	0.70	-4.02E-04	-0.20
Valencia 1	6.60E-04	0.47	-3.82E-04	-0.19
Valencia 2	9.85E-04	0.70	-2.90E-04	-0.14
VTT 2	1.36E-03	0.96	1.21E-03	0.60
VTT 1	9.70E-04	0.69	8.88E-04	0.44

Table 4.11. Deviations: moderator reactivity, Doppler reactivity and scram reactivity at end of transient

REACTIVITY	Moderator: Mean = 3.22E-02 $\sigma = 2.0E-03$		Doppler: Mean = 7.97E-03 $\sigma = 8.9E-04$		Scram: Mean = -4.53E-02 $\sigma = 0.00$	
Participant	Moderator reactivity		Doppler reactivity		Scram reactivity	
	E	Φ	e	Φ	e	Φ
British Energy	-7.27E-04	-0.37	-1.33E-03	-1.48	0.00E+00	–
CSA/GPUN/EPRI	-6.27E-04	-0.32	-8.96E-04	-1.00	0.00E+00	–
GRS	3.73E-04	0.19	-1.09E-03	-1.21	0.00E+00	–
Iberdrola	-1.93E-03	-0.99	4.04E-04	0.45	0.00E+00	–
IPSN/CEA	2.17E-03	1.11	6.44E-04	0.72	0.00E+00	–
Pisa/Zagreb	–	–	–	–	–	–
PSU	-3.43E-03	-1.75	1.21E-03	1.36	0.00E+00	–
Purdue/NRC	-2.73E-05	-0.01	-6.96E-04	-0.78	0.00E+00	–
Rosendorf	8.73E-04	0.45	9.84E-04	1.10	0.00E+00	–
Siemens/FZK	–	–	–	–	–	–
Valencia 1	-1.03E-03	-0.53	6.54E-04	0.73	0.00E+00	–
Valencia 2	-1.38E-03	-0.69	1.03E-03	1.15	0.00E+00	–
VTT 2	1.73E-03	0.09	-5.26E-04	-0.59	0.00E+00	–
VTT 1	4.73E-04	0.24	4.54E-04	0.51	0.00E+00	–

due to the MSSV's action and further evens and remains constant until the end of the transient. While there is general agreement about the behaviour of the masses in each SG, the analysis shows a great deal of disagreement about the values of the masses throughout the transient. This parameter shows the largest deviation out of all those presented in this report; however, this is not surprising when one considers the complexity involved with modelling the OTSG. Originally, it was thought that the SG mass discrepancy was the result of the differences in modelling of both the SG and the steam line. Since that time, the break nodalisation has been made uniform amongst all the participants and a great deal of additional information has been provided about the OTSG, concerning both the way it works and its geometry. The initial mass of the SG has been modified to remove the artificial increase of 3 000 kg that a number of the participants were having trouble reproducing. Putting the SG masses back to 26 000 kg has helped to make the results more uniform; however, discrepancies still exist.

Overall, the masses for both SGs are fairly consistent amongst all participants. All the participants were provided with the same base deck from which to take SG information, as well as the same subsequent information. As a result, any differences in the value or behaviour of this parameter throughout the transient can be attributed to three major factors:

1. Differences in the code models, which significantly influence the transient behaviour, like models for break flow rate, and steam-liquid interface friction or liquid entrainment during blow-down.
2. Differences in the heat transfer correlations used within each participant's code. This is especially true for the participants who use proprietary correlations that are specific to U-tube SGs in their codes, as a behaviour of an OTSG is much different than a U-tube SG, and also involves superheat, something U-tube SG users do not have to worry about modelling.
3. Differences in the noding of the SG, which can produce significant differences in the SG behaviour.

As a lot of time was spent making sure that the participants' models for the SG are the same, additional information for the transient SG behaviour was requested and compared in Figures 4.25-4.28. This approach certainly helped to explain the observed differences in the participants' predictions.

Sequence of events

The modelling sequence of events for the MSLB transient is specified in the final specifications and has been discussed at the benchmark workshops and meetings. The double-ended break occurs at 0.001 seconds. It is followed by an immediate closure of the turbine isolation valve of the broken SG and all flow from the broken SG goes out to break. Reactor trip is modelled to occur at the high neutron flux trip set point (with delay of 0.4 seconds) or at the low RCS pressure set point (with a delay of 0.5 seconds). The turbine trip begins at the reactor trip. At the turbine trip the turbine isolation valve for the intact SG closes with a closure time of 0.5 seconds. With increasing pressure in the intact steam line some of the safety relief valves (MSSVs) will open and subsequently close at the set points, defined in the final specification. High pressure injection (HPI) occurs when the primary system pressure drops to the defined set point with a 25 second delay.

Looking at Table B.1 of Appendix B it can be seen that there are variations among the participants in interpreting the modelling sequence of events. Some participants initiate the break at 0.01 seconds. Further, there are different interpretations of the time of the turbine trip and the closure of the turbine isolation valve for the intact SG. Some participants interpret the time of reactor trip as the time when

the trip condition is reached, while others are consider the time when the reactor scram begins, i.e. taking into account the delay. While these misinterpretations may not be significant, they contribute to the differences of the participants' predictions at the beginning of the transient. Later into the transient all the participants see a rise in power, twelve of them see a return to power and five of them (NETCorp, British Energy, Rossendorf, IPSN/CEA and Purdue/NRC) also see a return to criticality.

In summary the explanation of differences in the transient chronology predicted by participants is quite complex. The main parameter seems to be the broken SG break flow rate but the differences result from many other parameters, as was discusses above. These factors include break flow correlation, SG nodalisation, steam line pressure drop, liquid entrainment model, steam-liquid interface friction model, primary to secondary heat transfer calculation, primary flow rate and core mixing assumptions.

Figure 4.1. Total break flow rate

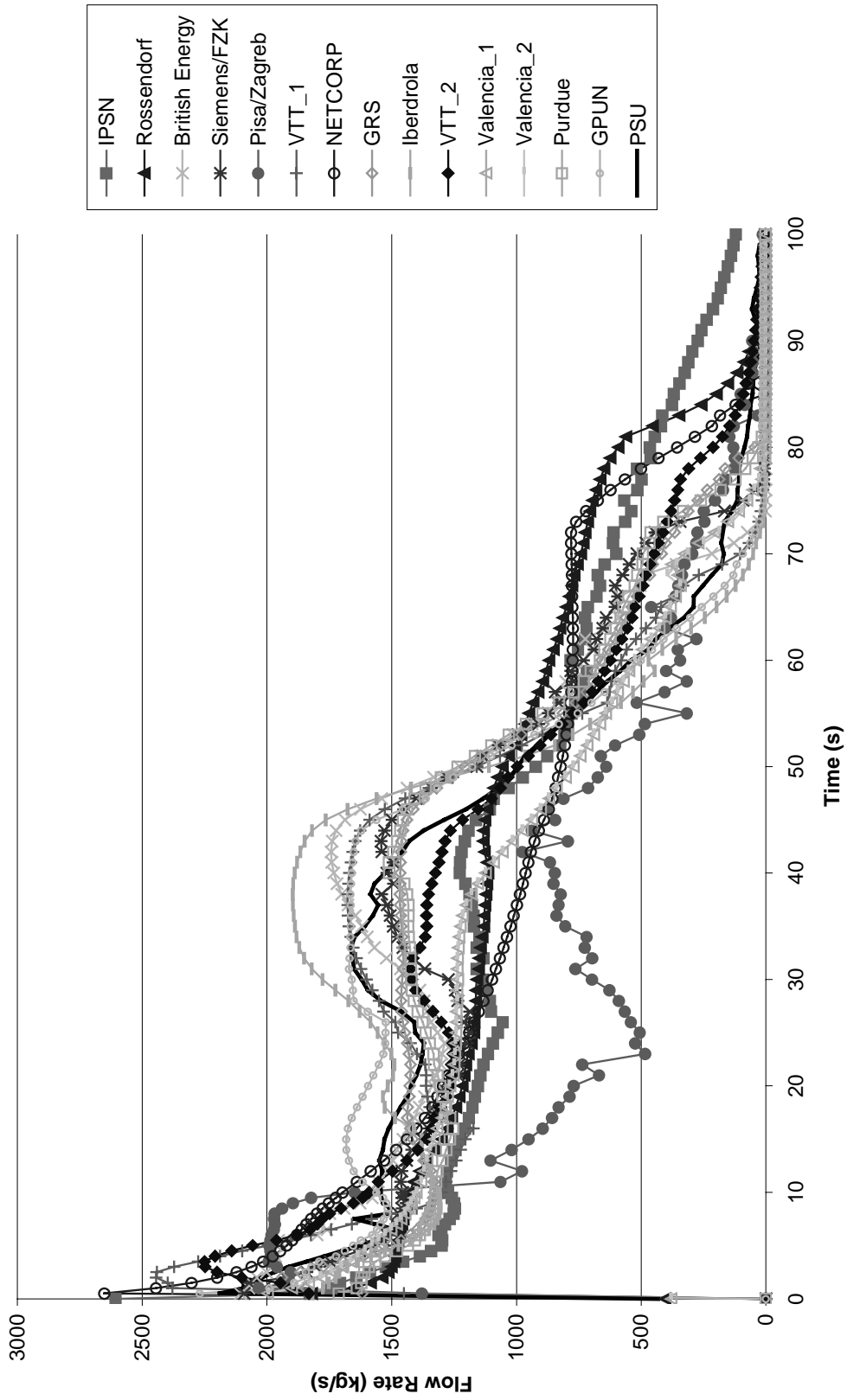


Figure 4.2. Break flow rate – 24 inch

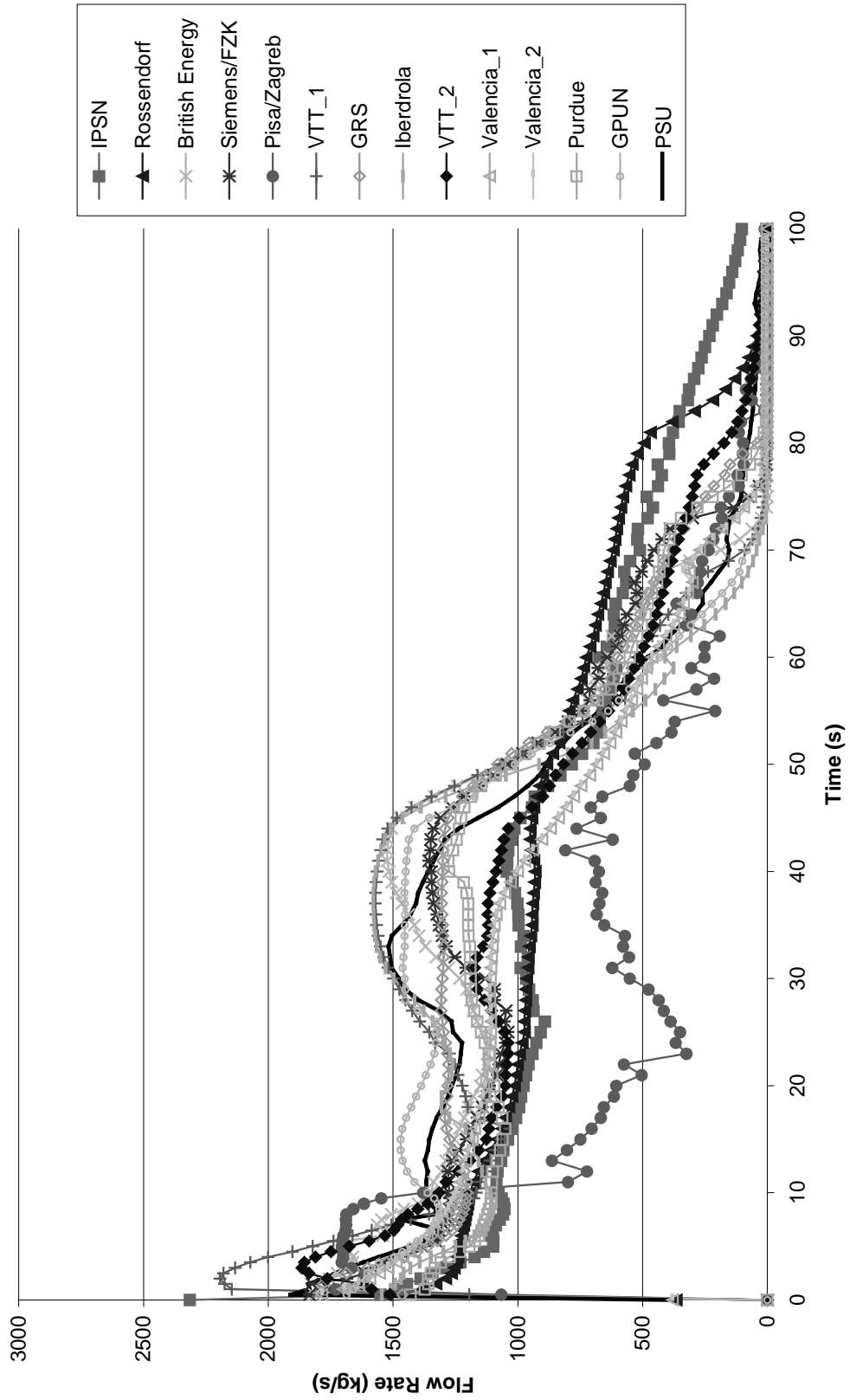


Figure 4.3. Break flow rate – 8 inch

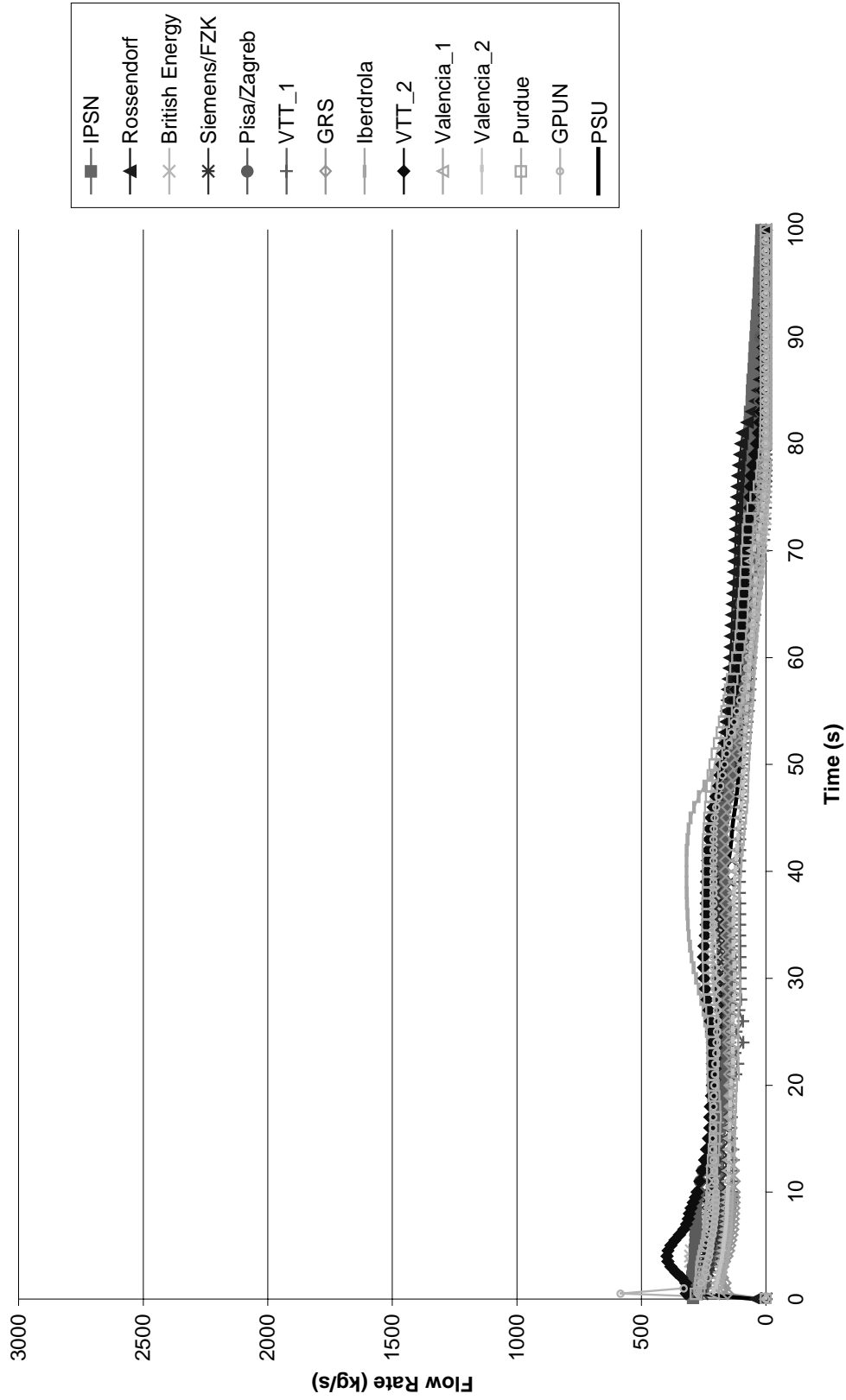


Figure 4.4. Average pressure

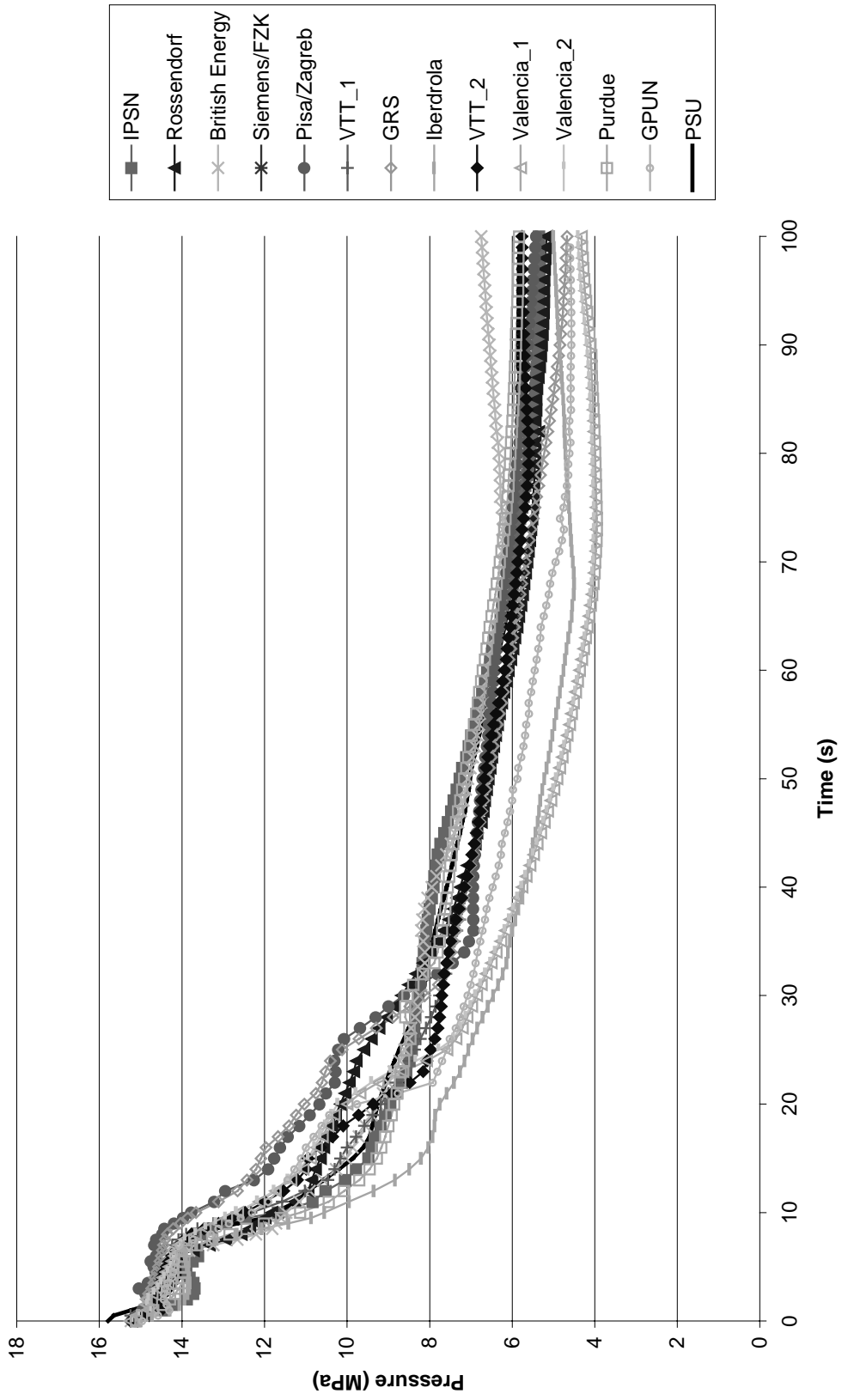


Figure 4.5. Broken loop pressure

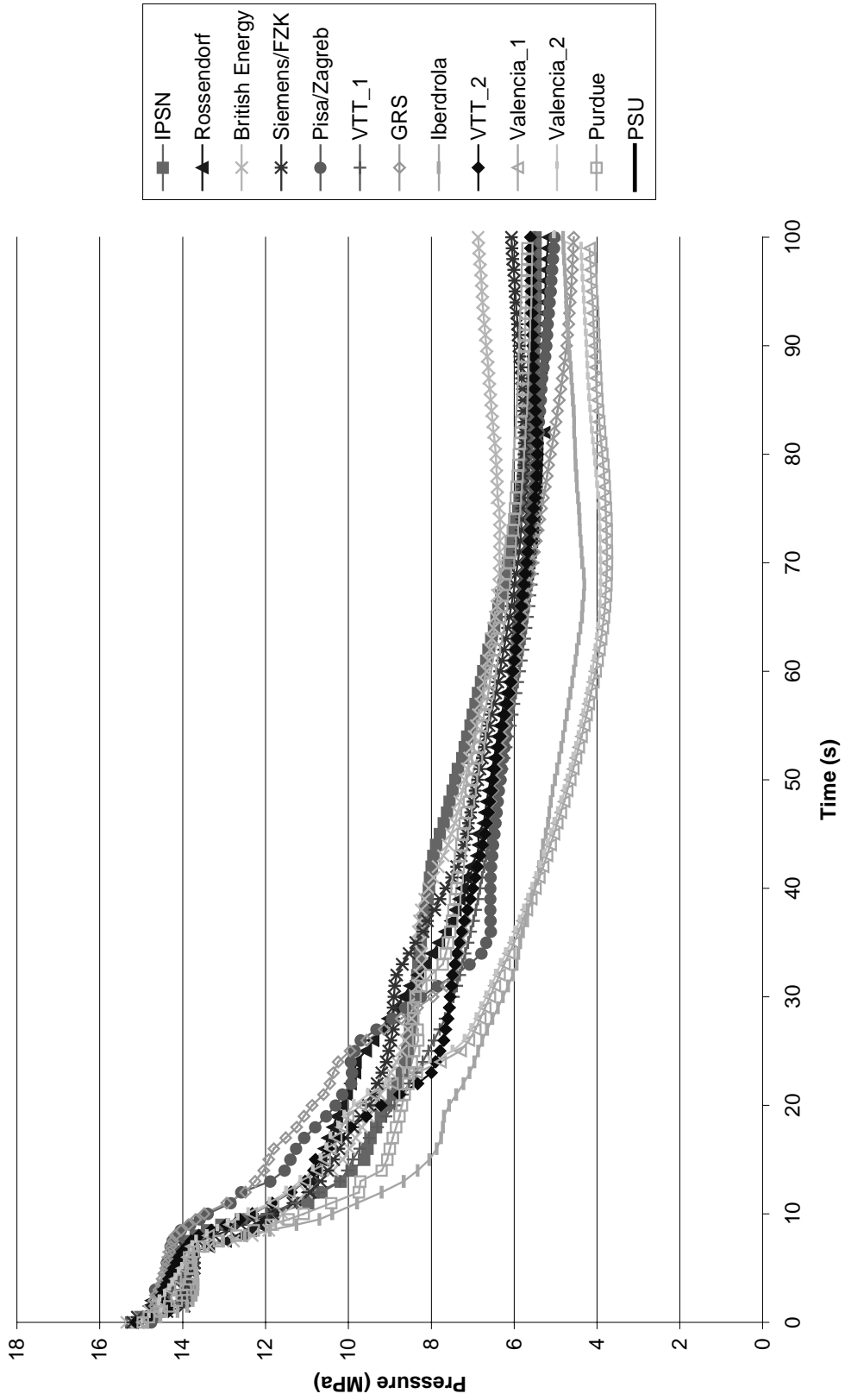


Figure 4.6. Intact loop pressure

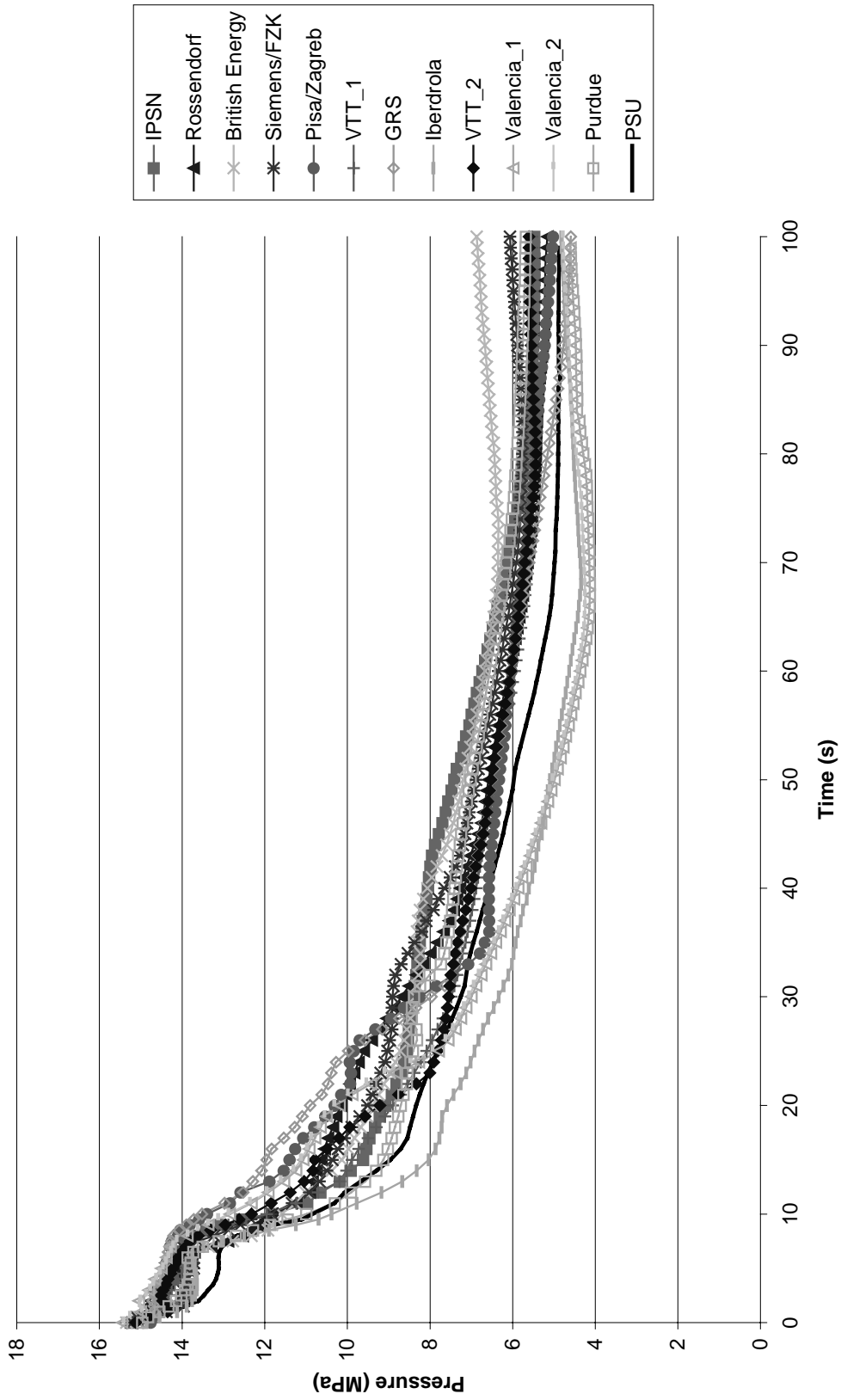


Figure 4.7. Pressuriser pressure

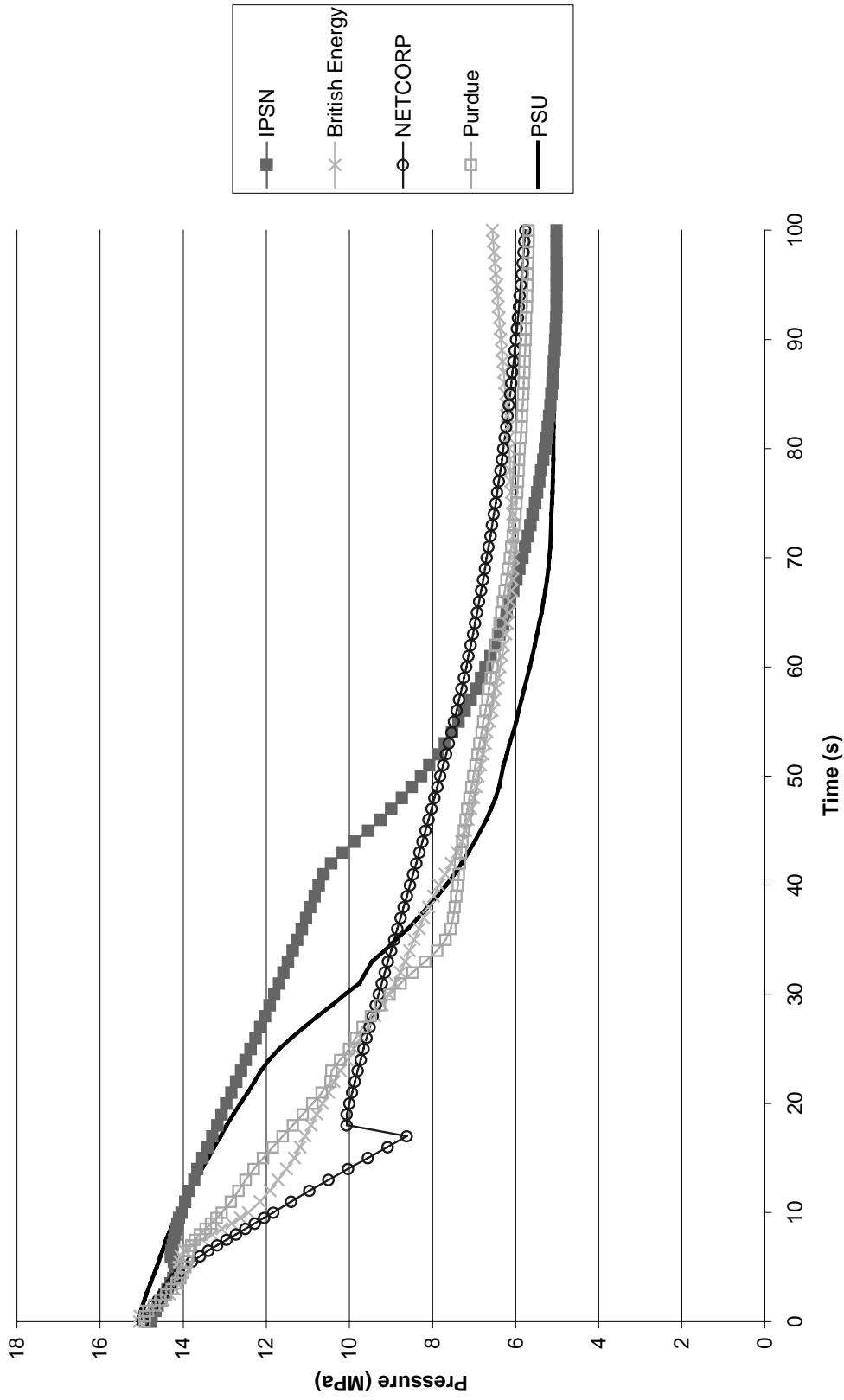


Figure 4.8. Broken steam line pressure

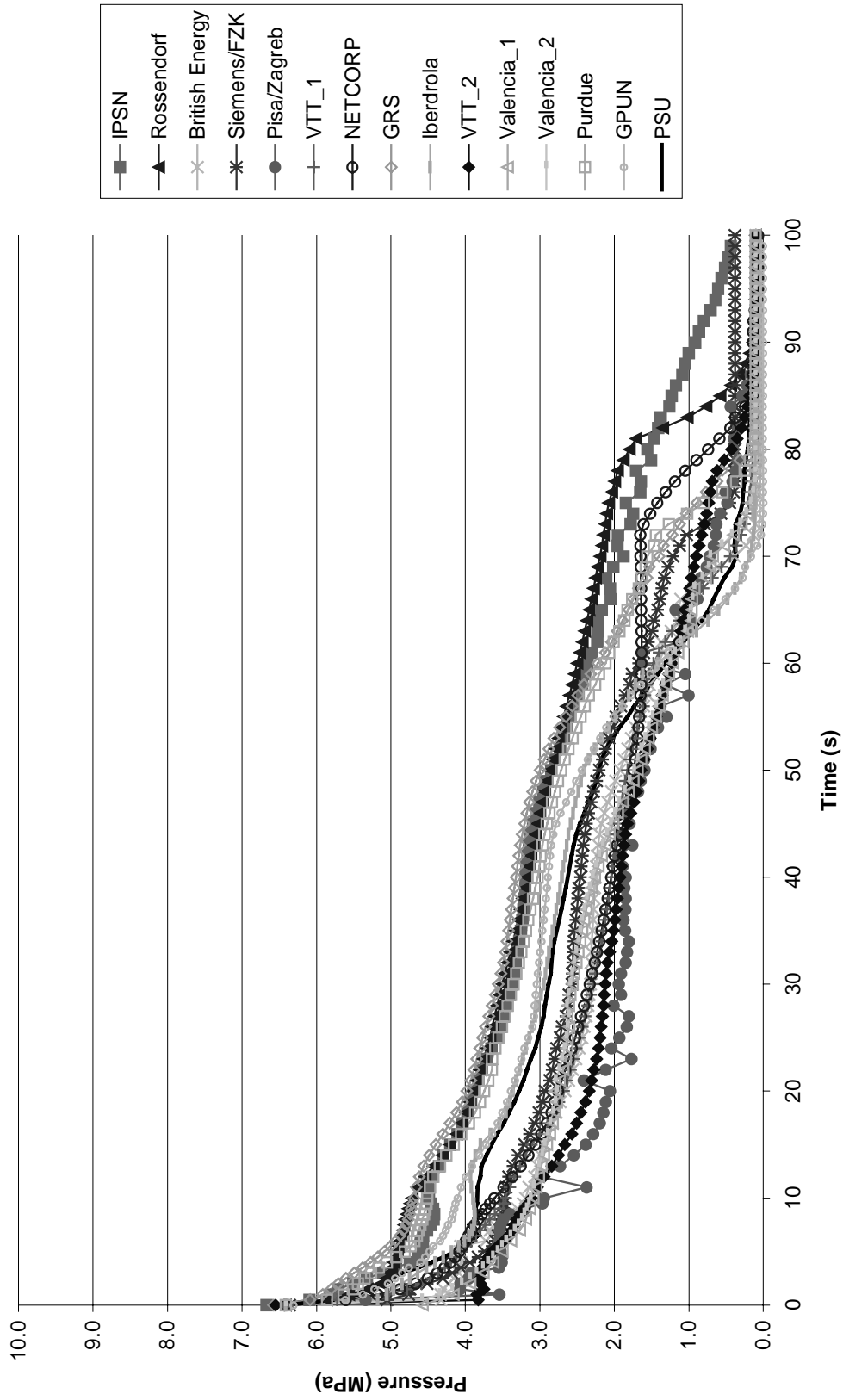


Figure 4.9. Intact steam line pressure

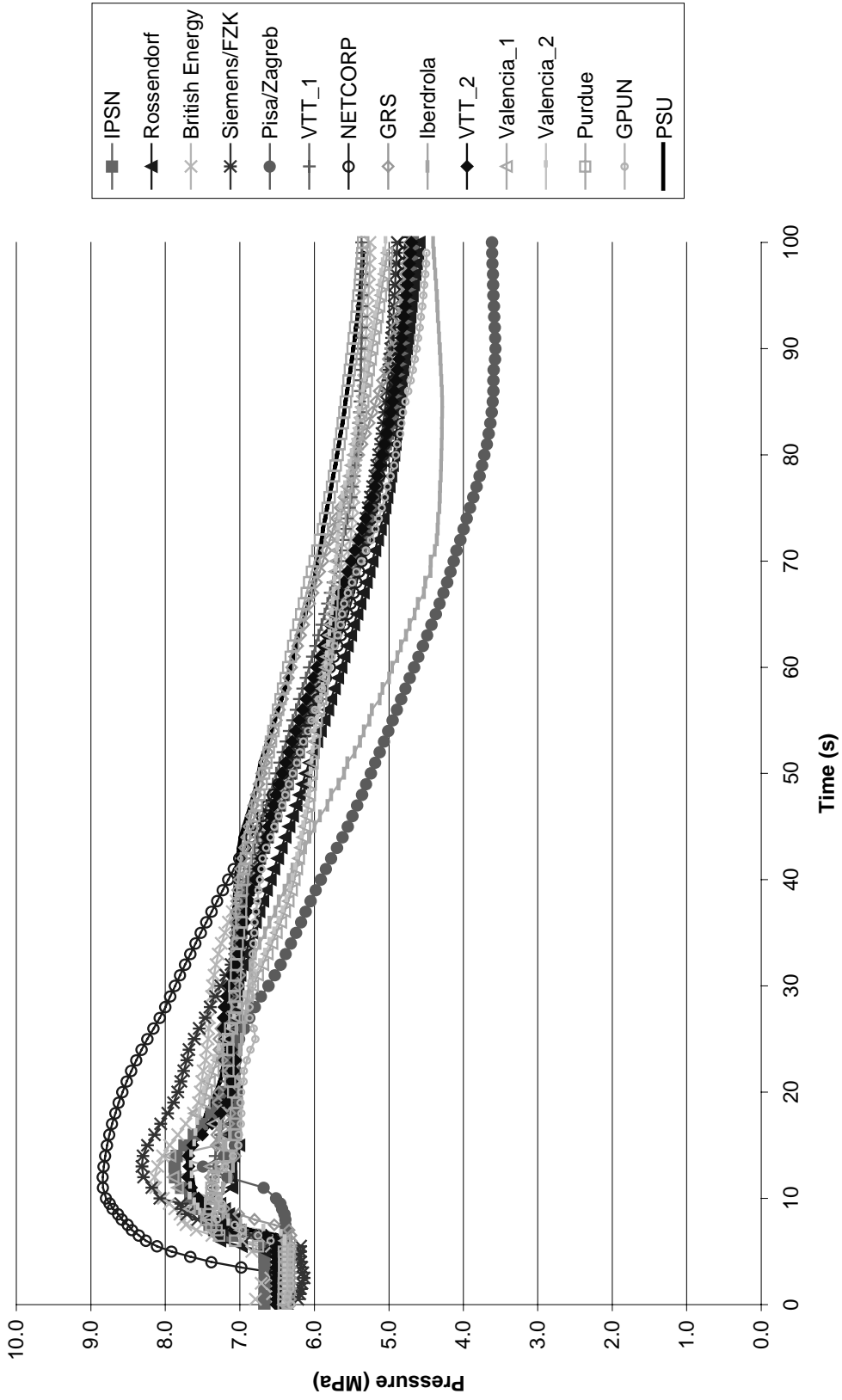


Figure 4.10. Average coolant temperature

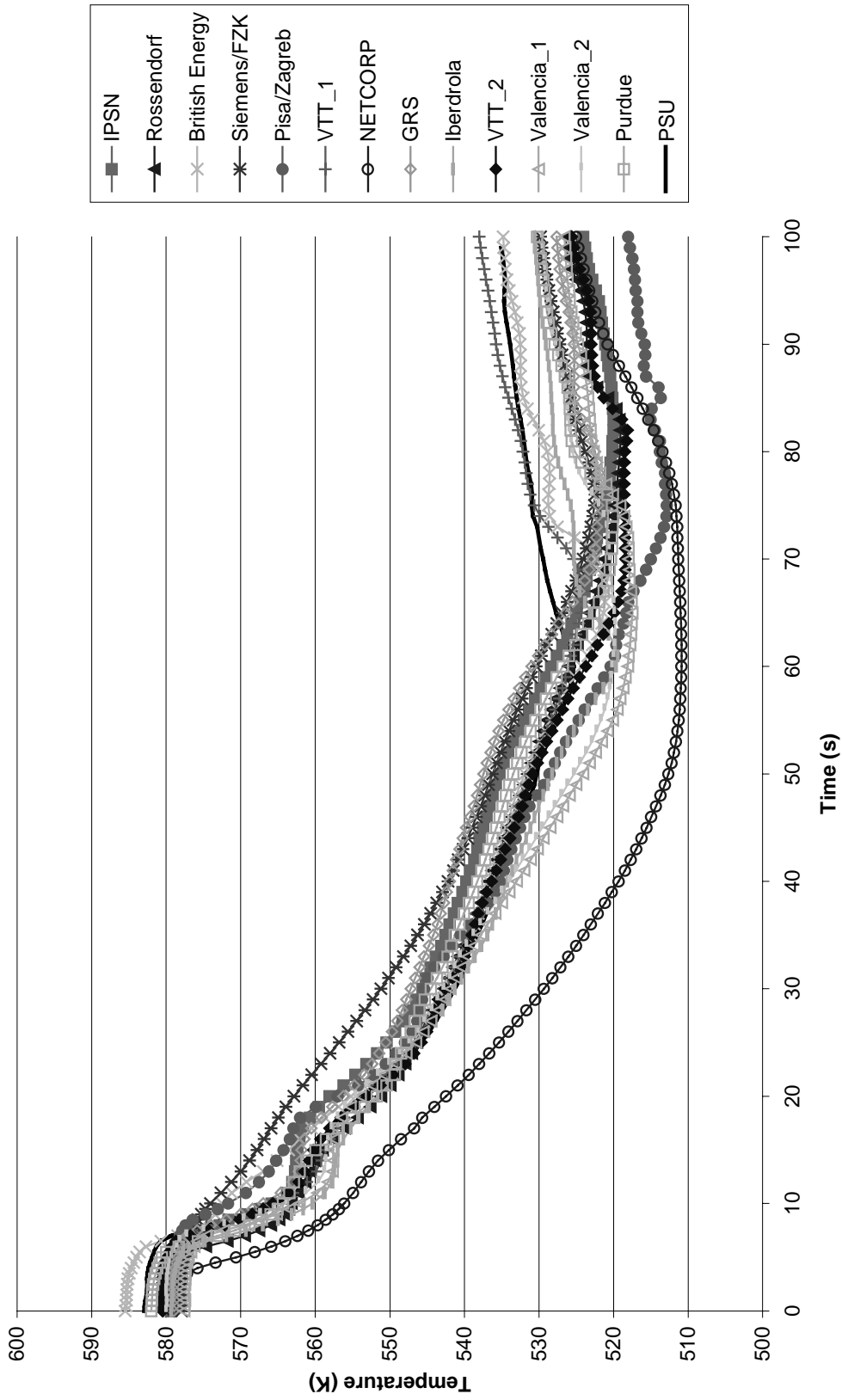


Figure 4.11. Broken hot leg temperature

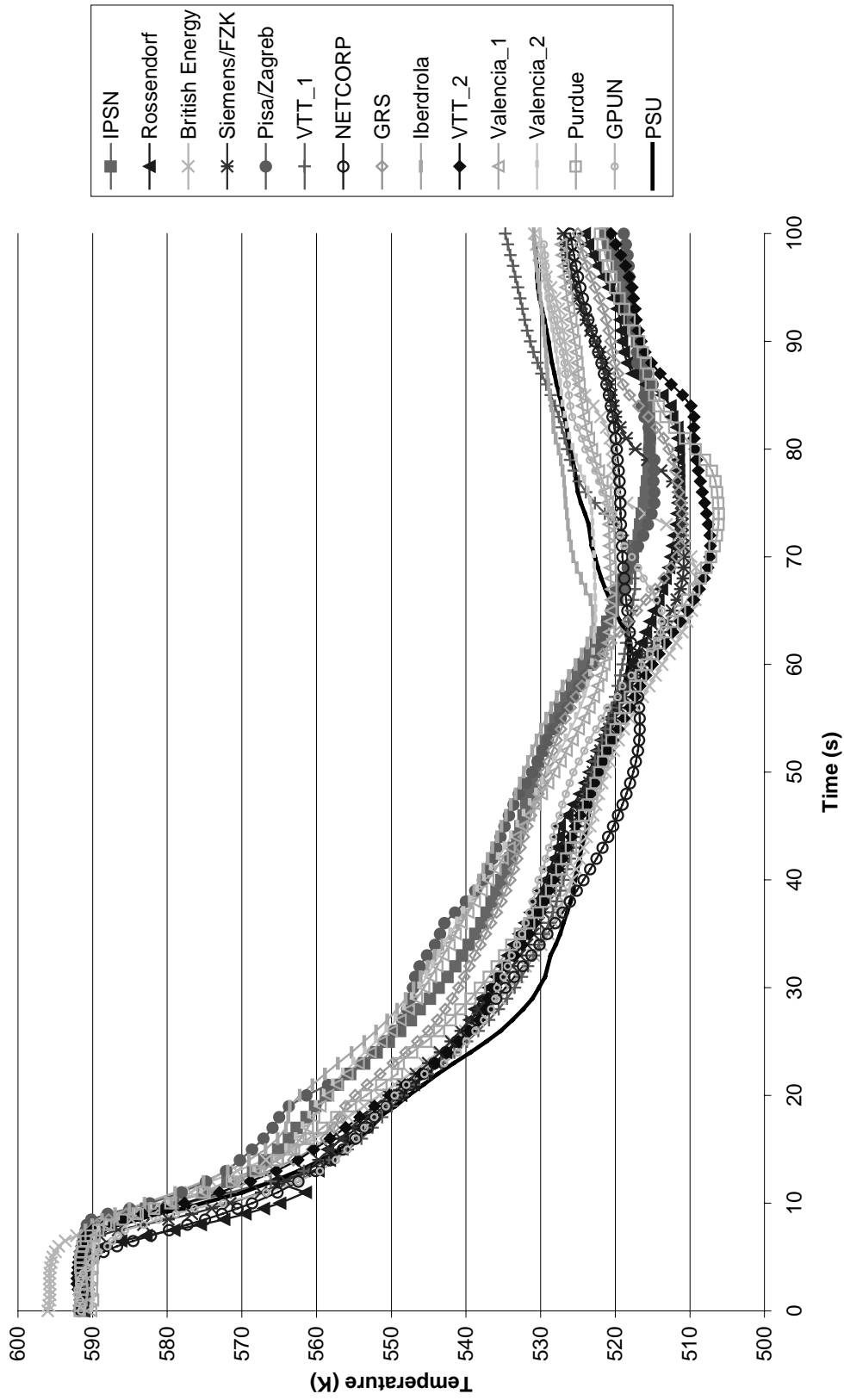


Figure 4.12. Intact hot leg temperature

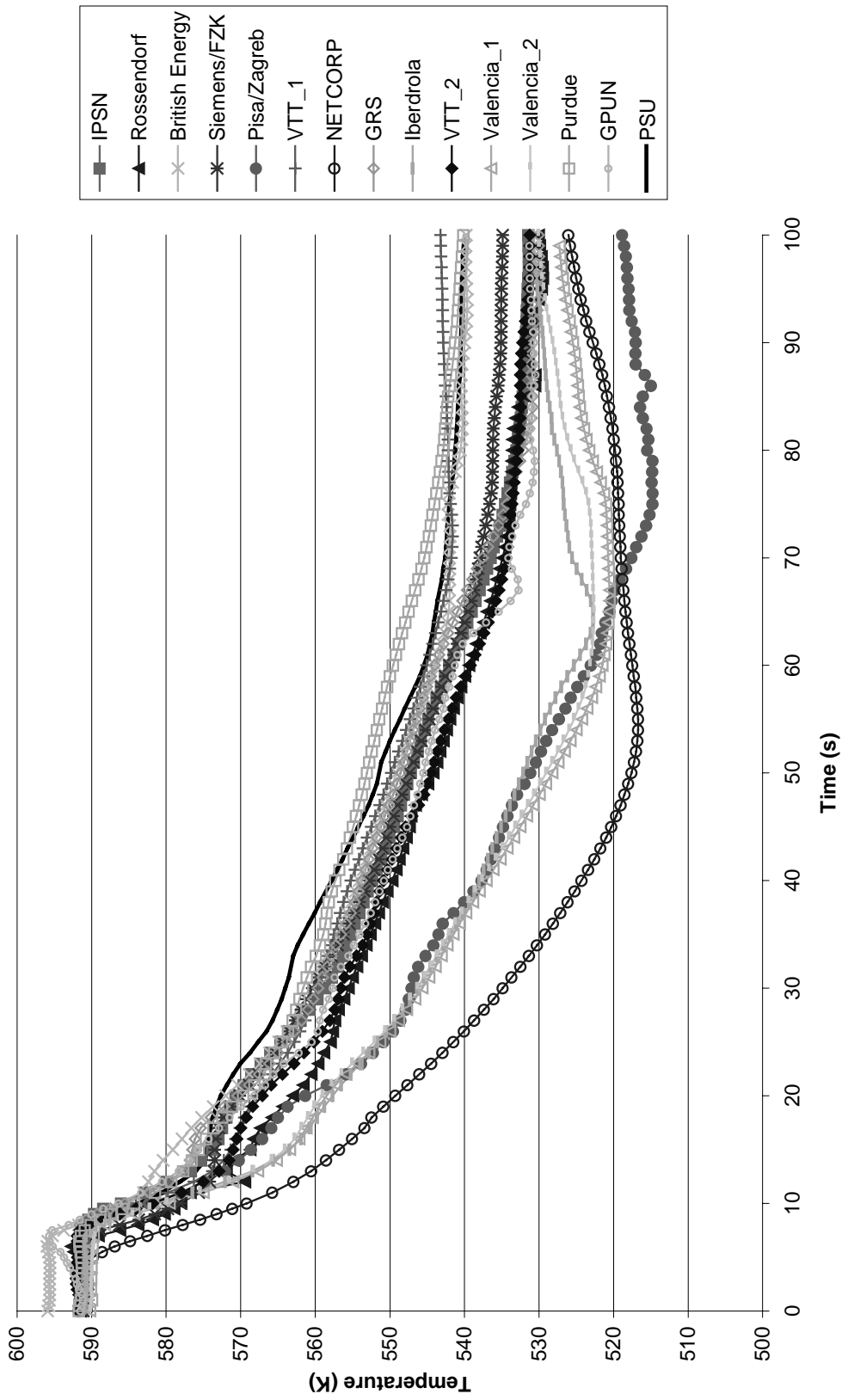


Figure 4.13. Broken cold leg temperature

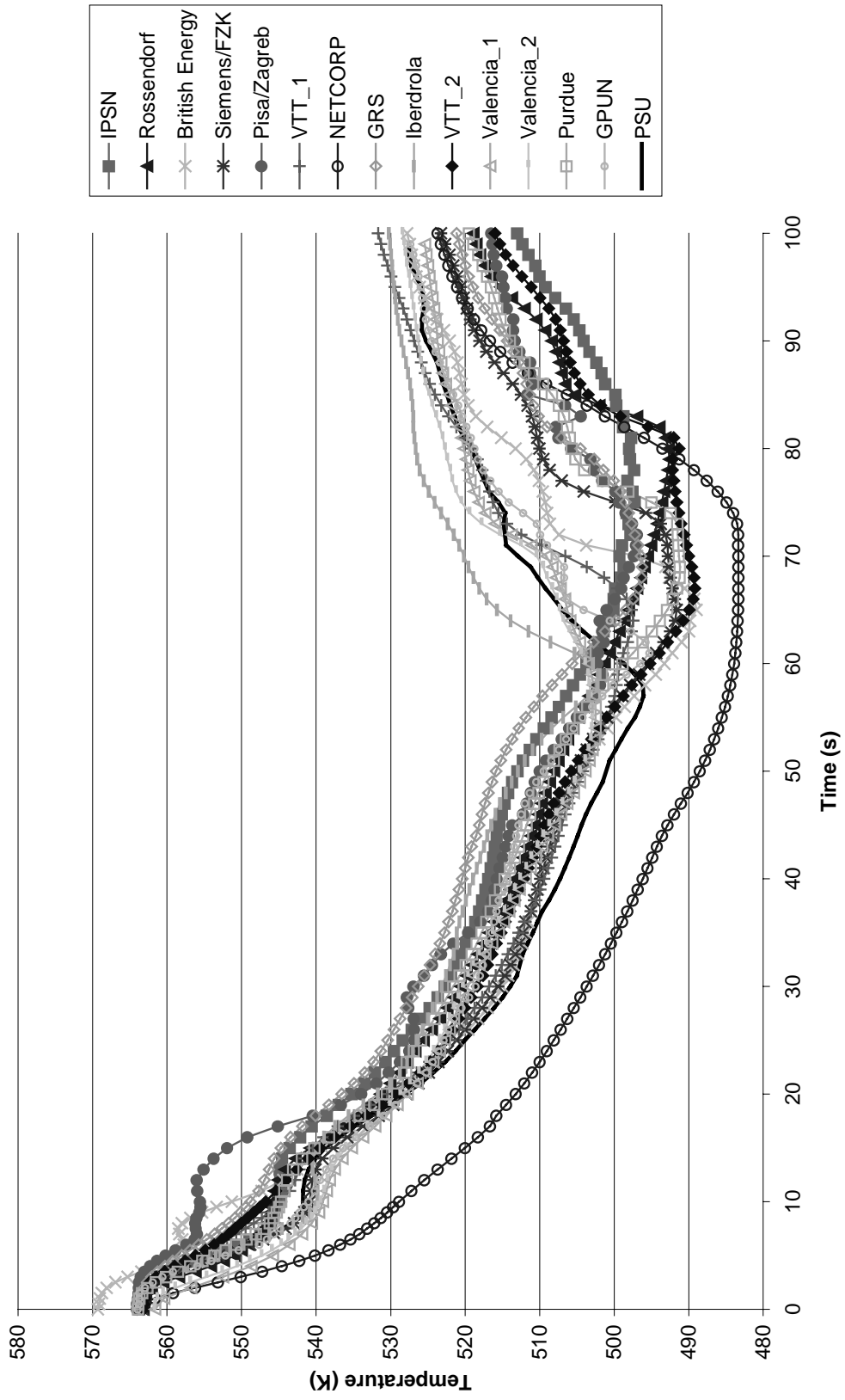


Figure 4.14. Intact cold leg temperature

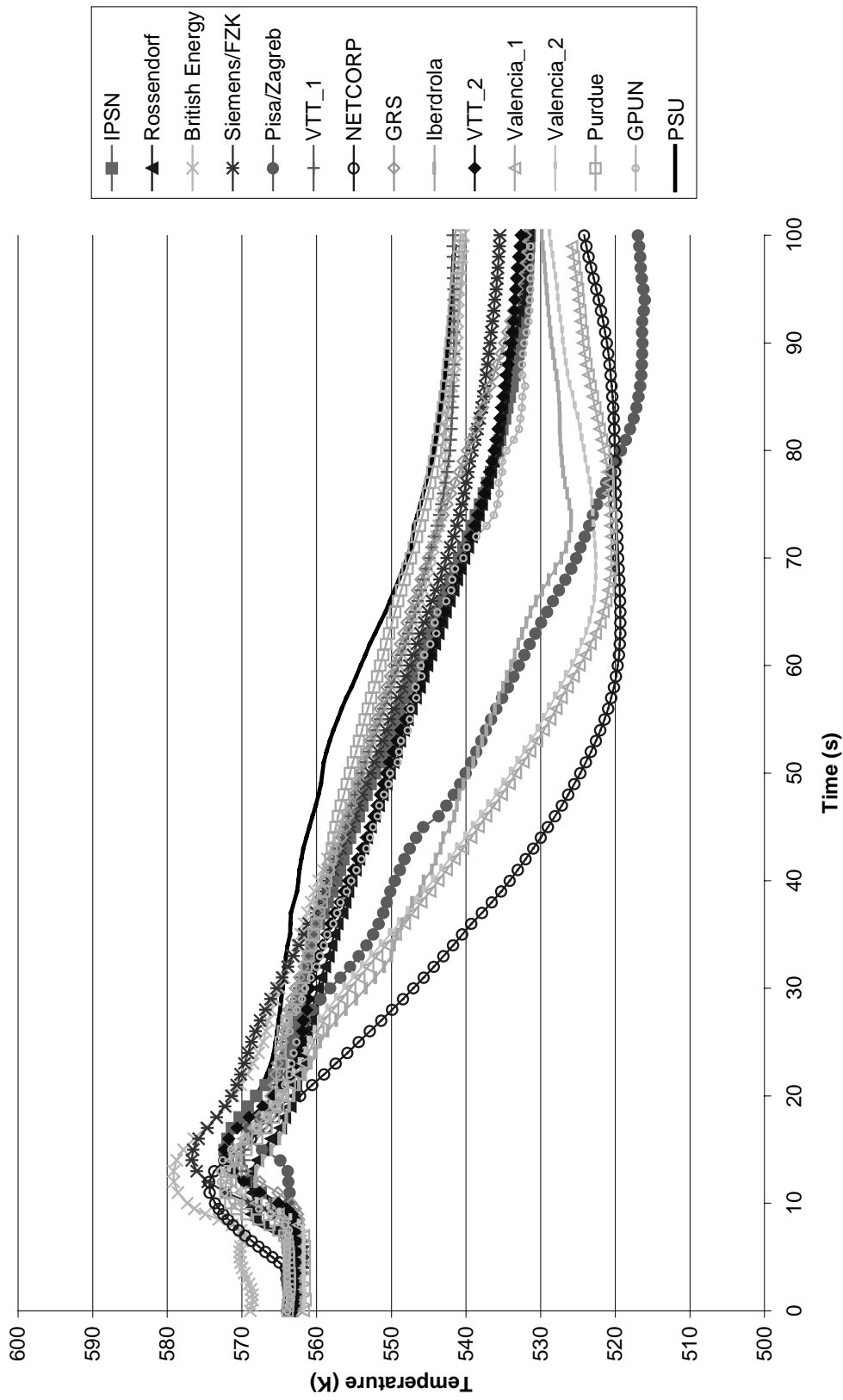


Figure 4.15. Fuel temperature

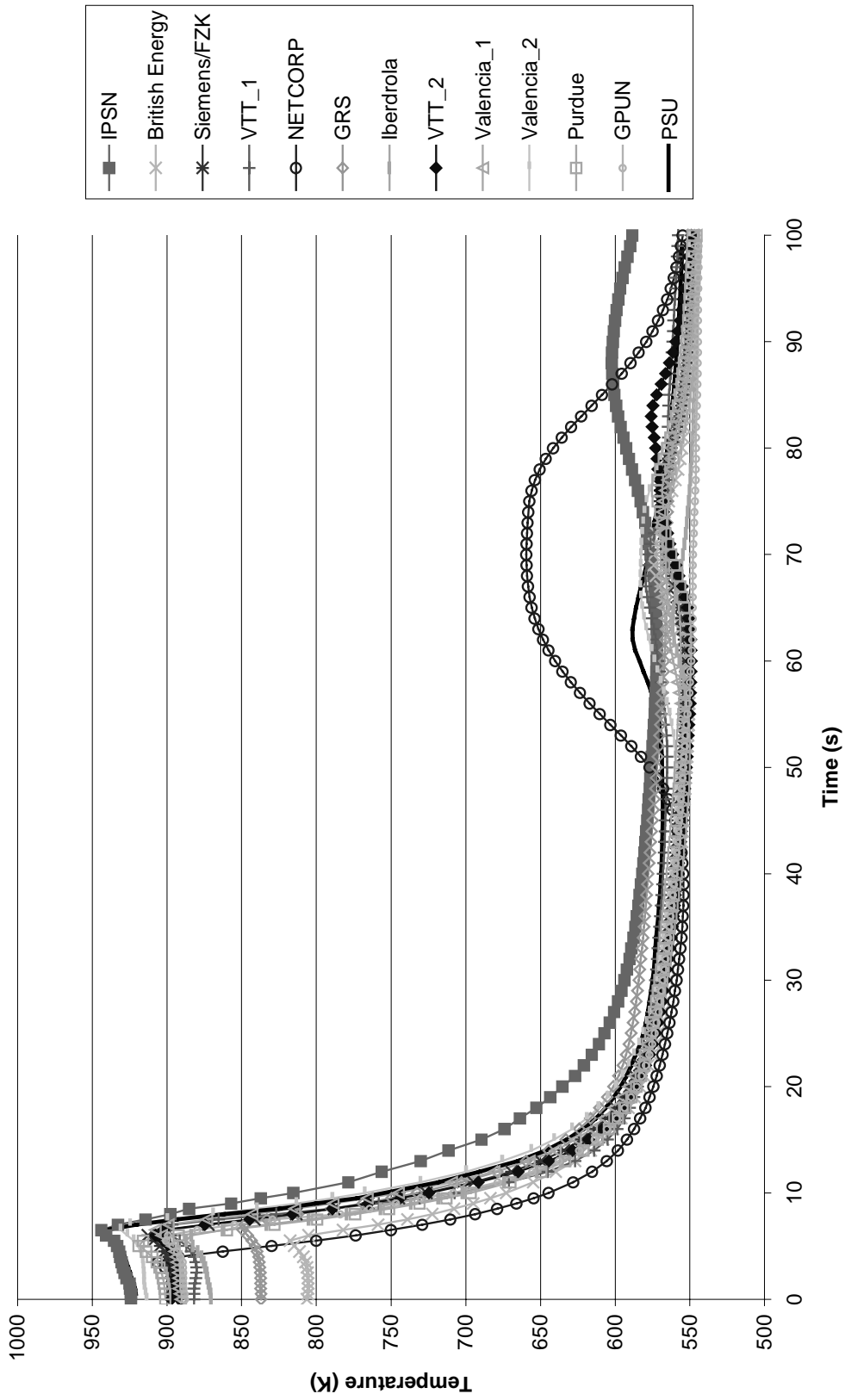


Figure 4.16. Fission power

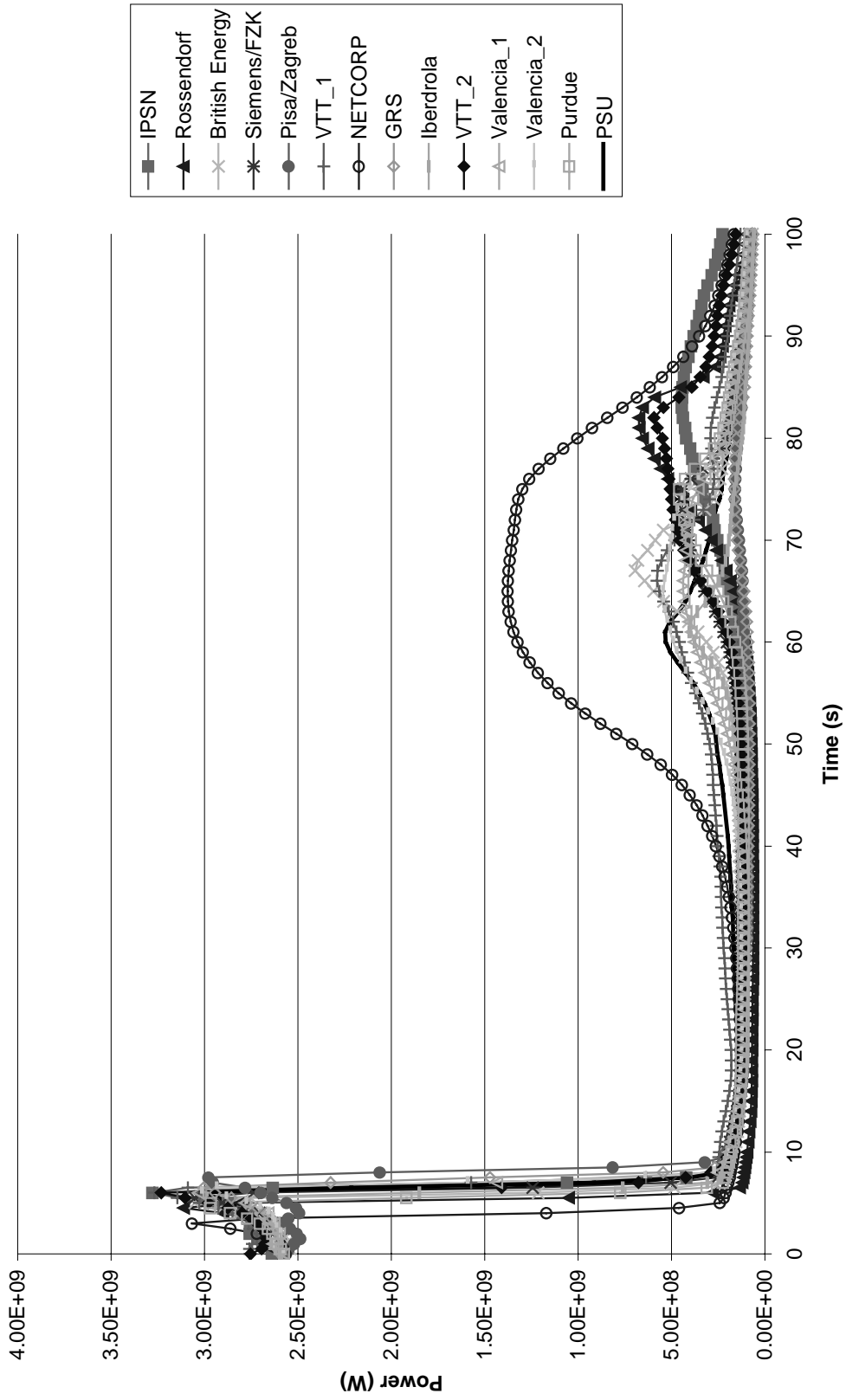


Figure 4.17. Total power

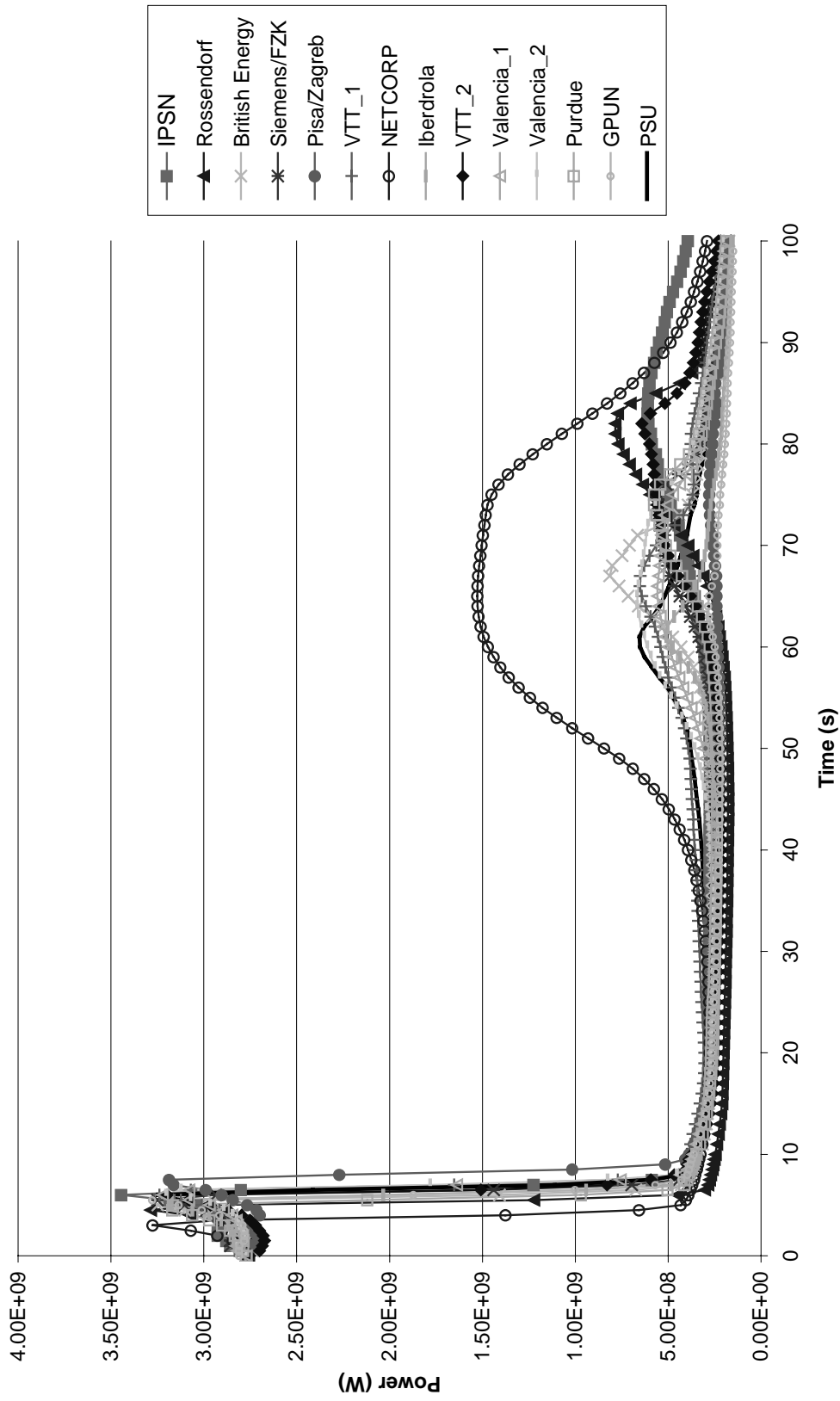


Figure 4.18. Decay power

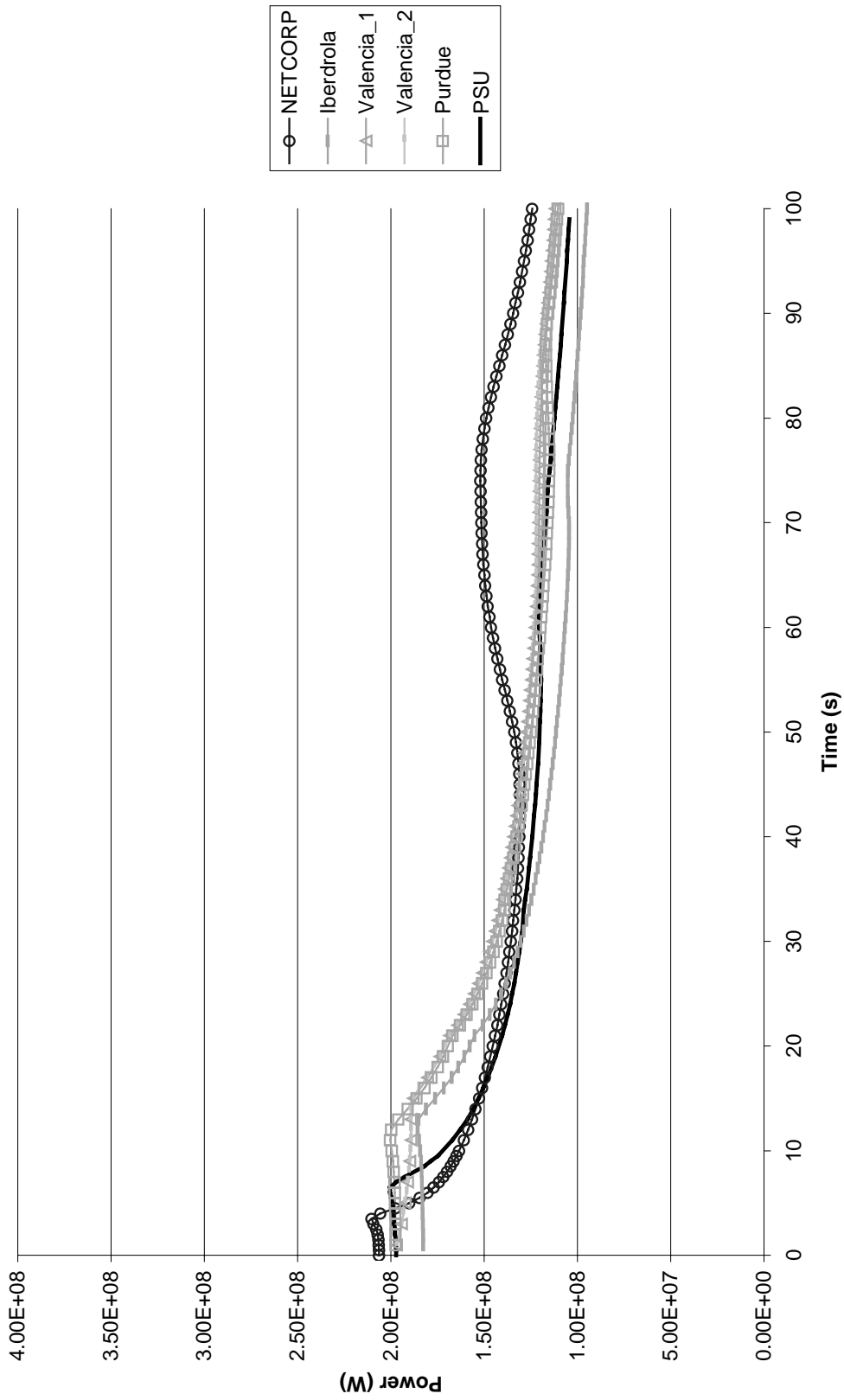


Figure 4.19. Total reactivity

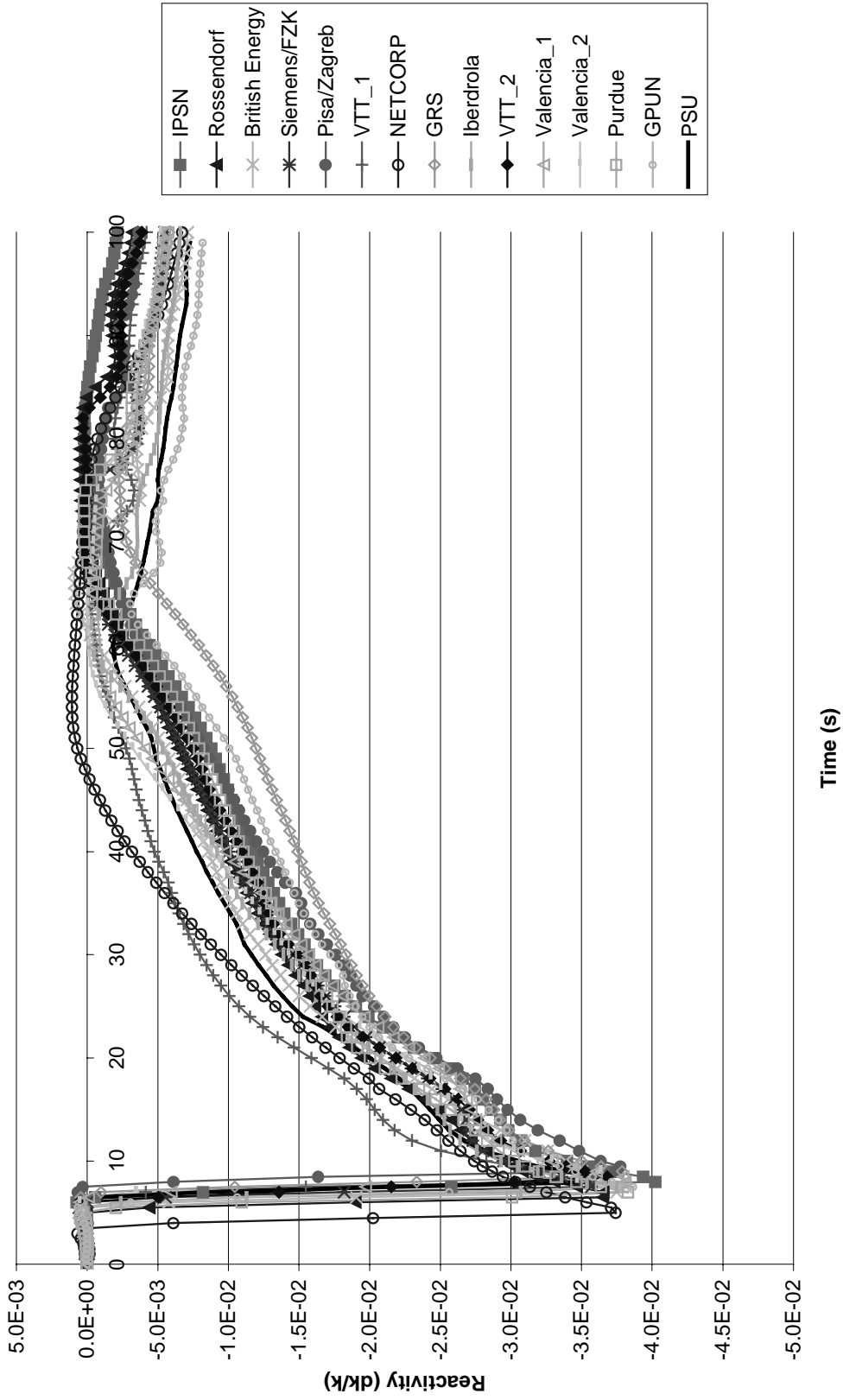


Figure 4.20. Moderator reactivity

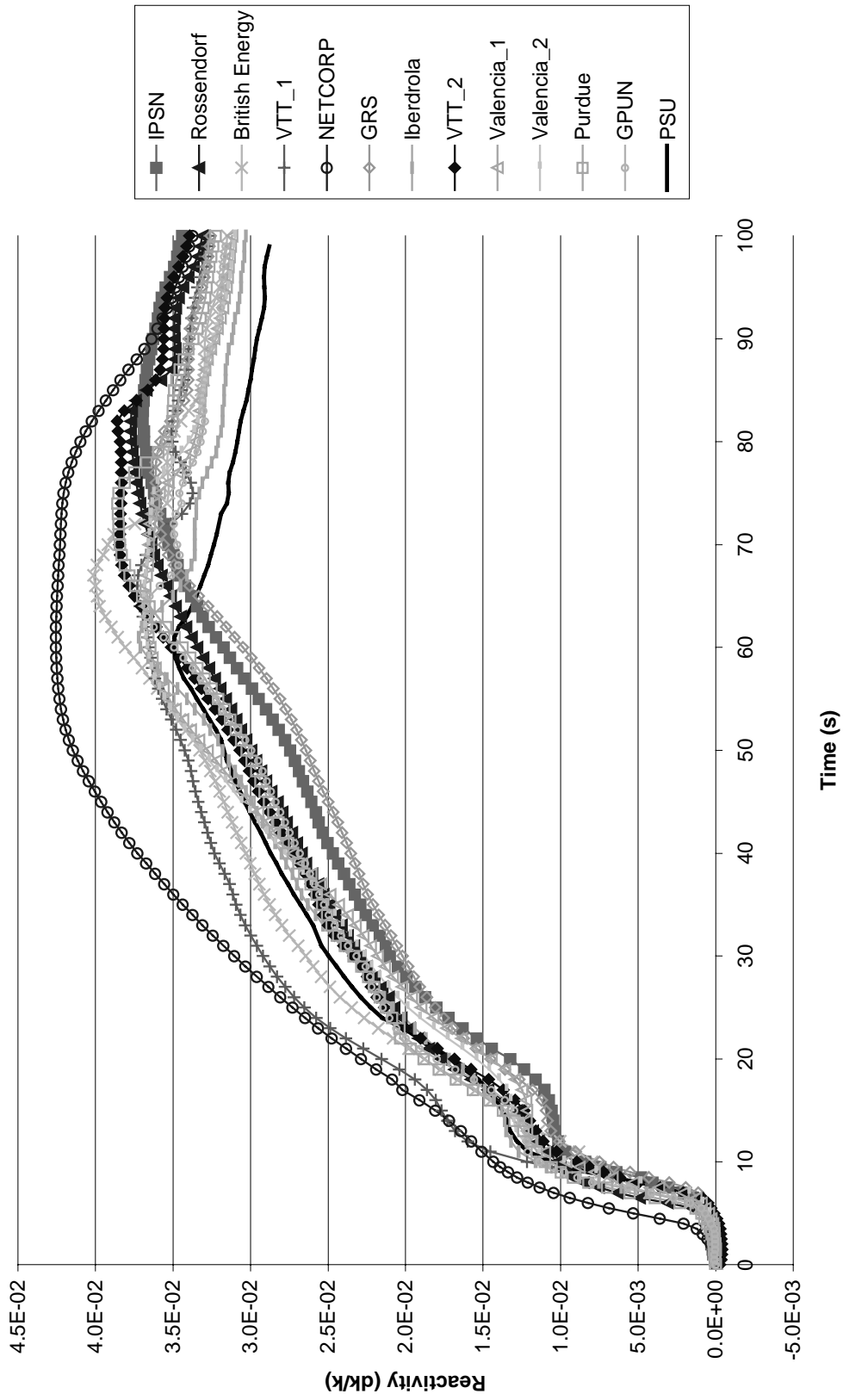


Figure 4.21. Doppler reactivity

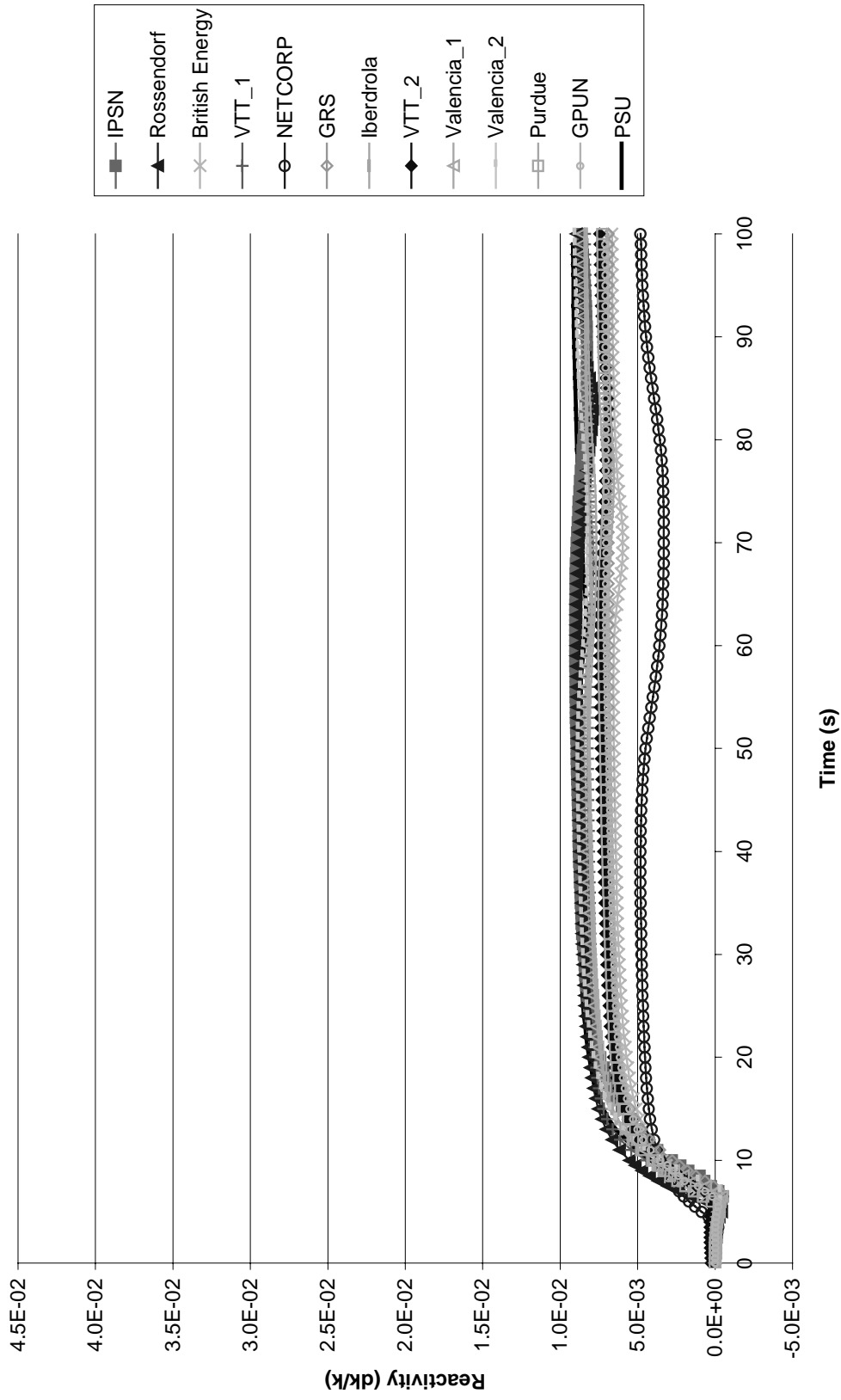


Figure 4.22. Scram reactivity

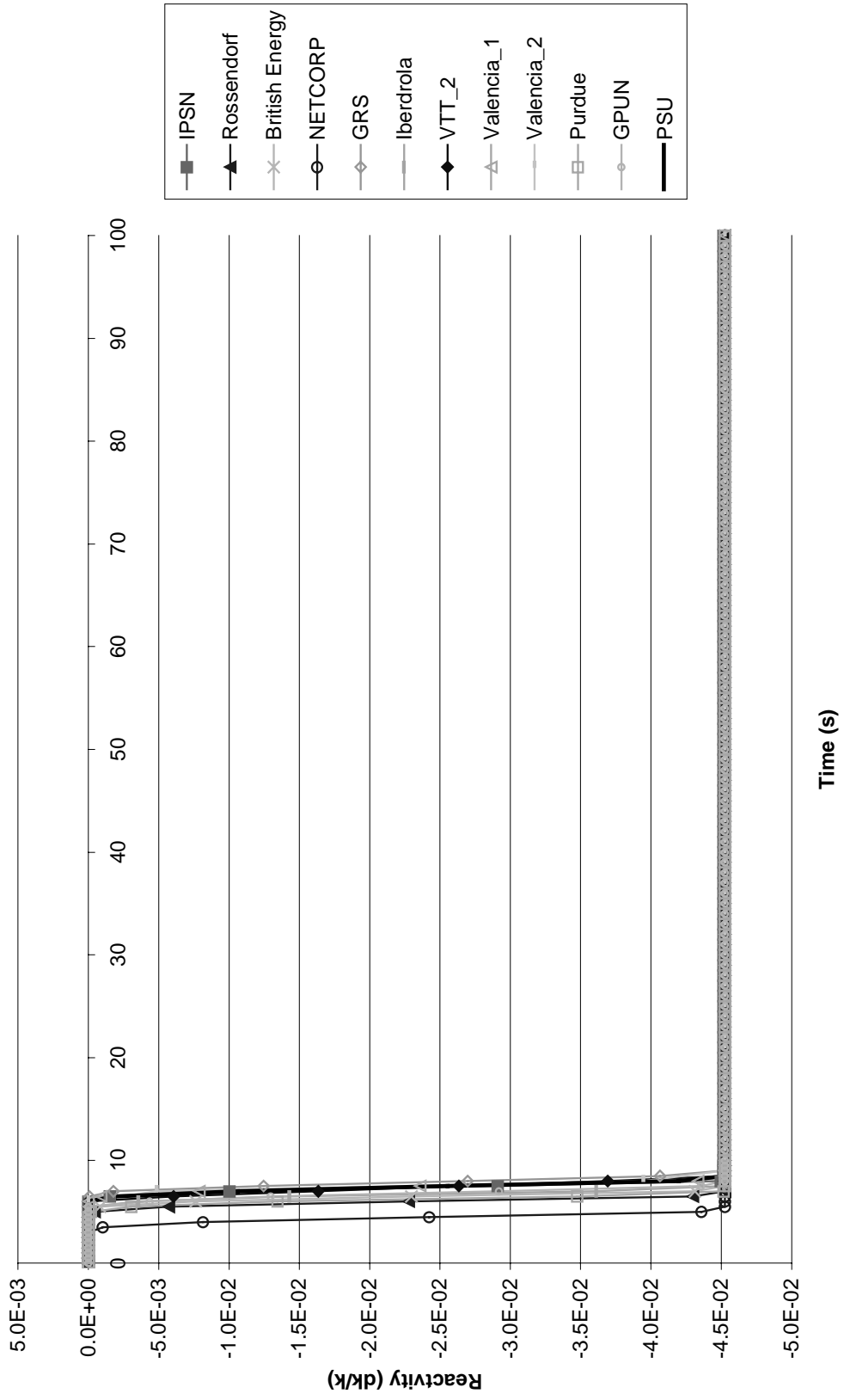


Figure 4.23. Broken steam generator mass

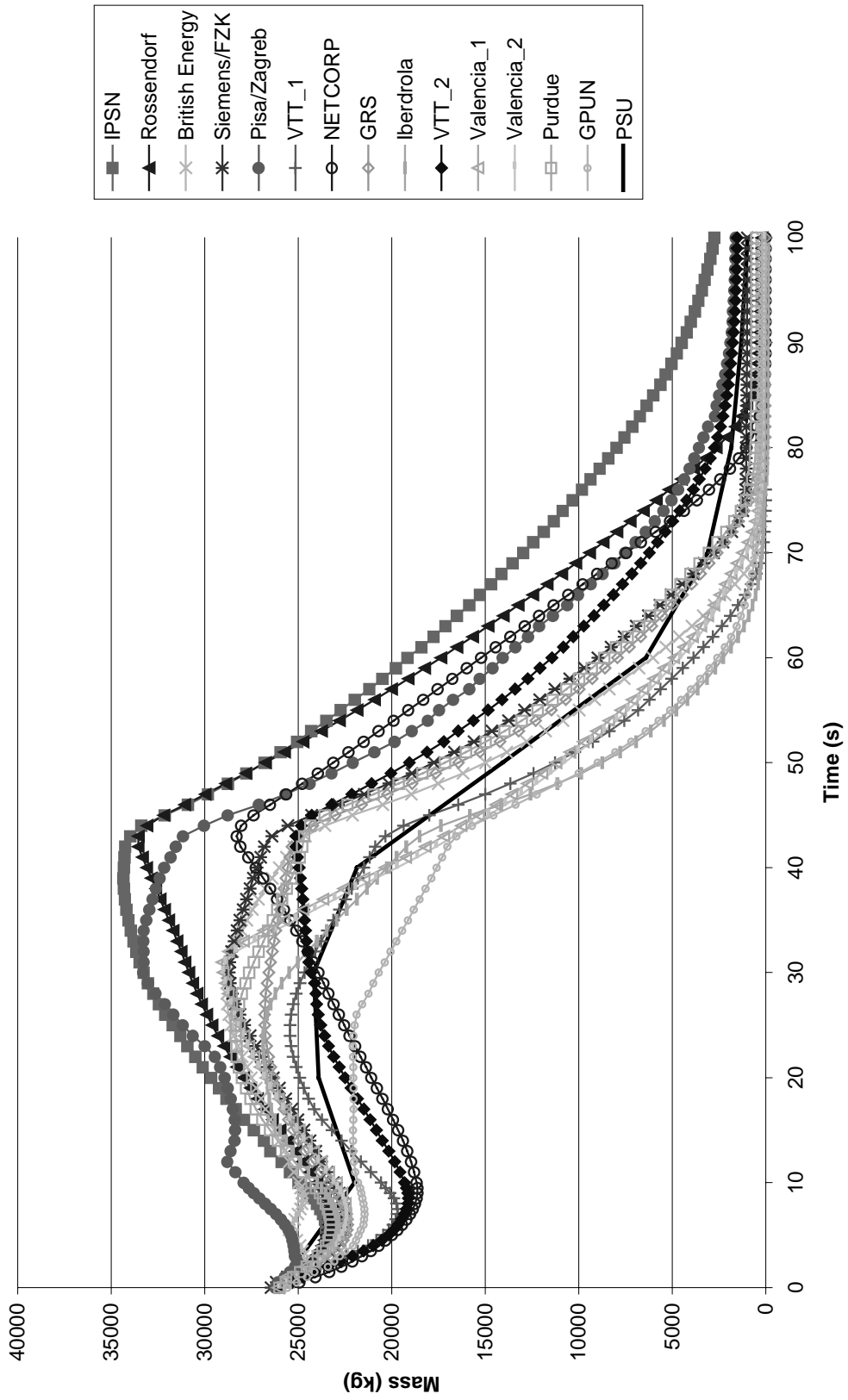


Figure 4.24. Intact steam generator mass

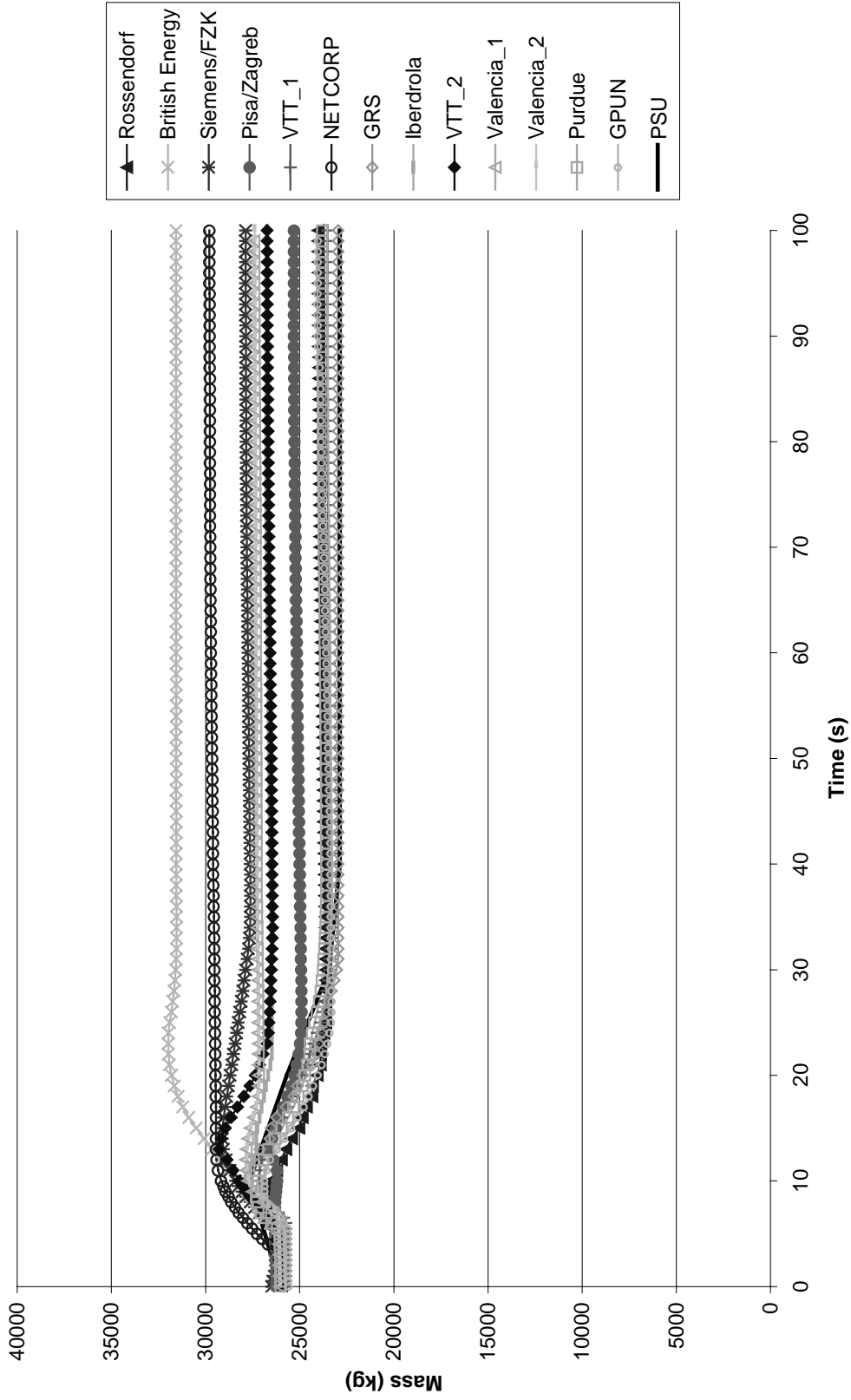


Figure 4.25. Heat transfer: broken steam generator

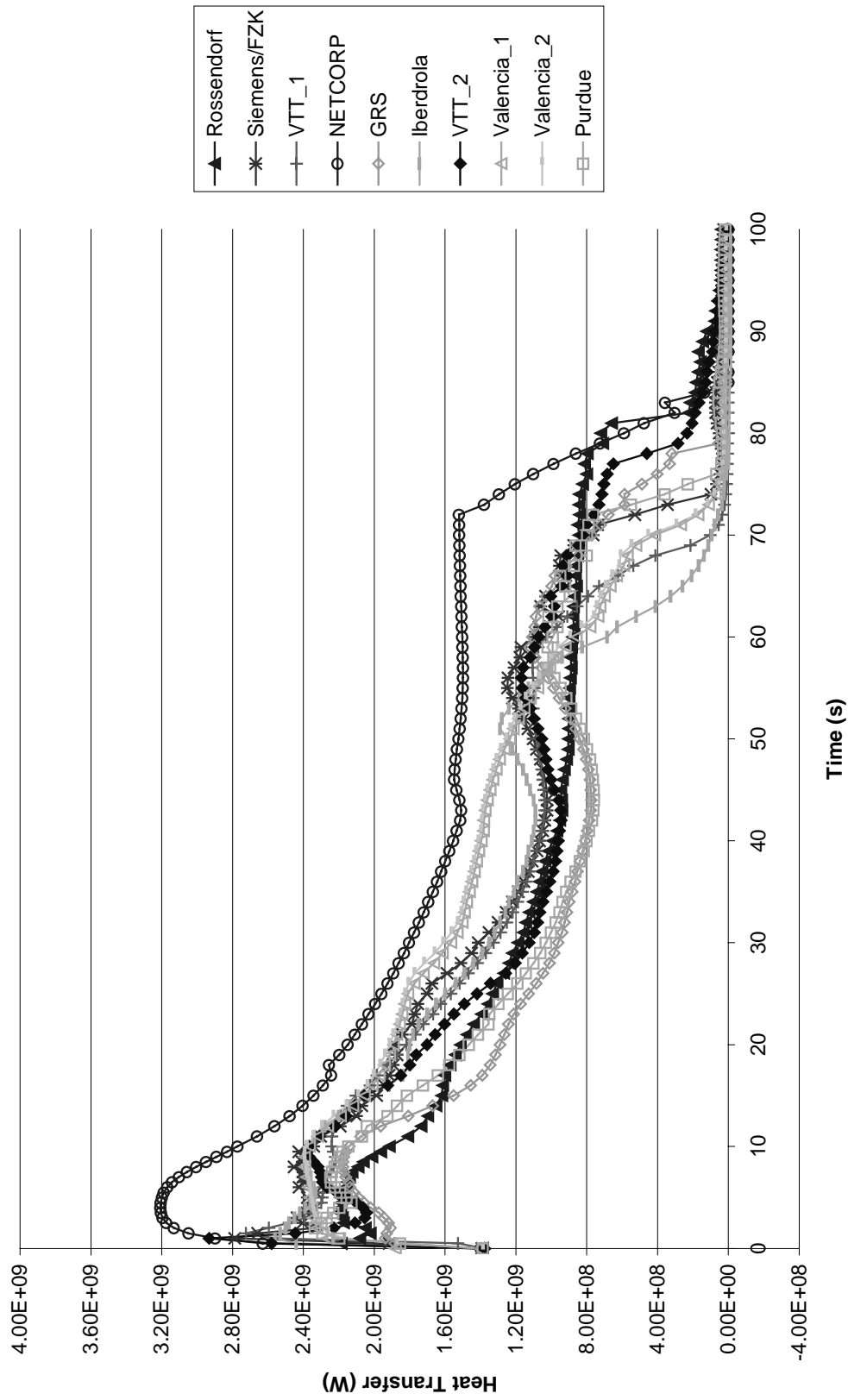


Figure 4.26. Heat transfer: intact steam generator

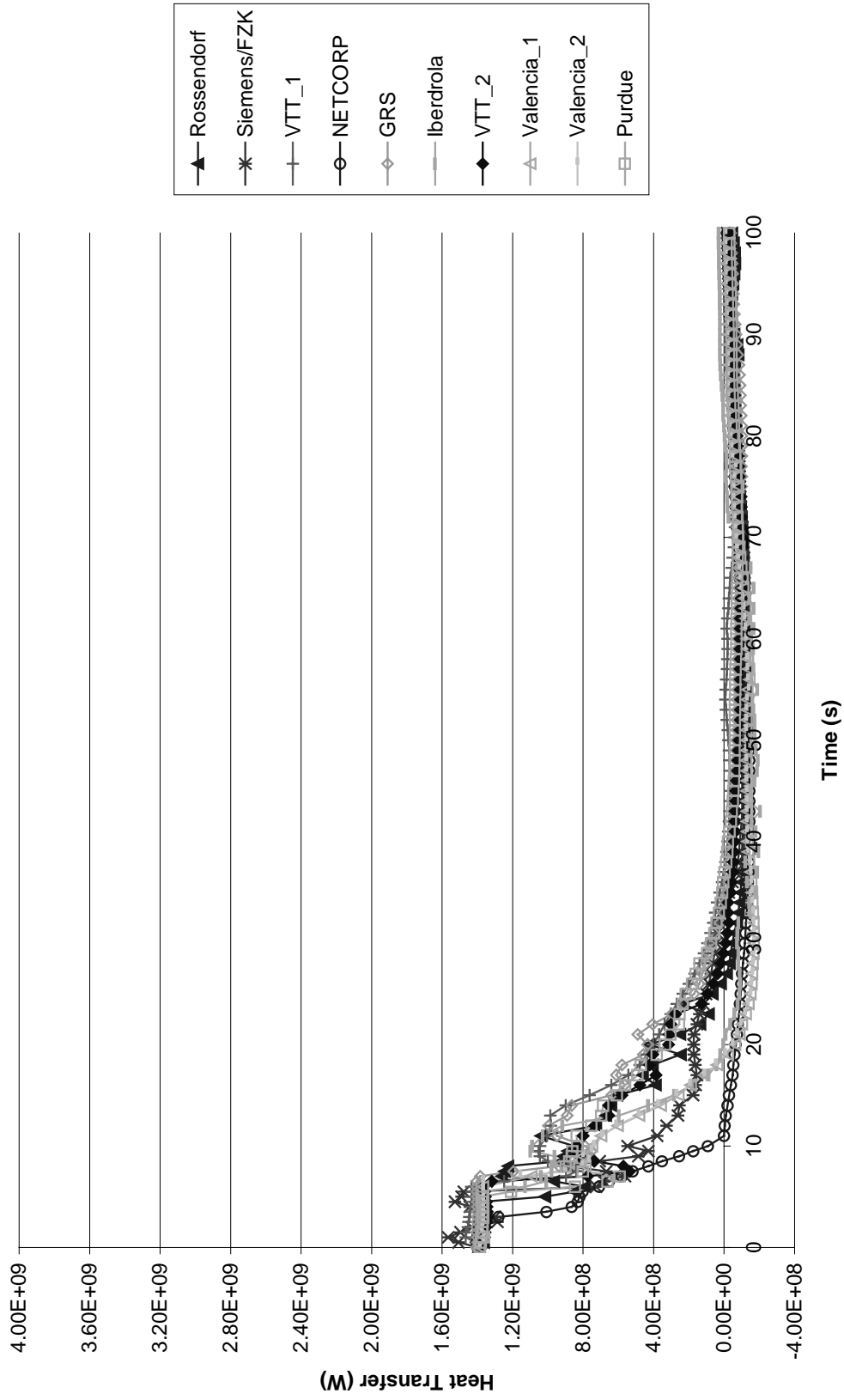


Figure 4.27. Integrated leakage: vapour mass

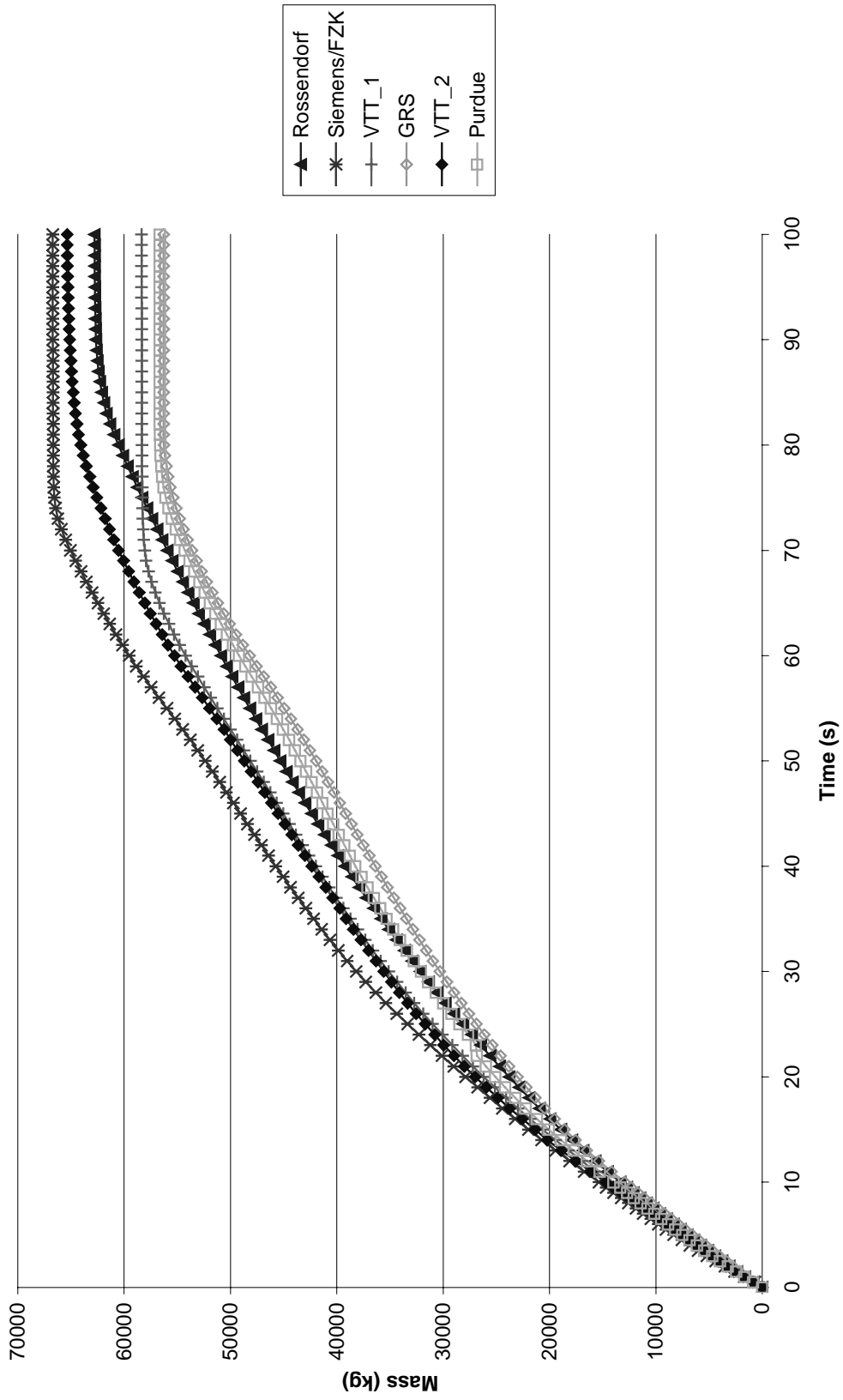
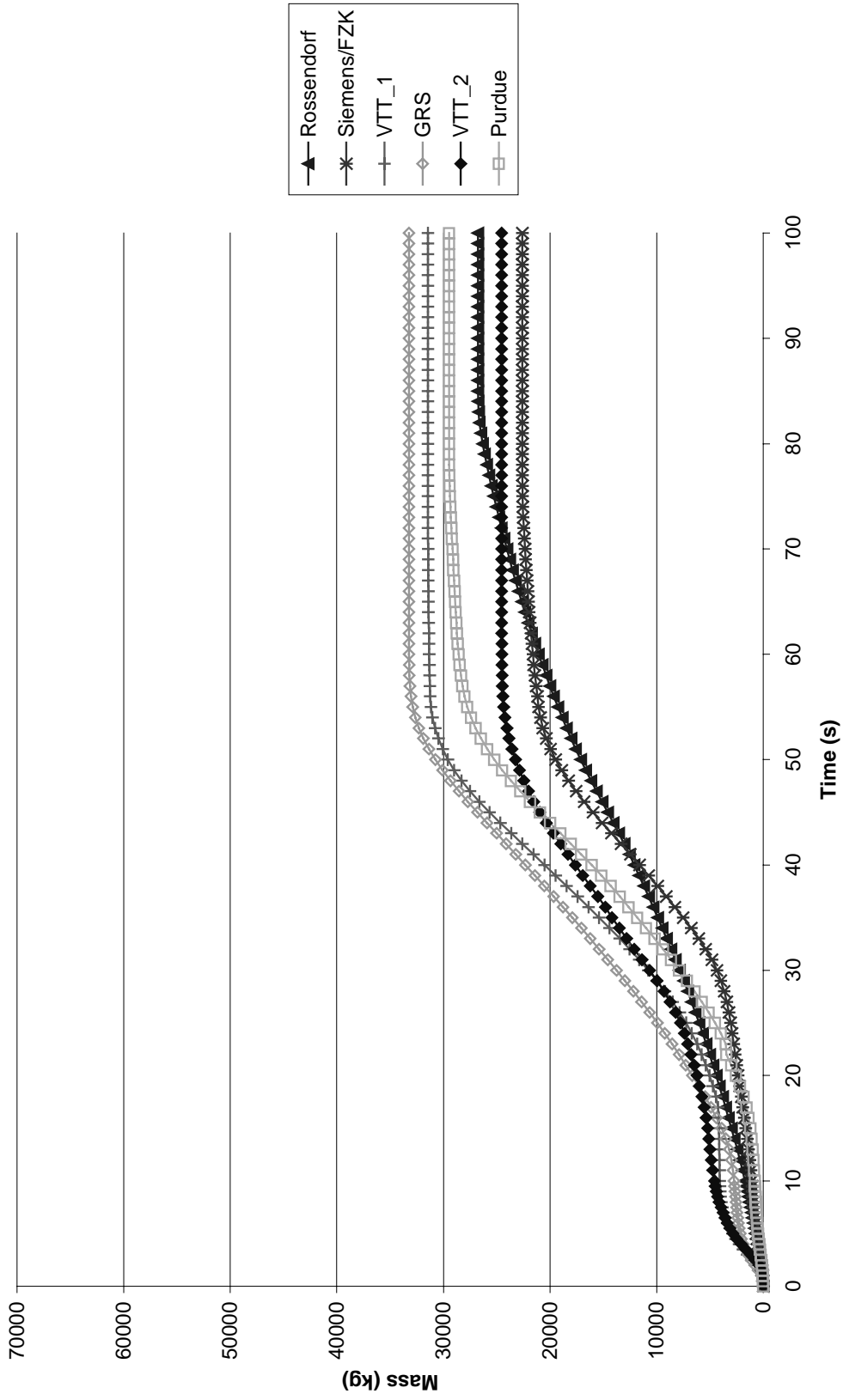


Figure 4.28. Integrated leakage: liquid mass



Chapter 5

CONCLUSIONS

In order to meet the objectives of the validation of best-estimate coupled codes a systematic approach has been introduced to evaluate the MSLB transient. Such codes use separate temporal and spatial models and numerical methods for core neutronics, core thermal-hydraulics and system thermal-hydraulics simulations. Therefore, the validation of these codes should include a testing of these models for the defined transient (in this case a MSLB) as phases (separate exercises) of the overall benchmark. The ultimate goal is to enable participants to initiate and verify these models before focusing on the major objective – testing of coupling methodologies in terms of numerics, temporal and spatial mesh overlays. This approach allows one to evaluate in a more consistent way the modelling of combined effects (determined by neutronics/T-H as well as core/plant interactions) by removing the uncertainties introduced with separate models. In order to perform such a comprehensive validation of coupled codes a multi-level methodology is employed. It includes the application of three exercises (phases), the evaluation of several steady states, and simulation of two transient scenarios.

The analysis of the MSLB benchmark has been performed in an iterative manner. Subsequent to preliminary calculations and comparisons, the specific list of relevant parameters for comparison in each exercise has finally been established. The practical experience gained in this benchmark shows that only after such preliminary stages of analysis can all peculiarities and requirements of modelling be fixed. In this context the international benchmark workshops and ad-hoc meetings (held in conjunction with international conferences) have played important roles as forums for discussing the obtained results and observed deviations as well as the sources of modelling uncertainties and subsequent modifications of the benchmark specification [6-8]. Over the course of the benchmark activities a professional community has been created, and its members became involved in an in-depth discussion of different aspects considered in the validation process.

Exercise 1 is defined as point kinetics (PK) plant simulation. The purpose of this exercise is to test the primary and secondary system model responses. Compatible point kinetics model inputs which preserve axial and radial power distributions and tripped rod reactivity are provided from the coupled three-dimensional (3-D) kinetics/system T-H calculations. During the course of benchmark calculations about fourteen participants from eight countries were assisted in modelling the first exercise and subsequently submitted their PK results. Overall, this benchmark has been well accepted internationally and a like number will be participating in the remaining two phases.

Based on the preliminary comparisons of participants' results it was concluded that the overall agreement of the compared parameters could be improved. The analysis performed demonstrated that the deviations are primarily due to the modelling differences rather than the different code theoretical models. These modelling differences were identified as follows: the conservative initial steam generator (SG) masses, modelling the additional feedwater to the broken SG, steam line break flow modelling, the flow paths to the upper head of reactor vessel and different reactor vessel mixing models. The need to resolve these issues was addressed by carrying out parametric studies which demonstrated sensitivity of power response during the MSLB transient to key input parameters. This initiated a detailed discussion concerning the main effects during a MSLB transient and the

sensitivity of these effects to the modelling assumptions. As a result a three-step procedure was applied: additional information was provided, some modelling assumptions were made explicit (such as the additional feedwater to the broken SG, which was specified as feedwater mass flow rate versus time) and other assumptions were made consistent (such as the SG initial mass).

Due to the sensitive nature of this transient to small variations in initial parameters, the participants were advised to follow the final specifications as closely as possible. To avoid possible misinterpretations, the benchmark team provided further clarifications before the final results were submitted. The motivation behind such clarifications were to narrow down to the extent possible the modelling differences for the initial steady state conditions as well as for the transient scenario. This strategy helped to obtain a cluster of solutions to be used as a basis for deviations. A statistical methodology for evaluation of discrepancies between different code predictions was employed for single value parameters.

In this volume, the first phase of the OECD/NRC PWR MSLB benchmark is discussed in detail. The final results submitted by the participants for the first phase are used to make code-to-code comparisons and a subsequent statistical analysis. This information encompasses approximately 26 thermal-hydraulic and neutronic parameters that affect the reactor behaviour during a MSLB accident, including powers, pressures, temperatures, reactivities, mass flow rates and SG masses throughout the transient. It is presented in plots graphically illustrating the agreement in different code predictions and tables containing relative differences for each of the participant's results for each parameter. The calculation is performed for single value parameters for chosen time points during the transient based on statistical mean value solution.

A detailed assessment of the differences between the calculated results submitted by the participants for the first exercise were presented in Chapter 4 of this volume. The power response and the magnitude of the return to power during the transient as predicted by different codes are functions of the total reactivity time evolution. Since the negative tripped rod reactivity inserted is specified, the differences arise from the predictions of moderator feedback and Doppler feedback reactivity components. The moderator reactivity component follows the cold leg temperature. The discrepancies in the cold leg temperature predictions are mostly due to differences in modelling the secondary side. It was observed that the major factors affecting the dynamics of the transient are break flow modelling (critical flow model), liquid entrainment, modelling of the aspirator flow and nodalisation of the SG down comer. These factors affect the SG mass parameter for both the broken and intact SGs. This parameter shows the greatest deviation amongst participant results, both in the value and behaviour of the SG masses throughout the transient. In addition the disagreement can be attributed to differences in the heat transfer correlations used within each participant's code. This is especially true for the participants who use proprietary correlations that are specific to U-tube SGs in their codes, as the behaviour of a OTSG is much different than a U-tube SGs, and also involves superheat, something U-tube SGs do not have. The Doppler feedback reactivity predictions are sensitive to the relation for Doppler fuel temperature used as well as to the radial and axial nodalisation of the heat structure used (fuel rod).

Overall, it was determined that for the first phase of this benchmark, the key parameters were the SG masses, the break flow rates, the coolant and fuel temperatures and the powers. The other parameters were useful to analyse because they helped to determine what was causing the behaviour of the key parameters. As expected, the break flow rates/modelling was very sensitive to the SG masses/modelling and vice versa. In addition, it was proven that the SG model has a great effect on the power throughout the transient. In particular, the way the additional feedwater was introduced into the steam generator, the aspirator junction area, down comer nodalisation and the OTSG model in general proved to be a source for many differences in the preliminary results. Various interpretations of the steam line break

also caused a great deal of uncertainty before the model was made uniform amongst all participants. One of the most important lessons learned from the first phase of the benchmark was that it is extremely important, as well as very difficult, to ensure consistency in the modelling for any problem.

This type of analysis requires considerably more output than was required by previous benchmarks, and this is especially true of the remaining phases. In addition to requesting more output, the process of determining which parameters to request from the participants must be completed well in advance. From the benchmark team's experiences to date, it is evident that for any future large-scale coupled analyses, closer attention must be paid to the thermal-hydraulic aspect of the benchmark. In addition to doing a better job specifying the transient scenario, it should be designated in such a way that multiple interpretations are not possible. Overall it was determined that:

- The possible redefinition of the problem to help clarify the participants' understanding should be allowed for.
- The participants should be provided with a standard file into which they insert data.
- It is not possible to do a "blind" benchmark of this complexity.

Numerous questions arose despite a concerted effort, including a participant review, to generate a complete and accurate benchmark specification. Problems with the interpretation of the transient scenario, the physics and the models used in various codes led to numerous requests for clarification and changes to the final specification. While certain problems were anticipated, such as modelling of the OTSG, many others came as a surprise. The participants had difficulty with the break and flow distribution information, the kinetics parameters, reactor vessel mixing and the feedwater flow piping and mass flow parameters provided in the original specification. Difficulties led to an interactive process stretching the benchmark to a three-year effort, and required several iterations on results to obtain a consistent interpretation of the specification and the transient.

While some of the lessons learned by the benchmark team came as a surprise, the point kinetics results were as expected. They verify that point kinetics analysis may be overly conservative and thus may limit the operational flexibility of NPPs in the areas of higher burn-ups, longer fuel cycles and power upgrades. The results of the first phase will be combined with results from the next two phases of the PWR MSLB benchmark to help verify coupled 3-D neutronics/thermal-hydraulic system codes results and to assist the users in gaining a more in-depth knowledge of these best estimate codes. The recent progress in computer technology made the development of such advanced codes for realistic modelling of plant transient and accident conditions feasible and they will play a critical role in the future of nuclear analysis.

REFERENCES

- [1] C. Jackson and H. Finnemann, "Verification of the Coupled RELAP5/PANBOX System with the NEACRP LWR Core Transient Benchmark", Proc. of the International Conference on Mathematics and Computations, Reactor Physics, and Environmental Analyses, Portland, Oregon, 30 April-1 May 1995, p. 297.
- [2] K. Ivanov, T. Beam, A. Baratta, A. Irani and N. Trikoros, "PWR MSLB Benchmark. Volume 1: Final Specifications", NEA/NSC/DOC(99)8, April 1999.
- [3] T. Beam, K. Ivanov and A. Baratta, "Benchmarking Advanced Coupled Neutronic/Thermal-Hydraulic Computer Code Models for Nuclear Power Plants", Proc. of the Joint International Conference on Mathematical Methods and Supercomputing for Nuclear Applications, Vol. 1, Saratoga Springs, New York, 5-9 October 1997, p. 263.
- [4] K. Ivanov, T. Beam, A. Baratta, A. Irani and N. Trikoros, "MSLB Analysis of TMI Unit-1 Using TRAC-PF1/NEM", Proceedings of the International RETRAN Conference 1998, EPRI TR-109622, pp. 28-17 to 28-56, June 1998.
- [5] B. Taylor and K. Ivanov, "Statistical Methods Used for Code-to-Code Comparisons in the OECD/NRC PWR MSLB Benchmark", *Annals of Nuclear Energy*, 27 (2000), 1589-1605.
- [6] "Summary of the 2nd PWR MSLB Benchmark Workshop", Madrid, Spain, 25-26 June 1998, NEA/NSC/DOC(98)4.
- [7] "Summary of the 3rd PWR MSLB Benchmark Workshop", Garching, Germany, 24-25 Mar. 1999, NEA/NSC/DOC(99)6.
- [8] "Summary of the 4th PWR MSLB Benchmark Workshop", Paris, France, 24-25 January 2000, NEA/NSC/DOC(2000)2.
- [9] K. Ivanov, A. Baratta and E. Sartori, "OECD/NRC MSLB Benchmark – A Systematic Approach to Validate Best-Estimate Coupled Codes Using a Multi-Level Methodology", Proceedings of CSNI/NRC Workshop on Best Estimate Methods and Codes, Barcelona, Spain, 15-19 April 2000.

APPENDIX A

Description of Computer Codes Used for Analysis in the First Phase of the PWR MSLB Benchmark

SMABRE (VTT-1)

The SMABRE computer code is used by VTT for the point kinetics phase of the benchmark exercise. This computer code has 1-D kinetics and thermal-hydraulics; however, it is able to model 3-D thermal-hydraulic effects using parallel channel nodalisation. SMABRE contains a five-equation, two-phase, thermal-hydraulic model, using the drift flux model. The point kinetics model allows for one energy group and six delayed neutron groups, with cross-sections coming from polynomials using feedback reactivity coefficients or from a user defined table. The numerical solution method used in SMABRE is a predictor-corrector type non-iterative solution. The code has been used by VTT for analysis of VVER reactor transients.

RELAP5/MOD3.2 (FZK/Siemens-KWU, Germany; Universities of Pisa and Zagreb, Italy and Croatia; and BE, United Kingdom)

RELAP5/MOD3.2 is a full six equations, two-phase flow, thermal-hydraulic code developed by INEEL/NRC to simulate both operational transients and loss of coolant accidents in light water reactors. The code models the primary and secondary reactor coolant system as well as the reactor with a one-dimensional approach. A point kinetics model is available to predict the core kinetics with related feedback mechanisms. By the use of one-dimensional flow channels and cross-flow junctions a limited 3-D modelling of the flow inside the RPV is possible. The RELAP5 system model is solved numerically using a semi-implicit finite difference technique. Here, a direct sparse matrix solution technique is used. The user that allows violation of the material Courant limit can also select a nearly implicit finite difference technique.

RELAP5/MOD3 (Purdue University/NRC, USA)

The RELAP5 code has been developed for best-estimate transient simulation of light water reactor coolant systems during postulated accidents. RELAP5 is a highly generic code that, in addition to calculating the behaviour of a reactor coolant system during a transient, can be used for simulation of a wide variety of hydraulic and thermal transients in both nuclear and non-nuclear systems involving mixtures of steam, water, non-condensable and solute.

The RELAP5/MOD3 code is based on a non-homogeneous and non-equilibrium model for the two-phase system that is solved by a fast, partially implicit numerical scheme to permit economical calculation of system transients. The code includes many generic component models from which general systems can be simulated. The component models include pumps, valves, pipes, heat releasing or absorbing structures, reactor point kinetics, electric heaters, jet pumps, turbines, separators, accumulators and control system components. In addition, special process models are included for effects such as form loss, flow at an abrupt area change, branching, choked flow, boron tracking and non-condensable gas transport.

ATHLET (GRS and FZR, Germany)

The ATHLET code is under development by GRS and the Nuclear Research Centre Rossendorf and is a best estimate code for the analysis of anticipated and abnormal transients, small and intermediate breaks as well as large breaks in light water reactors. This code will be used by GRS and RCR for modelling the thermal-hydraulic aspect of the benchmark. It employs point and one-dimensional kinetics. It can be coupled to a three-dimensional kinetics code using a generalised interface.

Using a channelised model, the core can be simulated in a multi-dimensional manner. The code is a two-fluid thermal-hydraulic code using either a five- or four-equation model. A full range drift-flux model is available for calculating relative phasic velocities. A full two-fluid six-equation version is under development.

DYNODE-P 3/D (NETCorp, USA)

Nuclear Engineering Technology Corporation uses the DYNODE-P 3/D code for the benchmark. The code has point and multi-dimensional spatial kinetics models for calculation of core power. The code solves for the change in enthalpy within a volume based on the change in pressure and heat sources in the volume and the flow of mass into the volume. A series of component models are used to describe the system. Each is hardwired to represent different components.

RETRAN-3D (GPUN/CSA/EPRI, USA; and IBERDROLA, Spain)

While similar to RETRAN 03, the RETRAN 3D code includes a three-dimensional kinetics module. The reactor core is modelled as a series of parallel channels coupled to the kinetics module. Iberdrola is working in this benchmark with the version MOD002. This version does not have a decay heat model in the 3-D mode.

CATHARE2 (IPSN/CEA, France)

The CATHARE2 code features a full six-equation, two-fluid, non-equilibrium, non-homogeneous, three-dimensional hydrodynamic model. The numerics are fully implicit in the one-dimensional components and semi-implicit in the three-dimensional components.

The CATHARE code is a French system code for nuclear thermal-hydraulics developed at CEA Grenoble by EDF, FRAMATOME and IPSN for PWR safety analysis. Two-phase flows are described using a full six-equation, two-fluid, non-equilibrium, non-homogeneous two-fluid model. The presence of an incondensable can be taken in account by one to four additive transport equations.

CATHARE has a modular structure. Various modules (0-D, 1-D and 3-D) can be connected to model the primary and secondary circuits of any PWR. Sub-modules can be used to calculate the neutronics, the fuel thermo-mechanics, the pump characteristics, accumulators, sources, sinks, walls and re-flooding. All kinds of two-phase flow patterns are modelled. Co-current and counter-current flows are modelled with prediction of counter current flow limitation. Heat transfer with wall structures and fuel are calculated taking into account all heat transfer processes (natural and forced convection with liquid, with gas, sub-cooled and saturated nucleate boiling, critical heat flux, film boiling, film condensation). The interfacial heat and mass transfers describe the vaporisation due to superheated steam and the direct condensation due to sub-cooled liquid, but also the steam condensation or liquid flashing due to metastable sub-cooled steam or superheated liquid.

The calculations for Exercise 1 of the MSLB benchmark have been performed with the version V1.3L_1, which contains revision 5.

TRAC-PF1/MOD2 (Polytechnic University of Valencia, Spain; and PSU, USA)

The TRAC series of codes use a two-fluid (six-equation), non-equilibrium, non-homogeneous, three-dimensional hydrodynamic model in the reactor vessel. The balance of the plant is modelled

using one-dimensional flow. The solution method used is the semi-implicit SETS method. Based on version 5.4 from LANL, the Penn State version of TRAC-PF1/MOD2 was modified to include several new options, including axial decay heat model, an improved fuel element model and an improved boron-tracking algorithm.

APROS (VTT-2)

APROS (Advanced PROcess Simulator) is a multi-functional simulation environment for the dynamic simulation of nuclear and conventional power plant processes and for the simulation of industrial process dynamics. The Technical Research Centre of Finland (VTT) has developed it with Fortum Engineering Ltd. The APROS simulation environment consists of an executive system, model packages, equation solvers, a real-time database and interface models. APROS has been programmed using Fortran 77 and C languages. All the physical models, like neutronics or thermal-hydraulics, are written with Fortran 77.

The essential models in the calculations performed within the MSLB have been the core point kinetics model for Phase I and the six-equation thermal-hydraulic model. In the APROS calculation of the MSLB benchmark with point kinetics model the reactor core was divided into six independent flow channels in thermal-hydraulics. Each flow channel was divided into 12 axial nodes. For the point kinetics calculation a conventional point kinetics model had to be programmed into APROS. Also for the point kinetics calculation, the average values of fuel and coolant temperatures obtained from the thermal-hydraulic channels were used. In the renewed calculation the coolant temperature coefficient was used according to the proper benchmark definition. The fuel pellet dimensions and material properties according to the updated final specifications were used. The axial and radial profile definitions given in the benchmark could not be taken into account in the point kinetics calculation.

The six-equation thermal-hydraulic model describes the behaviour of one-dimensional two-phase flow. The model is based on the conservation equations of mass, momentum and energy for the gas and liquid phases separately. The equations are coupled with empirical correlations describing various two-phase phenomena. The pressures and velocities, volume fractions and enthalpies of each phase are solved from the discretised equations using an iterative procedure. Heat transfer modules connect the six-equation thermal-hydraulic model with heat conduction solution. Boric acid concentration solution is included in the thermal-hydraulic part. The thermal-hydraulic part also contains calculation of fuel enthalpy and oxide layer thickness on cladding surface and power production by cladding oxidation according to the Baker-Just model. For the calculation of fuel rod temperatures the fuel rod is described as a solid heat structure consisting of three materials: fuel, fuel-cladding gap and cladding. The one-dimensional heat conduction solution in the fuel rod is calculated using ten radial nodes.

APPENDIX B

Sequence of Events for the First Phase of the PWR MSLB Benchmark

Table B.1. Sequence of events for the first phase of the PWR MSLB benchmark problem

Event	NETCorp	IPSN/CEA	VTT 1 (SMABRE)	Univ. of Valencia V 1/V 2	Univ. of Pisa and Zagreb
Break opens	0.000	0.0010	0.000	0.0001/0.0001	0.000
Turbine isolation valve closes – broken SG	N/A	N/A	0.500	N/A	N/A
High neutron flux set point	N/A	5.5700	5.700	N/A	N/A
Low RCS pressure set point	N/A	N/A	N/A	N/A	N/A
Reactor trip	3.075	6.0300	6.200	6.2575/6.1919	7.390
Turbine isolation valve closes – intact SG	2.670	6.0300	6.600	6.7575/6.6919	8.39
Steam line B small safety valve opens	N/A	6.9100	7.200	7.51/8.011	N/A
Steam line B safety valve Group 1 opens	N/A	6.9600	7.400	8.011/8.011	N/A
Steam line B safety valve Group 2 opens	N/A	6.9600	7.400	N/A	N/A
Steam line B safety valve Group 3 opens	N/A	7.6000	7.600	N/A	N/A
HPI initiated	N/A	N/A	10.900	N/A	N/A
Steam line B safety valve Group 3 closed	N/A	22.1700	28.1000	N/A	N/A
Steam line B safety valve Group 2 closed	N/A	31.9400	34.9000	N/A	N/A
Steam line B safety valve Group 1 closed	N/A	31.9400	34.900	19.51/17.52	N/A
Steam line B small safety valve closed	N/A	35.2700	38.000	21.51/21.02	N/A
HPI starts	36.140	35.5500	35.900	37.7944/37.5497	45.530
Return to criticality	48.00	77.00	N/A	N/A	N/A
Point of maximum power after trip	65.00	82.78	66.0	65.66/6589	75.00
Transient ends	100.000	100.00	100.000	100.000	100.000

Table B.1. Sequence of events for the first phase of the PWR MSLB benchmark problem (cont.)

Event	GRS	Rossendorf	Purdue/ NRC	BE	GPUN/CSA/ EPRI	VIT 2 (APROS)
Break opens	0.0	0.1	0.001	0.0	0.001	0.01
Turbine isolation valve closes – broken SG	N/A	N/A	0.001	N/A	N/A	N/A
High neutron flux set point	N/A	4.21	4.5	N/A	N/A	N/A
Low RCS pressure set point	N/A	N/A	N/A	N/A	N/A	N/A
Reactor trip	6.56	4.61	4.9	5.4	5.5	6.135
Turbine isolation valve closes – intact SG	6.56	N/A	5.4	5.9	5.7	6.7
Steam line B small safety valve opens	N/A	N/A	6.2	N/A	6.55	N/A
Steam line B safety valve Group 1 opens	N/A	N/A	6.6	N/A	7.14	N/A
Steam line B safety valve Group 2 opens	N/A	N/A	6.6	N/A	7.14	N/A
Steam line B safety valve Group 3 opens	N/A	N/A	7.7	N/A	11.8	N/A
HPI initiated	N/A	N/A	10.0	N/A	N/A	N/A
Steam line B safety valve Group 3 closed	N/A	N/A	14.7	N/A	15.15	N/A
Steam line B safety valve Group 2 closed	N/A	N/A	31.8	N/A	21.1	N/A
Steam line B safety valve Group 1 closed	N/A	N/A	17.9	N/A	21.2	N/A
Steam line B small safety valve closed	N/A	N/A	37.2	N/A	23.8	N/A
HPI starts	42.95	35.89	35.0	27.75	38.5	39.1
Return to criticality	N/A	70.2	67.2	62.0	N/A	68.0
Point of maximum power after trip	77.0	81.60	73.5	67.50	64.00	81.8
Transient ends	100	100	100	100	100	N/A

Table B.1. Sequence of events for the first phase of the PWR MSLB benchmark problem (cont.)

Event	Siemens/FZK	Iberdrola	PSU
Break opens	0.15	0.001	0.001
Turbine isolation valve closes – broken SG	0.15	N/A	0.001
High neutron flux set point	5.2	N/A	5.60
Low RCS pressure set point	N/A	N/A	N/A
Reactor trip	5.6	5.327	6.01
Turbine isolation valve closes – intact SG	5.6	5.9	6.51
Steam line B small safety valve opens	7.44	8.402	8.4467
Steam line B safety valve Group 1 opens	7.62	8.9713	9.1587
Steam line B safety valve Group 2 opens	7.62	N/A	10.2061
Steam line B safety valve Group 3 opens	7.8	N/A	N/A
HPI initiated	11.375	N/A	12.8774
Steam line B safety valve Group 3 closed	32.23	N/A	N/A
Steam line B safety valve Group 2 closed	33.76	N/A	31.7471
Steam line B safety valve Group 1 closed	33.91	12.5374	40.7525
Steam line B small safety valve closed	36.75	21.4102	40.7525
HPI starts	36.375	34.069	37.9483
Return to criticality	N/A	N/A	N/A
Point of maximum power after trip	74.0	61.0	61.0
Transient ends	100	100	100

APPENDIX C

Questionnaire for the First Phase of the PWR MSLB Benchmark

QUESTIONNAIRE FOR THE FIRST EXERCISE

I. Primary system

1. Vessel thermal-hydraulic (T-H) model and nodalisation (1-D, 3-D and number T-H channels or cells) – how are channels/T-H cells chosen?
2. Mixing model – how is the required mixing ratio implemented?
3. Upper plenum and upper head (of reactor vessel) paths (junctions) modelling?
4. Radial and axial heat structure (fuel rod) nodalisation?
5. Relation used for Doppler temperature?

II. Secondary system

1. Initial steam generator (SG) mass inventory?
2. SG down-comer nodalisation?
3. Aspirator flow modelling?
4. Steam line modelling?
5. Break flow modelling and critical flow model?
6. Are you using the updated steam safety relief valves data (see Updated Specifications, April 1999, Table 5.4.2, p. 69)?
7. Are you using the updated additional feedwater mass data (between the feedwater isolation valve and the broken SG) (see Updated Specifications, April 1999, Table 5.4.3, p. 69)?

III. General

1. Deviations from the updated final specifications (April 1999, NEA/NSC/DOC(99)8)?
2. User assumptions?
3. Specific features of the codes used?

FZR
Germany

I. Primary system

1. Vessel thermal-hydraulic (T-H) model and nodalisation (1-D, 3-D and number T-H channels or cells) – how are channels/T-H cells chosen?

One-dimensional vessel model: two parallel and independent flow paths (see 1.2) simulating the flow from the cold legs outlet through the down-comer and the lower plenum to the core, the core is modelled with two channels for the fuel assemblies and two channels for the bypass, from the core outlet the flow paths go through the upper plenum to the inlet of the hot legs, additional flow paths for the upper head: see 1.3, connections between the flow paths: see 1.2.

2. Mixing model – how is the required mixing ratio implemented?

The primary circuit is fully split into two parts, two connection points are introduced between these parts for pressure balance (core reflector and upper head) – at each time step the actual mixing ratio is determined – by means of a controller energy is exchanged in the lower and the upper plenum to match the required value of 0.5.

3. Upper plenum and upper head (of reactor vessel) paths (junctions) modelling?

Two flow paths (one for each half of the circuit) are modelled from the upper plenum to the upper head and back to the upper plenum to ensure the cooling of the upper head (the summary flow rate is about 1 000 kg/s).

4. Radial and axial heat structure (fuel rod) nodalisation?

Two fuel rods are modelled each with 24 nodes in axial and five nodes in radial direction.

5. Relation used for Doppler temperature?

Standard ATHLET approach (?).

II. Secondary system

1. Initial steam generator (SG) mass inventory?

26 077 kg.

2. SG down-comer nodalisation?

Eleven nodes.

3. Aspirator flow modelling?

Aspirator flow is modelled as a junction between the SG and the SG down-comer, the flow rate in the initial state is about 80 kg/s.

4. Steam line modelling?

For the broken SG two steam lines are modelled, the cross connection is modelled, and each steam line also has 10 nodes up to the break.

5. Break flow modelling and critical flow model?

The break is modelled as double ended rupture within 0.1 s > for the description of the critical flow the 1-D finite difference critical discharge model of ATHLET is used. It is a four-equation model, the field equations for this two-phase flow model are based on the 1-D stationary conservation laws for liquid mass, vapour mass, mixture energy and mixture momentum.

Due to convergence problems, the Moody model could not be used, but investigations at the early stage of the benchmark work showed that the differences between these two models are negligible.

6. Are you using the updated steam safety relief valves data (see Updated Specifications, April 1999, Table 5.4.2, p. 69)?

Yes.

7. Are you using the updated additional feedwater mass data (between the feedwater isolation valve and the broken SG) (see Updated Specifications, April 1999, Table 5.4.3, p. 69)?

Yes.

III. General

1. Deviations from the updated final specifications (April 1999, NEA/NSC/DOC(99)8)?

Critical flow model and determination of the Doppler temperature (probably).

2. User assumptions?

3. Specific features of the codes used?

FZK/SKWU

Germany

I. Primary system

1. Vessel thermal-hydraulic (T-H) model and nodalisation (1-D, 3-D and number T-H channels or cells) – how are channels/T-H cells chosen?

To model the vessel (RPV) thermal-hydraulics for the MSLB transient the RPV was split almost into two equal halves, one half connected to the coolant stream of the broken Loop A and the other one to the coolant stream of the intact Loop B. Each RPV half consists of following fluid volumes along the main flow streams: RPV inlet, down-comer, lower plenum, core bypass, core, core outlet, upper plenum, one annular region between baffle and the core support shield and one dead-end annular region formed by the core support shield and the RPV wall. The uppermost upper plenum volume connects both RPV halves to each other. In addition there are two volumes in the upper plenum for the mixing modelling. Four volume stacks (two per loop) thermal-hydraulically represent the core itself with 10 axial nodes. The two volume stacks belonging to a core half are hydraulically connected at each axial node by a cross-connection junction. There is no connection between the core volumes of both Loop A and Loop B. The main in-vessel structures and the RPV walls are also modelled. In total 64 fluid volumes are used to represent the whole RPV with its main flow paths.

2. Mixing model – how is the required mixing ratio implemented?

A precondition to model the coolant mixing according to the specification was the splitting of the RPV. So, at the lower plenum the mixing was reached adding two junctions to connect Loop A with Loop B. To get the recommended mixing ratio of 0.5, appropriate flow areas of the connecting junctions had to be defined. In this way a mixing ratio close to 0.5 was obtained during almost the whole transient calculation.

3. Upper plenum and upper head (of reactor vessel) paths (junctions) modelling?

At the upper plenum, the main flow paths are defined by the baffle and the baffle holes as well as by the annular region between the baffle and the core support shield. As earlier mentioned six volumes in three elevations were considered per core halves. Two additional volumes were defined (elevation 2 and 3) for mixing of both loops (A and B) occurs. The uppermost volume connects both loops. In addition, two representative guide tubes per halves were modelled that conjoin the core outlet volumes (of Loop A and Loop B) with the uppermost volume.

4. Radial and axial heat structure (fuel rod) nodalisation?

Four heat structures, each one representing a quarter of the total core fuel rods, were modelled. Each heat structure is connected with one volume stack (core channel) by convective boundary conditions. Axially the same number of nodes as the corresponding flow channels were chosen,

i.e. 10 nodes. Each heat structure consists radially of three material zones: UO₂, gap and Zry cladding. The pellet and cladding are subdivided in two zones respectively. The axial power profile provided in the Final Specifications was used. No radial power peaking distribution was considered in the model for the Phase I since a point kinetics approach is used for total core reactivity and total core power prediction.

5. Relation used for Doppler temperature?

In RELAP5 the node wise volume average fuel temperature is used to predict the Doppler reactivity feedback. A test calculation have shown that the Doppler temperature calculated by the relation given in the Final Specification is close to the average fuel temperature used in RELAP5. Thus the RELAP5 approach, which is comparable to the PSU procedure, was used in Phase I.

II. Secondary system

1. Initial steam generator (SG) mass inventory?

26 450 kg.

2. SG down-comer nodalisation?

An annulus volume with four internal volumes models the steam generator down-comer. Feedwater is injected at the down comer top and flows out of the down-comer to the volume representing the lower tube sheet, which is modelled as a branch. From this branch the flow is directed upward through two volume stacks representing the boiler part of the steam generator.

3. Aspirator flow modelling?

The aspirator is modelled by a cross-flow junction that connects the boiler (at an elevation of 9.73 m) with the down-comer top. The aspirator flow area mounts to 0.972 m² but it was reduced to 0.1858 m² to obtain the initial fluid inventory of about 26 tonnes.

4. Steam line modelling?

The steam lines are modelled in detail considering their whole length as recommended by the Specifications. It was represented by a RELAP5 pipe with 15 internal volumes. A cross-connection line per loop was also considered in the model only for the intact loop. For this Loop B four banks of main steam safety valves (SRV) were modelled as prescribed in the Specifications. A turbine stop valve (MSIV) per steam line, i.e. four in total, was also modelled. Finally the common header, the turbine check valve and the turbine itself (as pressure boundary) were also included in the modelling of the steam lines.

5. Break flow modelling and critical flow model?

Modelling the breaks the default choking model of RELAP5/MOD3.2, i.e. the Trapp & Ramson model, together with the abrupt area option were used. To use the Moody critical flow model, modifications of the RELAP5 code beyond the scope of this benchmark are necessary. Thus, the homogeneous instead of the non-homogeneous flow model was activated (recommendation of the RELAP5 manuals). An additional run was performed with the optional Henry Fauske model of

RELAP5/MOD3.2, which uses the thermal non-equilibrium model as default option. From the performed calculations it was concluded that the differences in the break outflow rate of both models are marginal.

6. Are you using the updated steam safety relief valves data (see Updated Specifications, April 1999, Table 5.4.2, p. 69)?

Yes.

7. Are you using the updated additional feedwater mass data (between the feedwater isolation valve and the broken SG) (see Updated Specifications, April 1999, Table 5.4.3, p. 69)?

Yes.

III. General

1. Deviations from the updated Final Specifications (April 1999, NEA/NSC/DOC(99)8)?

a) Use of the node-wise volume average fuel temperature instead of the relation given in the specification (exploring run demonstrated that both approach are comparable).

b) Use of the Trapp & Ramson critical flow model instead of the Moody model.

2. User assumptions?

a) No radial nodalisation of the fuel rods since a point kinetics model is used to predict the reactivity and power.

b) Reduction of the aspirator flow is to get the initial fluid inventory in the steam generator secondary side.

3. Specific features of the codes used?

a) Use of the node-wise volume average fuel temperature to predict the Doppler reactivity coefficient.

b) Trapp & Ramson critical flow model as default (Henry Fauske model as alternative).

CSA/GPU
United States of America

I. Primary system

1. Vessel thermal-hydraulic (T-H) model and nodalisation (1-D, 3-D and number T-H channels or cells) – how are channels/T-H cells chosen?

For point kinetics, two parallel core channels and three axial T-H nodes were used. This is consistent with the vessel diagram in Figure A.2 in the benchmark specification. Each core channel had 24 axial T-H nodes.

2. Mixing model – how is the required mixing ratio implemented?

The mixing model was implemented by exchanging energy between the two lower plenum and two upper plenum nodes. A control system was implemented to monitor the loop temperature difference and adjust the plenum energy exchange each time step to achieve the desired loop temperature difference. The two upper and lower plenums are consistent with the vessel diagram in Figure A.2 in the benchmark specification.

3. Upper plenum and upper head (of reactor vessel) paths (junctions) modelling?

Same as vessel diagram shown in Figure A.2 in the benchmark specification.

4. Radial and axial heat structure (fuel rod) nodalisation?

For Exercise I, the same as shown in the vessel diagram in Figure A.2 in the benchmark specification.

5. Relation used for Doppler temperature?

As defined in the benchmark specification.

II. Secondary system

1. Initial steam generator (SG) mass inventory?

As defined in the benchmark specification.

2. SG down-comer nodalisation?

Eight axial nodes.

3. Aspirator flow modelling?

As defined in the benchmark specification. The aspirator flow paths (junctions 150 and 250) shown in benchmark specification Figure A.1 are consistent with the way it was modelled.

4. Steam line modelling?

As defined in the benchmark specification and as shown in Figures A.3 and A.4.

5. Break flow modelling and critical flow model?

The geometry was as defined in the benchmark specification. An isoenthalpic critical flow model was used instead of the specified Moody critical flow model.

6. Are you using the updated steam safety relief valves data (see Updated Specifications, April 1999, Table 5.4.2, p. 69)?

Yes.

7. Are you using the updated additional feedwater mass data (between the feedwater isolation valve and the broken SG) (see Updated Specifications, April 1999, Table 5.4.3, p. 69)?

Yes.

III. General

1. Deviations from the updated Final Specifications (April 1999, NEA/NSC/DOC(99)8)?

There were three deviations from the specifications that we are aware of in our analysis. The first is the choice of critical flow models for Exercises I (see Question 4 above). The second is we used the 1979 ANS decay heat model within RETRAN rather than the specified decay heat. We compared decay heat values and the differences were insignificant.

2. User's assumptions?

None other than discussed above.

3. Specific features of the codes used?

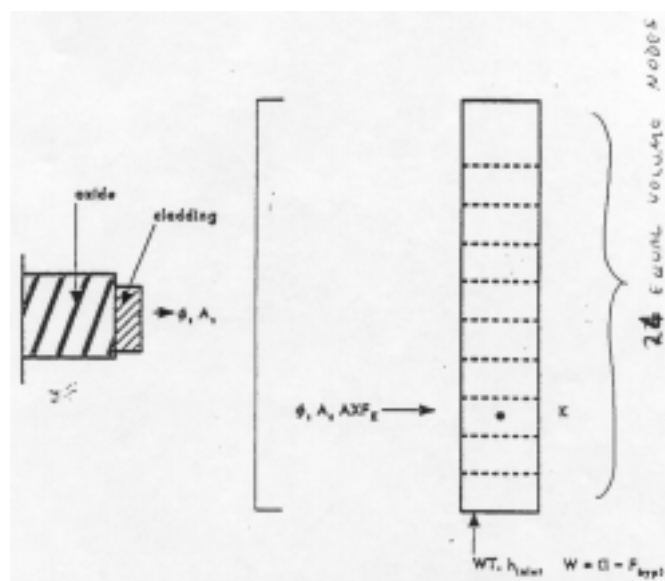
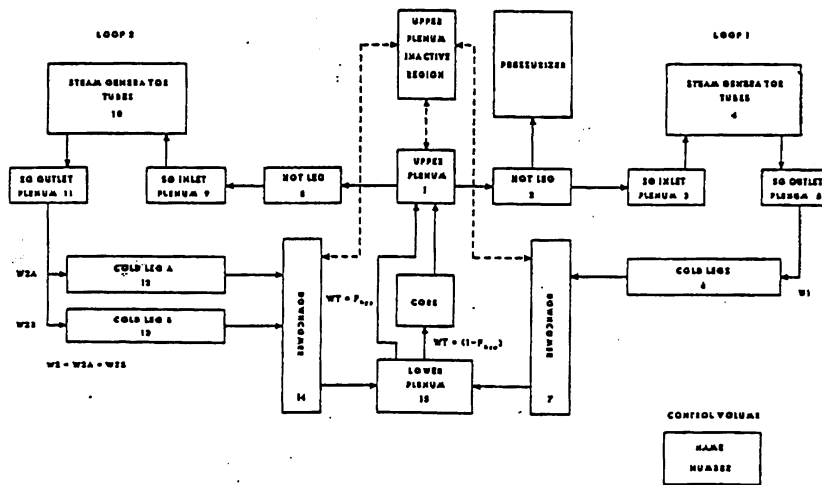
None.

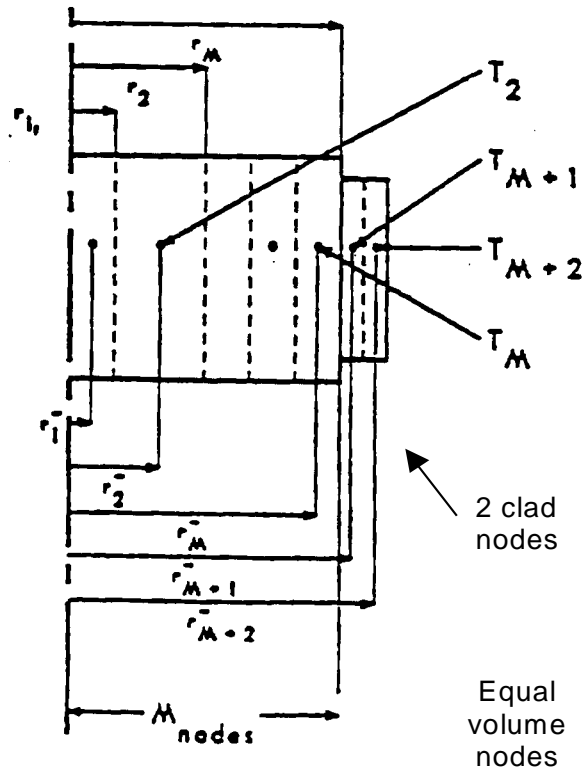
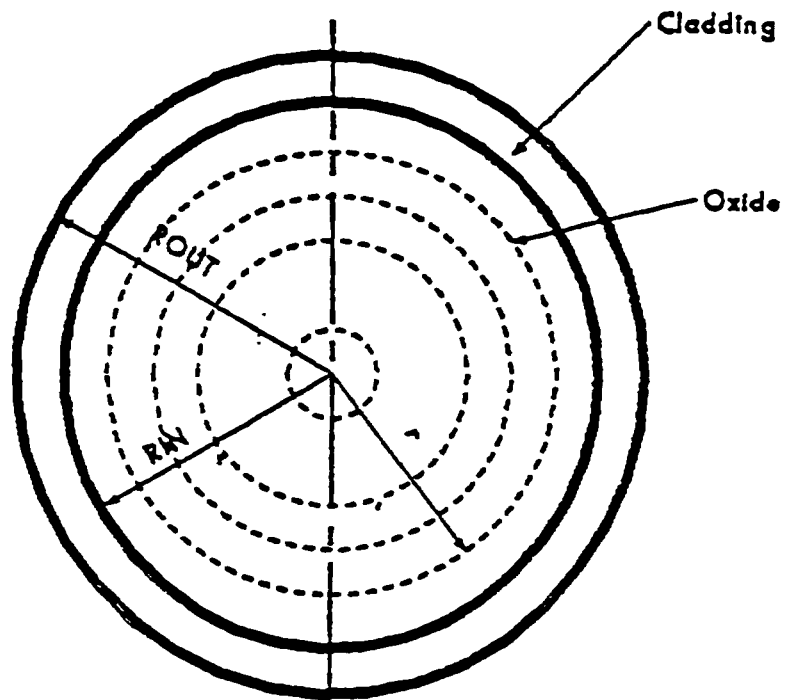
NETCorp
United States of America

I. Primary system

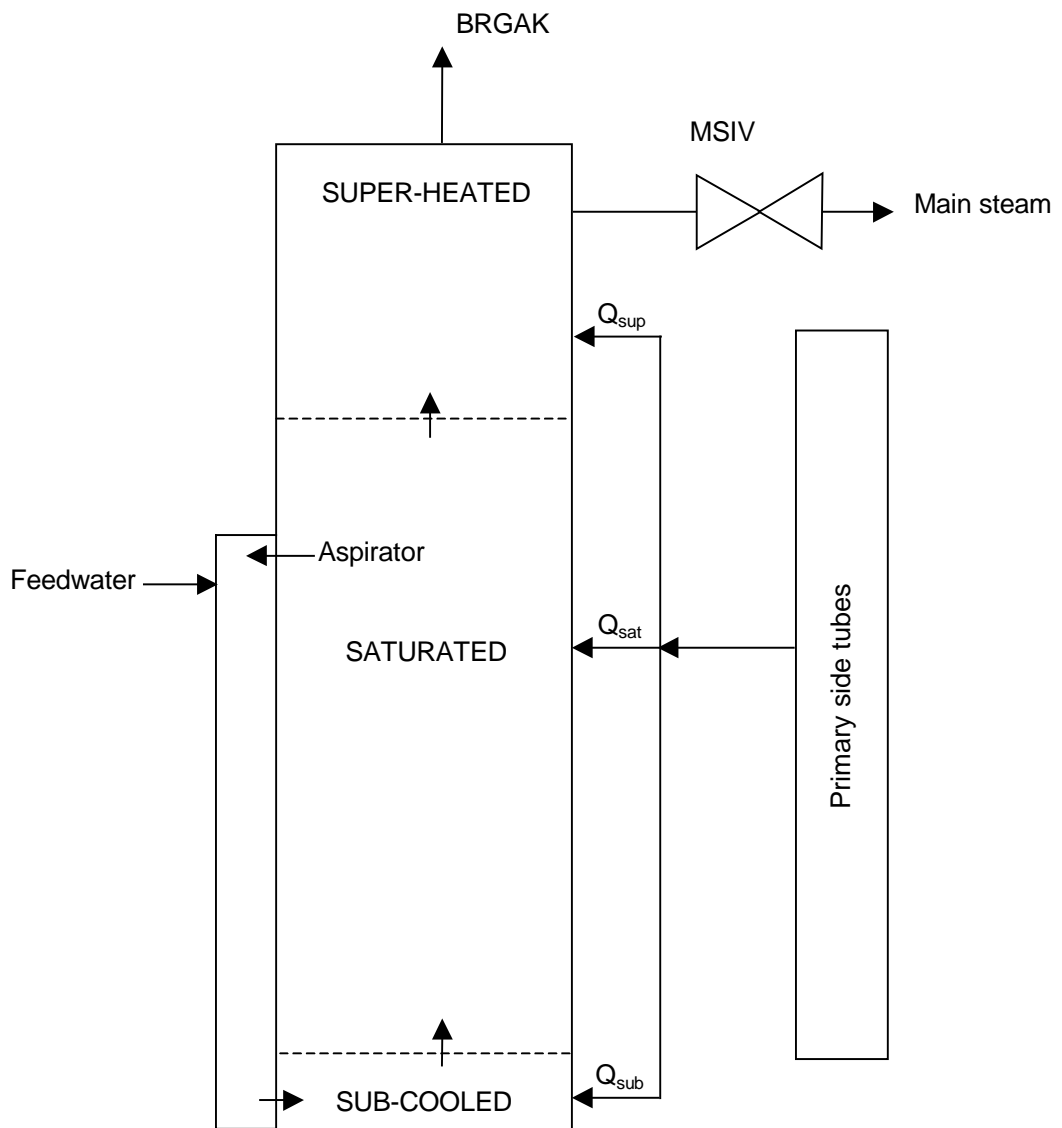
1. Vessel thermal-hydraulic (T-H) model and nodalisation (1-D, 3-D and number T-H channels or cells) – how are channels/T-H cells chosen?

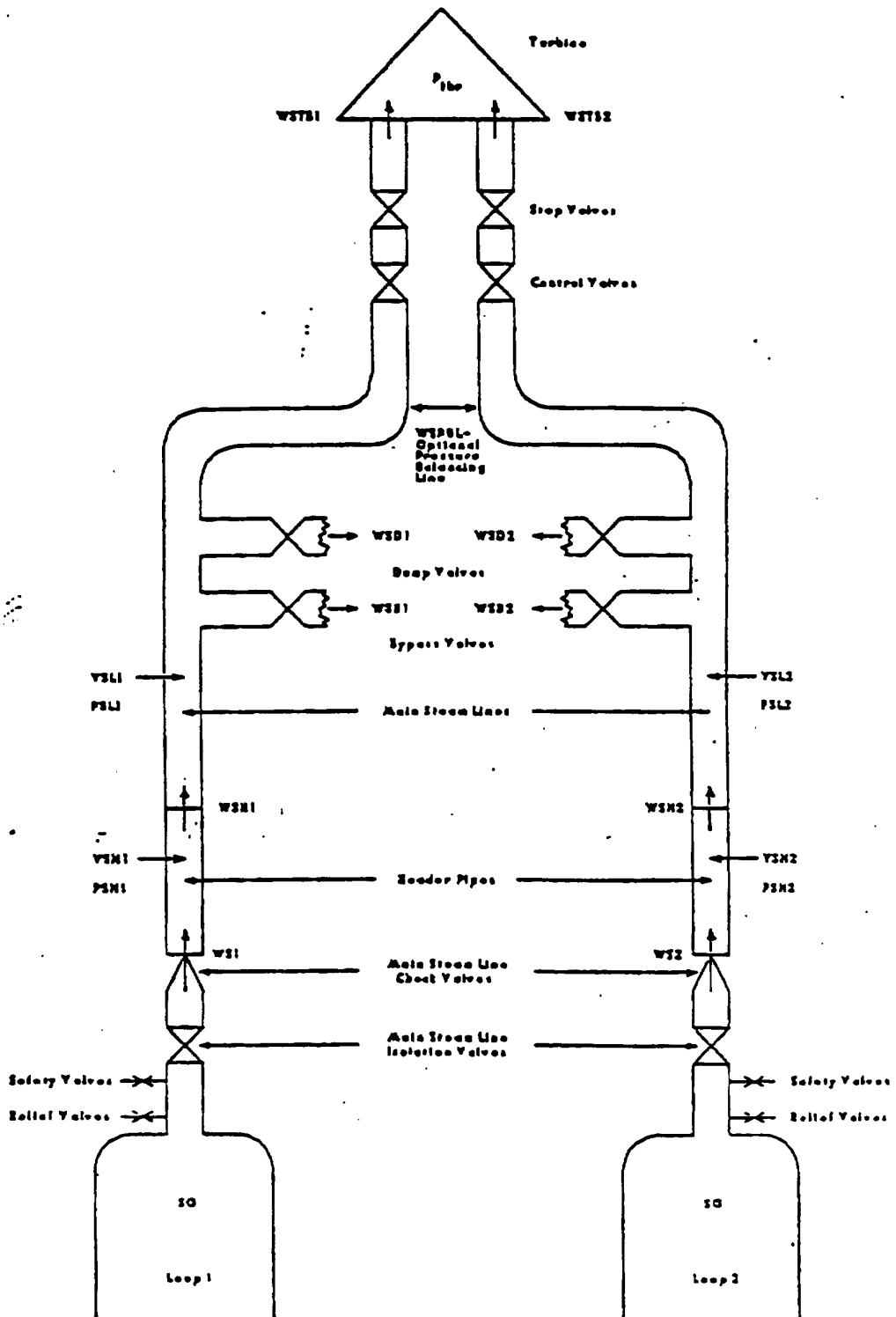
See the figures below.





$M = 5$





2. Mixing model – how is the required mixing ratio implemented?

DNP/3D did not use a mixing model for the first exercise.

3. Upper plenum and upper head (of reactor vessel) paths (junctions) modelling?

See Figures above.

4. Radial and axial heat structure (fuel rod) nodalisation?

See Figures above.

5. Relation used for Doppler temperature?

For the first exercise, the average fuel temperature was used for the Doppler reactivity.

II. Secondary system

1. Initial steam generator (SG) mass inventory?

Down-comer liquid = 36 023 lbm
Tube bundle liquid = 16 697 lbm
Tube bundle steam = 4 597 lbm
Total = 57 317 lbm

2. SG down-comer nodalisation?

See Figures above.

3. Aspirator flow modelling?

Initial aspirator flow based on raising feedwater flow to saturation.

4. Steam line modelling?

See Figures above.

5. Break flow modelling and critical flow model?

See Figures above.

Moody critical flow model assuming saturated steam at the exit plane.

No pressure drop losses from the steam dome to the exit plane.

6. Are you using the updated steam safety relief valves data (see Updated Specifications, April 1999, Table 5.4.2, p. 69)?

Yes.

7. Are you using the updated additional feedwater mass data (between the feedwater isolation valve and the broken SG) (see Updated Specifications, April 1999, Table 5.4.3, p. 69)?

Yes.

III. General

1. Deviations from the updated Final Specifications (April 1999, NEA/NSC/DOC(99)8)?

None known.

2. User assumptions?

Nothing special.

3. Specific features of the codes used?

OTSG model option.

UNIVERSITIES OF PISA AND ZAGREB

Italy and Croatia

I. Primary system

1. Vessel thermal-hydraulic (T-H) model and nodalisation (1-D, 3-D and number T-H channels or cells) – how are channels/T-H cells chosen?

The RPV geometry is 1-D (around 150 nodes are included). The core is also 1-D. However, one stack of hydraulic nodes for the active region and one stack for the bypass should be distinguished. In addition, the hydraulic stack for the active region includes four parallel thermal structure stacks. Each hydraulic (two) or structures (four) stacks consists of 24 axial nodes.

2. Mixing model – how is the required mixing ratio implemented?

Full mixing has been considered.

3. Upper plenum and upper head (of reactor vessel) paths (junctions) modelling?

All flow paths modelled: down-comer to upper head, upper head to upper plenum, upper head to upper plenum via control rod drive tubes, down-comer to hot legs.

4. Radial and axial heat structure (fuel rod) nodalisation?

See the answer to the Question 1.

5. Relation used for Doppler temperature?

The relation between fuel temperature and reactivity is the one supplied by the specifications (Table 5.3.1). However, the average fuel temperature has been estimated taking as reference only one of the four stacks of structures (see answer to Question 1). The considered stack includes the largest number of fuel assemblies (124 over 177).

II. Secondary system

1. Initial steam generator (SG) mass inventory?

Data are reported in Table 4 of NT 398. Taking as reference the submission of October 1999 (No. 3 in Table 4), the initial mass of SG is 26 230 (see Table 5 of the same report).

2. SG down-comer nodalisation?

The down-comer noding can be seen in Figure 2 of the report mentioned in the question above. Down-comer region modelled by 24 hydraulic nodes and a similar number of structures.

3. Aspirator flow modelling?

Modelled according to the latest information received (in other terms, all the received information has been considered).

4. Steam line modelling?

The steam line noding can be seen in Figure 2 of the report mentioned in Question 1 above. Sixty-four hydraulic nodes have been considered for the two branches of the steam line. Structures have been modelled in each branch.

5. Break flow modelling and critical flow model?

The steam line noding can be seen in Figure 2 of the report mentioned in Question 1 above (right part of the figure). The critical flow model adopted is embedded into the used version of the code. (See the code manual. Caution: actual critical flow results depend upon the model, the nodalisation, the triggering of user options and the way the model is implemented into the code.)

6. Are you using the updated steam safety relief valves data (see Updated Specifications, April 1999, Table 5.4.2, p. 69)?

Yes (run No. 3 of Table 2 of the mentioned report).

7. Are you using the updated additional feedwater mass data (between the feedwater isolation valve and the broken SG) (see Updated Specifications, April 1999, Table 5.4.3, p. 69)?

Yes (run No. 3 of Table 2 of the mentioned report).

III. General

1. Deviations from the updated Final Specifications (April 1999, NEA/NSC/DOC(99)8)?

Consideration of the mixing in the RPV (see the answer to Question I. 2).

2. User assumptions?

A number of user assumptions unavoidably are part of the input deck. However a standard procedure has been adopted. Therefore all user choices are commonly used at University of Pisa.

3. Specific features of the codes used?

The official versions of the code have been adopted. No modification to the code has been implemented.

VTT-1

Finland (SMABRE Code)

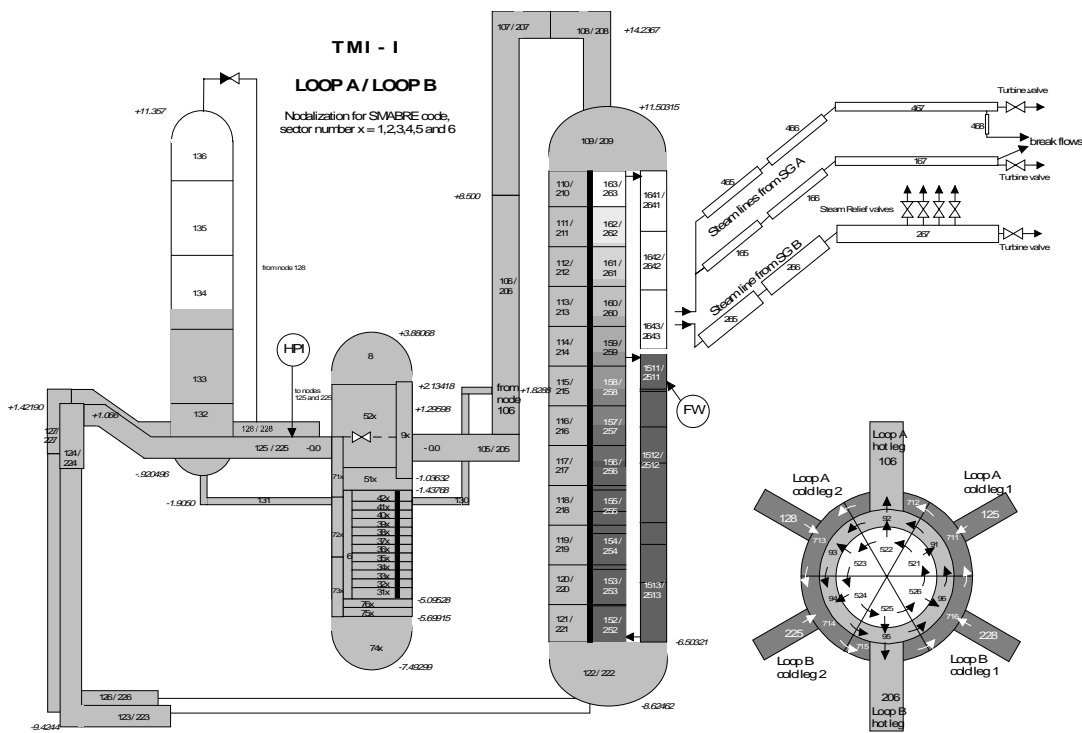
I. Primary system

1. Vessel thermal-hydraulic (T-H) model and nodalisation (1-D, 3-D and number T-H channels or cells) – how are channels/T-H cells chosen?

One-dimensional nodalisation. Vessel is divided in six sectors.

Number of T-H cells is 128 (72 in the core and 56 in the vessel).

Nodalisation is based on information given on RETRAN and TRAC models.



2. Mixing model – how is the required mixing ratio implemented?

The vessel is modelled with six sectors all the way from the down-comer to outlet plenum. This creates a basis for simulate mixing of cold water from the broken loop and hot water from intact loop. Mixing in the horizontal connections between the sectors is based mainly on the density difference between the nodes. Further, the requested mixing is achieved by using the turbulent mixing model in these junctions. The turbulent mixing model consists of the mixing of the enthalpy and boron concentration between the neighbouring nodes. The amount of turbulent mixing varies according the main flow rate.

3. Upper plenum and upper head (of reactor vessel) paths (junctions) modelling?

In the upper plenum the mixing is mainly based on the six parallel sectors and turbulent mixing model described above. Here the uppermost node, the upper head takes also part in mixing, since part of the flow in the model goes through the single node in upper head.

4. Radial and axial heat structure (fuel rod) nodalisation?

The core is divided in six sectors. Each sector is divided in 12 axial T-H and heat structure nodes. In radial direction the fuel rod is divided into three heat structure nodes. One layer for fuel pellet, one for gas cap and one for cladding.

5. Relation used for Doppler temperature?

Doppler temperature in SMABRE model is the average of fuel temperatures in 12 levels.

II. Secondary system

1. Initial steam generator (SG) mass inventory?

26 078 for A and 25 731 kg for steam generator B.

2. SG down-comer nodalisation?

Three nodes. See figure of the nodalisation in Question I.1.

3. Aspirator flow modelling?

The aspirator junction, steam out-take from tube bundle to down-comer to preheat the feedwater, is modelled with the given flow area, 0.96 m^2 . At the steady state in the SMABRE model 100 kg/s steam and also 400 kg/s of saturated water is flowing from the tube bundle to the top of down-comer. During the transient at the aspirator junction no reversal flow is allowed.

4. Steam line modelling?

*Steam line A1: three nodes until the break.
Steam line A2: four nodes until the break.
Steam line B: four nodes until the turbine valve.
See picture of nodalisation in Question I.1.*

5. Break flow modelling and critical flow model?

Main steam line:

- *Break area: 0.2462 m^2 .*
- *Hydraulic diameter: 0.5599 m.*

Cross-connect line:

- *Break area: 0.0324 m^2 .*
- *Hydraulic diameter: 0.2031 m.*

Critical flow:

- *The Moody model is used for critical break flow model with the contraction coefficient 1.0 for saturated flow.*

6. Are you using the updated steam safety relief valves data (see Updated Specifications, April 1999, Table 5.4.2, p. 69)?

Yes.

7. Are you using the updated additional feedwater mass data (between the feedwater isolation valve and the broken SG) (see Updated Specifications, April 1999, Table 5.4.3, p. 69).

Yes.

III. General

1. Deviations from the updated Final Specifications (April 1999, NEA/NSC/DOC(99)8)?

The superheating of the main steam flow in SMABRE model is 26°C instead of 19°C given in the specification.

2. User assumptions?

None.

3. Specific features of the codes used?

Turbulent mixing model (Q I.1).

PURDUE UNIVERSITY/NRC

United States of America

I. Primary system

1. Vessel thermal-hydraulic (T-H) model and nodalisation (1-D, 3-D and number T-H channels or cells) – how are channels/T-H cells chosen?

Core: 1-D pipe component, two parallel channels, six axial levels each.

Bypass: 1-D pipe component, six axial levels.

2. Mixing model – how is the required mixing ratio implemented?

Two parallel lower plenum channels and two parallel upper plenum channels were connected with junctions with no momentum transfer across junction ($s = 3$). The friction losses were adjusted to achieve the desired mixing ratio.

3. Upper plenum and upper head (of reactor vessel) paths (junctions) modelling?

Each of the core channels was connected to an upper plenum. Both upper plenums were connected to a single upper head and two parallel outlet plenums. The upper head was connected back to the outlet plenums. The outlet plenum was connected to a hot leg. The frictional losses were adjusted so that about 20% of the core flow goes through the upper head. This modelling was chosen to be similar to the RETRAN skeleton input deck included in the final specifications.

4. Radial and axial heat structure (fuel rod) nodalisation?

Six axial levels, corresponding to six T-H axial levels.

Nine radial intervals – six for the pellet (equally spaced), one for the gap and two for the clad (equally spaced).

5. Relation used for Doppler temperature?

The correlation from p. 29 of the April 99 specifications was used (0.3/0.7 fuel centreline/surface weighting).

II. Secondary system

1. Initial steam generator (SG) mass inventory?

~26 005 kg.

2. SG down-comer nodalisation?

Five axial levels.

3. Aspirator flow modelling?

A junction connecting SG 2/3 way up with FW inlet was used. Form losses were adjusted to achieve 10% of the outlet SG flow through the aspirator junction.

4. Steam line modelling?

Fifteen axial levels, from SG outlet plenum to the MSIV. One steam line on the intact side, two steam lines on the broken side. Four relief valves connected to the four last axial levels of the intact steam line.

5. Break flow modelling and critical flow model?

Henry-Fauske critical flow model for the break. The 24" and 8" breaks were connected to separate steam lines, both at 44.8 m of the steam line.

6. Are you using the updated steam safety relief valves data (see Updated Specifications, April 1999, Table 5.4.2, p. 69)?

Yes.

7. Are you using the updated additional feedwater mass data (between the feedwater isolation valve and the broken SG) (see Updated Specifications, April 1999, Table 5.4.3, p. 69)?

Yes.

III. General

1. Deviations from the updated Final Specifications (April 1999, NEA/NSC/DOC(99)8)?

Mixing ratio of 0.6 was used.

2. User assumptions?

Turbine sink pressure adjusted to achieve SL inlet pressure of 6.41 MPa.

3. Specific features of the codes used?

The RELAP5 code has been developed for best estimate transient simulation of light water reactor coolant systems during postulated accidents. RELAP5 is a highly generic code that, in addition to calculating the behaviour of a reactor coolant system during a transient, can be used for simulation of a wide variety of hydraulic and thermal transients in both nuclear and non-nuclear systems involving mixtures of steam, water, non-condensable and solute.

The RELAP5/MOD3 code is based on a non-homogeneous and non-equilibrium model for the two-phase system that is solved by a fast, partially implicit numerical scheme to permit economical calculation of system transients. The code includes many generic component models from which general systems can be simulated. The component models include pumps, valves, pipes, heat

releasing or absorbing structures, reactor point kinetics, electric heaters, jet pumps, turbines, separators, accumulators and control system components. In addition, special process models are included for effects such as form loss, flow at an abrupt area change, branching, choked flow, boron tracking and non-condensable gas transport.

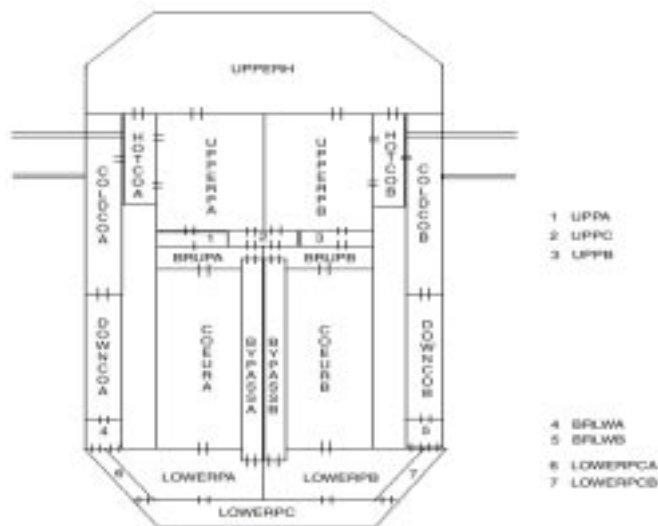
IPSN/CEA

France

I. Primary system

1. Vessel thermal-hydraulic (T-H) model and nodalisation (1-D, 3-D and number T-H channels or cells) – how are channels/T-H cells chosen?

The core is separated into two 1-D channels. The lower and upper plenums are separated in three volumes for mixing requirements.



2. Mixing model – how is the required mixing ratio implemented?

The lower plenum has been separated into three volumes:

- A volume LOWERPA connected to the intact leg.
- A volume LOWERPB connected to the broken leg.
- A volume LOWERPC connected to both intact and broken legs.

The mixing ratio of MSLB specifications has been obtained by choosing the size of Volume C for both lower and upper plenum. The upper plenum has been separated in two volumes UPPERPA and UPPERPB. Three others volumes are used for the junction with core. As for lower plenum, the size of these three volumes has been calculated in function of mixing ratio specifications.

- Upper plenum and upper head (of reactor vessel) paths (junctions) modelling?

Each volume UPPERPA and UPPERPB has a junction with the upper head and two junctions with hot leg inlet. A 1 409 kg/s flow between upper plenum and upper head exists at initial state.

- Radial and axial heat structure (fuel rod) nodalisation?

The axial fuel rod nodalisation has 24 cells. The radial fuel rod nodalisation has 10 cells.

- Relation used for Doppler temperature?

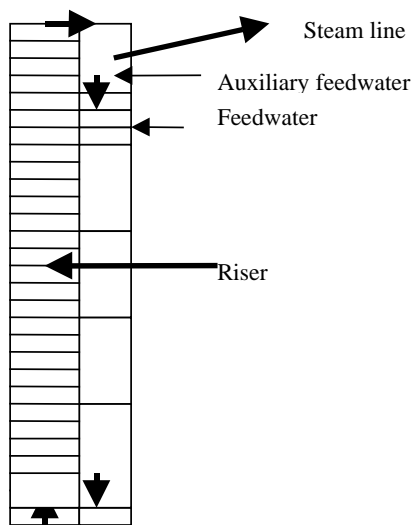
For each cells of axial fuel rod nodalisation, the Doppler temperature is calculated by the relation $T_{cell} = \alpha T_c + (1-\alpha)T_s$.

II. Secondary system

- Initial steam generator (SG) mass inventory?

26 tonnes.

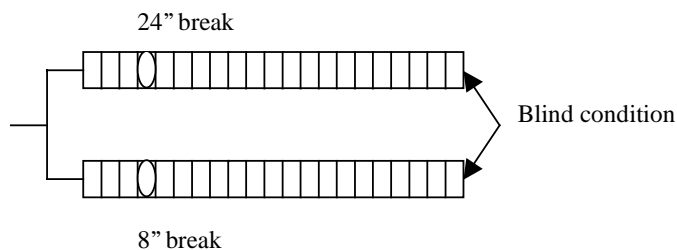
- SG down-comer nodalisation?



- Aspirator flow modelling?

A junction between the upper and lower part of down-comer.

- Steam line modelling?



5. Break flow modelling and critical flow model?

The 8" and 24" break flows are calculated by the Gros d'Aillon correlation.

6. Are you using the updated steam safety relief valves data (see Updated Specifications, April 1999, Table 5.4.2, p. 69)?

Yes.

7. Are you using the updated additional feedwater mass data (between the feedwater isolation valve and the broken SG) (see Updated Specifications, April 1999, Table 5.4.3, p. 69).

Yes.

III. General

1. Deviations from the updated Final Specifications (April 1999, NEA/NSC/DOC(99)8)?
2. User assumptions?
3. Specific features of the codes used?

GRS
Germany

I. Primary system

1. Vessel thermal-hydraulic (T-H) model and nodalisation (1-D, 3-D and number T-H channels or cells) – how are channels/T-H cells chosen?

The coolant flow through the reactor vessel and reactor core is modelled by two equal parallel flow paths by splitting the down-comer, the lower plenum, the reactor core and the upper plenum. These parallel flow paths consisting of 1-D pipe models behave independently, except of connections with the upper head volumes. The nodalisation is as follows:

Object	Nodes
<i>Upper down-comer</i>	<i>1</i>
<i>Lower down-comer</i>	<i>3</i>
<i>Lower head</i>	<i>1</i>
<i>Lower plenum</i>	<i>1</i>
<i>Active core</i>	<i>24</i>
<i>Bypass</i>	<i>24</i>
<i>Inner upper plenum</i>	<i>1</i>
<i>Outer upper plenum</i>	<i>1</i>
<i>Upper head</i>	<i>1</i>

In addition, mixing is modelled between the two halves of lower and upper plenum as specified.

2. Mixing model – how is the required mixing ratio implemented?

The required mixing ratio is modelled by exchanging energy between the two halves of lower and upper plenum. The mixing ratio of coolant temperatures in the hot and cold legs is calculated. The deviation from the specified value $R = 0.5$ is determined and corresponding to the difference power is exchanged within the lower and the upper plenum, as proposed 20% in the lower plenum and 80% in the upper plenum. The General Control System Module (GCSM) of ATHLET automatically calculates the value of exchange rate.

3. Upper plenum and upper head (of reactor vessel) paths (junctions) modelling?

For simulating the coolant flow between upper plenum and upper head, the upper plenum is divided in an inner and outer part. A junction pipe models the exchange between these parts. Junction pipes also model the flow between upper head and both volumes of upper plenum. The mass flow rates of these junctions correspond to the specification.

4. Radial and axial heat structure (fuel rod) nodalisation?

Four radial layers of equal volume, a specified gap and a cladding layer model the fuel rod. The number of axial nodes is 24.

5. Relation used for Doppler temperature?

The Doppler temperature is calculated as a weighted sum from the mean layer temperatures of the inner and outer fuel layer.

II. Secondary system

1. Initial steam generator (SG) mass inventory?

The initial steam generator mass inventory is $28 \cdot 10^3$ kg.

2. SG down-comer nodalisation?

The steam generator model for the unaffected and affected loop is different. The model for the unaffected loop only has two nodes on the secondary side and no down-comer. The SG model for the affected loop is more detailed. The down-comer consists of two parts. The lower down-comer has 14 nodes; the upper down-comer has 10 nodes. Between the riser and the down-comer heat conduction is considered.

3. Aspirator flow modelling?

The aspirator flow between the riser and the lower down-comer is modelled. The initial value is 100 kg/s, the time dependence is calculated by the pressure difference.

4. Steam line modelling?

The steam line for the affected SG is simulated as a single pipe. The distance between the SG outlet and the discharge is 38 m, discretised by four nodes. The cross-connect is located at a distance of 35 m.

5. Break flow modelling and critical flow model?

The break flow modelling consists of two discharge valves, one for the steam line and one for the cross-connect. The Moody model calculates the critical discharge rate.

6. Are you using the updated steam safety relief valves data (see Updated Specifications, April 1999, Table 5.4.2, p. 69)?

The updated steam safety relief valves as proposed in Table 5.4.2 are used.

7. Are you using the updated additional feedwater mass data (between the feedwater isolation valve and the broken SG) (see updated specifications, April 1999, Table 5.4.3, p. 69)?

The additional feedwater mass data as proposed in Table 5.4.3 are used.

III. General

1. Deviations from the updated Final Specifications (April 1999, NEA/NSC/DOC(99)8)?

No relevant deviations from the specifications.

2. User assumptions?

No.

3. Specific features of the codes used?

No.

IBERDROLA

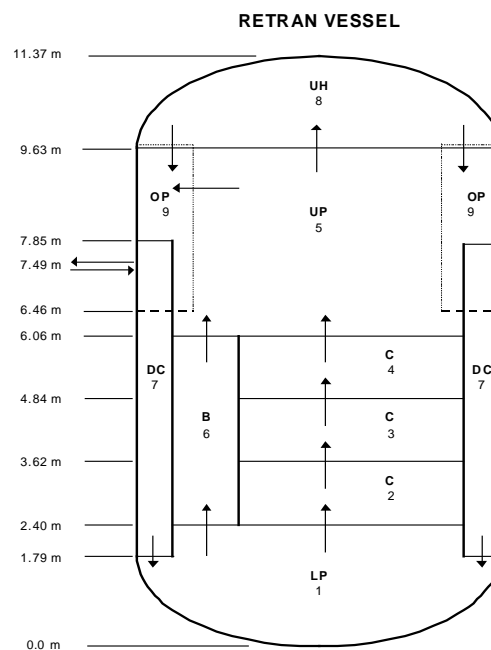
Spain

I. Primary system

1. Vessel thermal-hydraulic (T-H) model and nodalisation (1-D, 3-D and number T-H channels or cells) – how are channels/T-H cells chosen?

The vessel model and nodalisation used by RETRAN-3D MOD002 was selected according to the specifications.

Vessel nodalisation: specifications (Figure 3.1).



*Number of vessel volumes: 9
Number of core volumes: 3
Number of heat conductors: 3*

*Core volume: 3: Heat conductor 25
Core volume: 4: Heat conductor 26
Core volume: 5: Heat conductor 27*

Characteristics of the vessel volumes: according to specifications (Appendix A).

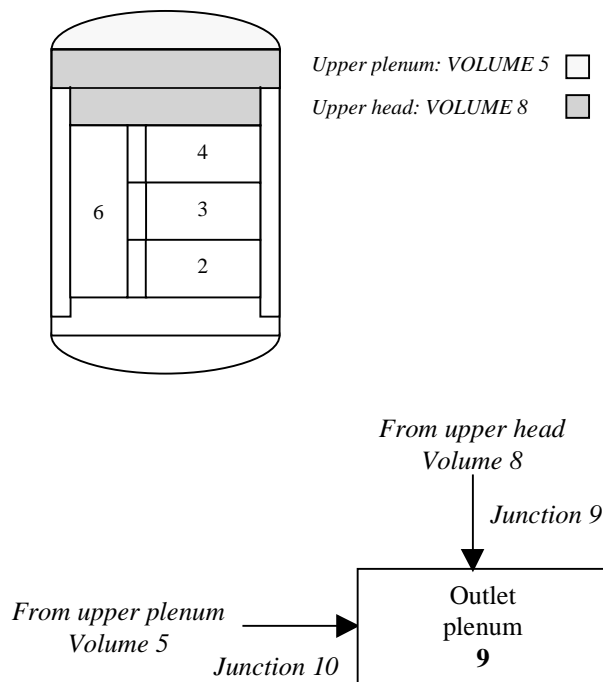
Reactor vessel						
	<u>Volume</u>	<u>Z Volume</u>	<u>FlowA</u>	<u>DiamV</u>	<u>Elev</u>	
001	621.64	7.8665	38.95	3.84	-24.5833	Lower plenum
002	196.862	4.00	49.2154	0.04277	-16.7168	Core – lower sect
003	196.862	4.00	49.2154	0.04277	-12.7168	Core – middle sect
004	196.682	4.00	49.2154	0.04277	-8.7169	Core – upper sect
005	877.90	11.7187	81.4	0.5783	-4.7168	Upper plenum
006	193.23	12.00	17.11	0.0349	-16.7168	Core bypass
007	689.37	19.865	35.13	1.67	-18.698	Reactor down-comer
008	492.57	5.73	104.58	7.11	7.0019	Upper head
009	247.96	10.65	23.29	1.29	-3.40	Outlet plenum

2. Mixing model – how is the required mixing ratio implemented?

The mixing model is not implemented in RETRAN-3D.

3. Upper plenum and upper head (of reactor vessel) paths (junctions) modelling?

Upper plenum and upper head are modelled with volumes as usual in RETRAN-3D:



Function modelling: specifications (Appendix A):

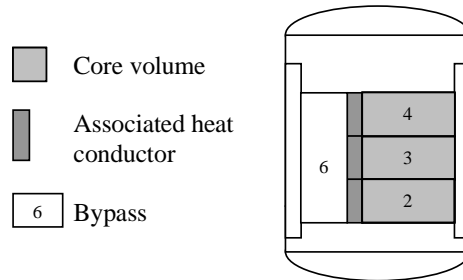
From	To	Junction area	Junction elev.	
8	9	8.564	7.0019	From upper head to outer plenum
5	9	50.750	4.2519	From upper plenum to outer plenum

4. Radial and axial heat structure nodalisation?

The nodalisation corresponds to the heat core T-H sectors of the core.

Radially: Core section is modelled with one volume which represents the active core and another volume which represents the bypass.

Axially: The axial heat structure consists of three volumes the total height of the active core, and the bypass is modelled with only one volume.



5. Relation used for Doppler temperature?

*Doppler temperature has been modelled using an averaged fuel temperature, and the relation $T_f = 0.3 * T_{f,c} + 0.7 * T_{f,s}$ has not been used, because the code does not have this option.*

II. Secondary system

1. Initial steam generator (SG) mass inventory?

26 048 kg for both steam generators.

2. SG down-comer nodalisation?

YES [Volume 251 (intact), Volume 151 (broken)].



3. Aspirator flow modelling?

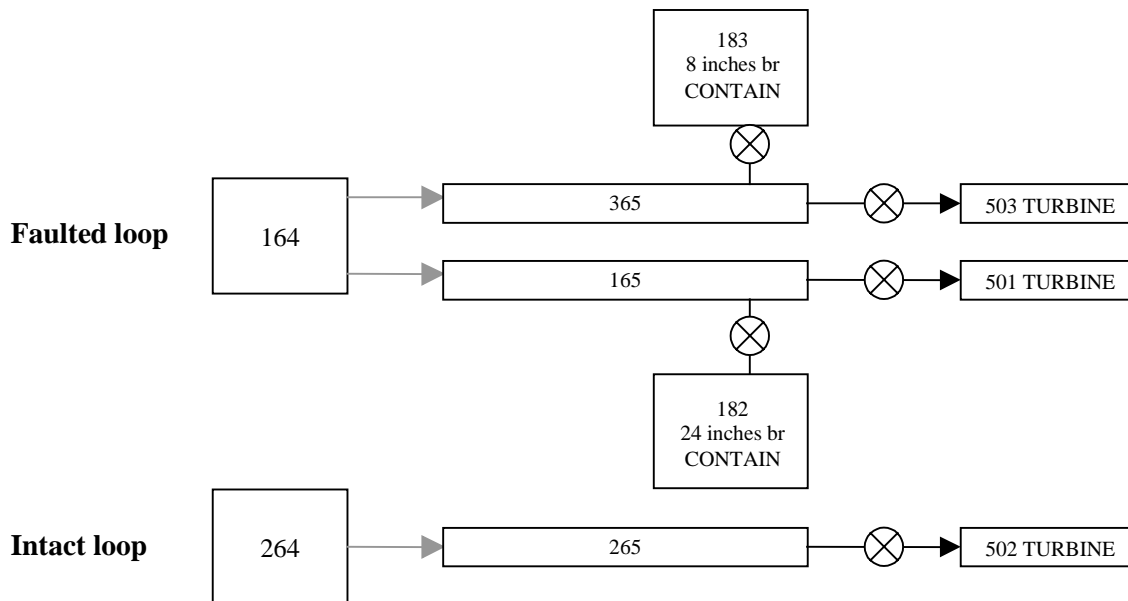
Bypass connects the steam generator with the inlet water, in the secondary side steam generator.

INTACT steam: Junction 250 (from: 259 to: 25).

FAULTED steam: Junction 150 (from: 159 to: 151).



4. Steam line modelling?



5. Break flow modelling and critical flow model?

The break flow has been modelled for both breaks, by the use of one valve joint to a time dependent volume (TDV) simulating the break.

No choking flow model is used in this exercise.

6. Are you using the updated steam safety relief valves data (see Updated Specifications, April 1999, Table 5.4.2, p. 69)?

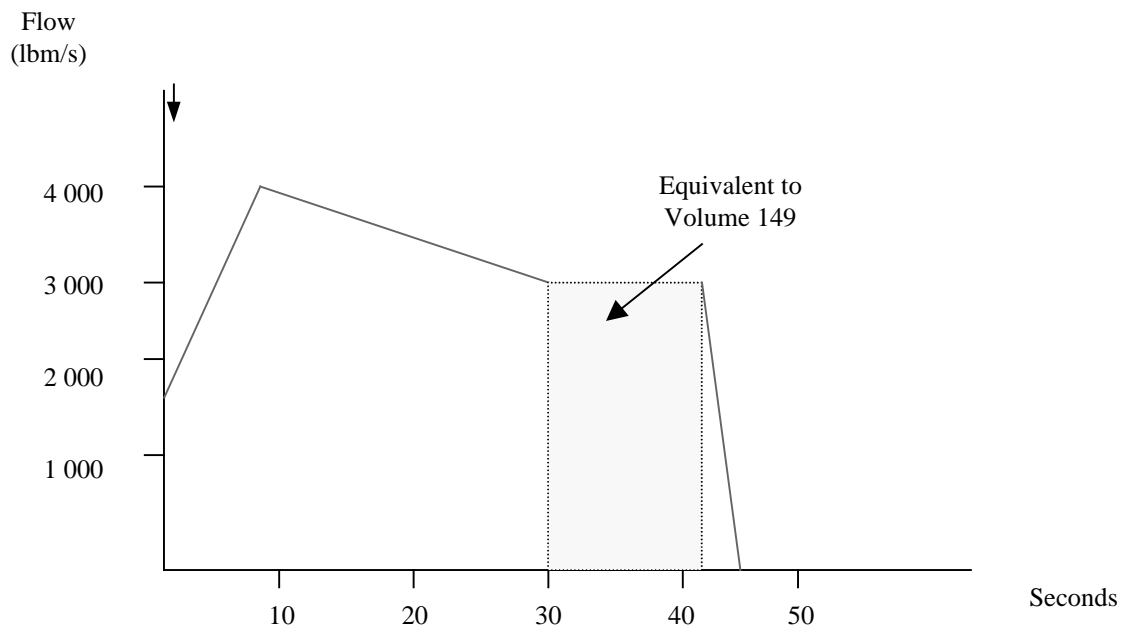
No updated steam safety relief valves have been used.

7. Are you using the updated additional feedwater mass data (between the feedwater isolation valve and the broken SG) (see updated specifications, April 1999, Table 5.4.3, p. 69)?

Yes, the additional feedwater mass is included in a FILL as follows:

Table 5.4.3 (Specifications)

Time (sec)	Flow (lb/sec /kg/sec)
0	1 679.0/761.59
10	4 000.0/1 814.4
30	3 000.0/1 360.8
42	3 000.0/1 360.8
45	0.0/0.0



III. General

1. Deviations from the updated Final Specifications (April 1999, NEA/NSC/DOC(99)8)?

No.

2. User assumptions?

No.

3. Specific features of the codes used?

Vessel and SG nodalisation using volumes, as usual in RETRAN3D-MOD002.

UNIVERSITY OF VALENCIA

Spain

I. Primary system

1. Vessel thermal-hydraulic (T-H) model and nodalisation (1-D, 3-D and number T-H channels or cells) – how are channels/T-H cells chosen?

We have model the vessel with the vessel component TRAC. The vessel consists of six levels and eighteen thermal-hydraulic sectors. We only have modelled the core reactor.

2. Mixing model – how is the required mixing ratio implemented?

No mixing is implemented.

3. Upper plenum and upper head (of reactor vessel) paths (junctions) modelling?

We have used the PLENUM TRAC component to model the upper plenum and upper head.

4. Radial and axial heat structure (fuel rod) nodalisation?

The radial and axial heat structures correspond to the heat core T-H sectors of the core. More accurately, we only have an axial heat structure per T-H sector in the core. On the other hand, axially, each heat structure consists of seven nodal nodes.

5. Relation used for Doppler temperature?

Averaged fuel temperature has been used in order to calculate Doppler temperature. Furthermore, in graphical representation, the following relation has not been used:

$$T_f = 0.3 * T_{f,c} + 0.7 * T_{f,s}$$

We have used this relation for the second and third exercise.

II. Secondary system

1. Initial steam generator (SG) mass inventory?

The secondary side mass inventory is 26 031 kg in steam generators 1 and 2.

2. SG down-comer nodalisation?

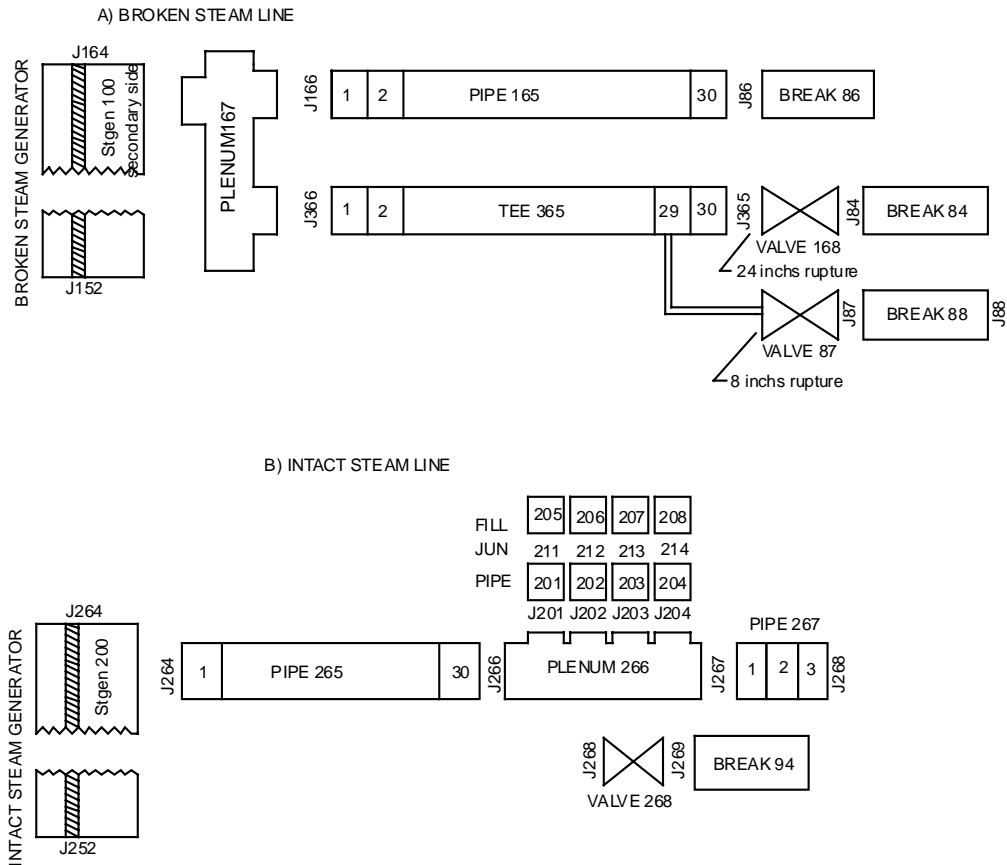
We did not model the bypass connecting the steam with the inlet water in the secondary side steam generator.

3. Aspirator flow modelling?

We did not model the bypass connecting the steam with the inlet water in the secondary side steam generator.

4. Steam line modelling?

We have two-steam line modelling. It has been represented in the following diagram.



5. Break flow modelling and critical flow model?

We have modelled the break flow by means of a valve followed by a BREAK TRAC component. The pressure in component “BREAK 84” is 6.31E6 Pa and in time 0.5 seconds after trip the VALVE 168 is closed. The small break is also modelled with the VALVE 87 followed by a BREAK 88, which maintains a pressure of 1.03419E5 during the transient. The critical flow model used is the choked flow model developed in TRAC.

6. Are you using the updated steam safety relief valves data (see Updated Specifications, April 1999, Table 5.4.2, p. 69)?

Yes, but with an exception: we have considered the same point of pressure. It is located in Cell 21 of PIPE 265.

7. Are you using the updated additional feedwater mass data (between the feedwater isolation valve and the broken SG) (see Updated Specifications, April 1999, Table 5.4.3, p. 69)?

Yes, but we have considered 16 103 kg of water inside a pipe and do not in the FILL during the interval from 30-42 seconds of transient.

III. General

1. Deviations from the updated Final Specifications (April 1999, NEA/NSC/DOC(99)8)?
2. User assumptions?
3. Specific features of the codes used?

BE
United Kingdom

I. Primary system

1. Vessel thermal-hydraulic (T-H) model and nodalisation (1-D, 3-D and number T-H channels or cells) – how are channels/T-H cells chosen?

Principally, we obtained the RELAP5 input deck from the US NRC. We modified the core along similar lines as to how we model Sizewell B. The model has two equal, parallel core channels that communicate fluid only at the inlet and outlet plenum. Each half of the core is associated with one of the steam generator loops. Each core channel contains 12 equal volumes and receives heat from half of the fuel. The axial variation of heat output from the fuel (which is also in twelve equal lengths) is taken from the specification.

There is a single guide tube connecting the upper plenum and the upper head. This feature introduces a mixing flow between the two core halves, which is in addition to any mixing in the upper and lower plenum.

The loops contain all the significant features and were not modified except in the steam generators where the number of primary side (and secondary side) axial nodes was increased (now 34 of equal length) to achieve the initial secondary side steam conditions.

The total volume of all primary components/volumes (and secondary volumes) is not identical to the specification, however, we are within a few per cent and the difference was judged to be negligible.

In the 3-D calculations the only difference is that the heat supplied to each of the 24 core nodes is calculated explicitly with PANTHER.

2. Mixing model – how is the required mixing ratio implemented?

The RELAP5 model was modified such that the cold leg temperatures were made constant, with a temperature difference between one half of the model and the other half. Valves were installed at both the inlet and the outlet of the core between the two halves of the core and the inlet/outlet plenum to enable to mixing to be varied. The mixing ratio was calculated according to the specification using the ratio of hot and cold leg temperatures. Once the desired mixing ratio had been achieved the area of each valve was frozen.

3. Upper plenum and upper head (of reactor vessel) paths (junctions) modelling?

As above, there is a single guide tube connecting the upper plenum and the upper head. The upper head splits in two and each half connects to the top of a down-comer (there are two, one associated with each loop). The single guide tube introduces a mixing flow between the two core halves, which is in addition to any mixing in the upper and lower plenum.

4. Radial and axial heat structure (fuel rod) nodalisation?

Yes, the radial noding was followed. Axially only twelve nodes were modelled for compatibility with the hydraulic nodes.

5. Relation used for Doppler temperature?

Yes, the Doppler temperature was calculated according to the specification. The average was a weighted sum using the power factors to represent a flux weighting. Each half of the core was weighted equally.

II. Secondary system

1. Initial steam generator (SG) mass inventory?

We achieve the revised specification.

2. SG down-comer nodalisation?

This is modelled as an annulus with eight equal length axial nodes.

3. Aspirator flow modelling?

A connection from the riser to the top of the down-comer inside the steam generator is used to model the aspirator flow. We have no experience with the once-through steam generator design and have therefore copied this data from one of the other participants using RELAP5 (Purdue).

4. Steam line modelling?

The arrangement of the steam pipes, including the length of the steam piping, is modelled according to the specification.

5. Break flow modelling and critical flow model?

The break flow and critical flow model is RELAP5's own since we do not have control over this (we believe that this is a feature of development versions). The flow through the break is homogeneous and goes through an abrupt area change. The flow does not choke.

6. Are you using the updated steam safety relief valves data (see Updated Specifications, April 1999, Table 5.4.2, p. 69)?

The steam safety valves on the unaffected steam generator have been modelled according to the specification. This is implemented by a flow versus pressure table since the specification did not include values to assume for accumulation and blow down of the valves. It was judged that this treatment for the relief on this steam generator was adequate for this problem.

7. Are you using the updated additional feedwater mass data (between the feedwater isolation valve and the broken SG) (see Updated Specifications, April 1999, Table 5.4.3, p. 69)?

Yes, we are using the updated feed flow data specification.

III. General

1. Deviations from the updated Final Specifications (April 1999, NEA/NSC/DOC(99)8)?

Specifically, none.

2. User assumptions?

Although it is not mentioned in the specification, it has been assumed that there is no transient control on the mixing ratio. We did not believe a transient control system to be practical or realistic.

3. Specific features of the codes used?

As above, we do not have control over the break flow model in this release of RELAP5 and therefore cannot guarantee that we are using the Moody correlation.

PSU
United States of America

I. Primary system

1. Vessel thermal-hydraulic (T-H) model and nodalisation (1-D, 3-D and number T-H channels or cells) – how are channels/T-H cells chosen?

The TRAC-PF1 VESSEL component is used to model thermal-hydraulically the TMI-1 vessel in 3-D cylindrical geometry. The vessel model is subdivided into 14 axial layers, five radial rings, and six azimuthal sectors for a total of 420 hydrodynamic cells as shown in Figures 1.1 and 1.3.

2. Mixing model – how is the required mixing ratio implemented?

Since TRAC-PF1 has a 3-D vessel fluid-dynamic capability and by explicitly modelling radial cross-flows between thermal-hydraulic cells, the code accounts for thermal loop flow mixing in a best-estimate manner.

3. Upper plenum and upper head (of reactor vessel) paths (junctions) modelling?

See Figures 1.1 and 1.2.

4. Radial and axial heat structure (fuel rod) nodalisation?

The radial and axial heat structure nodalisation follows the thermal-hydraulic nodalisation of the core region. The heat structure consist of 18 fuel rods radially and six axial layers.

5. Relation used for Doppler temperature?

Pellet volume averaged fuel temperature value is used for Doppler temperature relation.

II. Secondary system

1. Initial steam generator (SG) mass inventory?

26 000 kg.

2. SG down-comer nodalisation?

See Figure 2.1 – eight nodes.

3. Aspirator flow modelling?

According to the Final Specifications – see Figure 2.1.

4. Steam line modelling?

See Figure 2.2.

5. Break flow modelling and critical flow model?

The critical flow model used is the TRAC-PF1 choked flow model.

6. Are you using the updated steam safety relief valves data (see Updated Specifications, April 1999, Table 5.4.2, p. 69)?

Yes.

7. Are you using the updated additional feedwater mass data (between the feedwater isolation valve and the broken SG) (see Updated Specifications, April 1999, Table 5.4.3, p. 69)?

Yes.

III. General

1. Deviations from the updated Final Specifications (April 1999, NEA/NSC/DOC(99)8)?

Doppler temperature relation.

2. User assumptions?

None.

3. Specific features of the codes used?

3-D vessel thermal-hydraulic capability.

Figure 1.1. Axial nodalisation of the TMI-1 TRAC-PF1 vessel

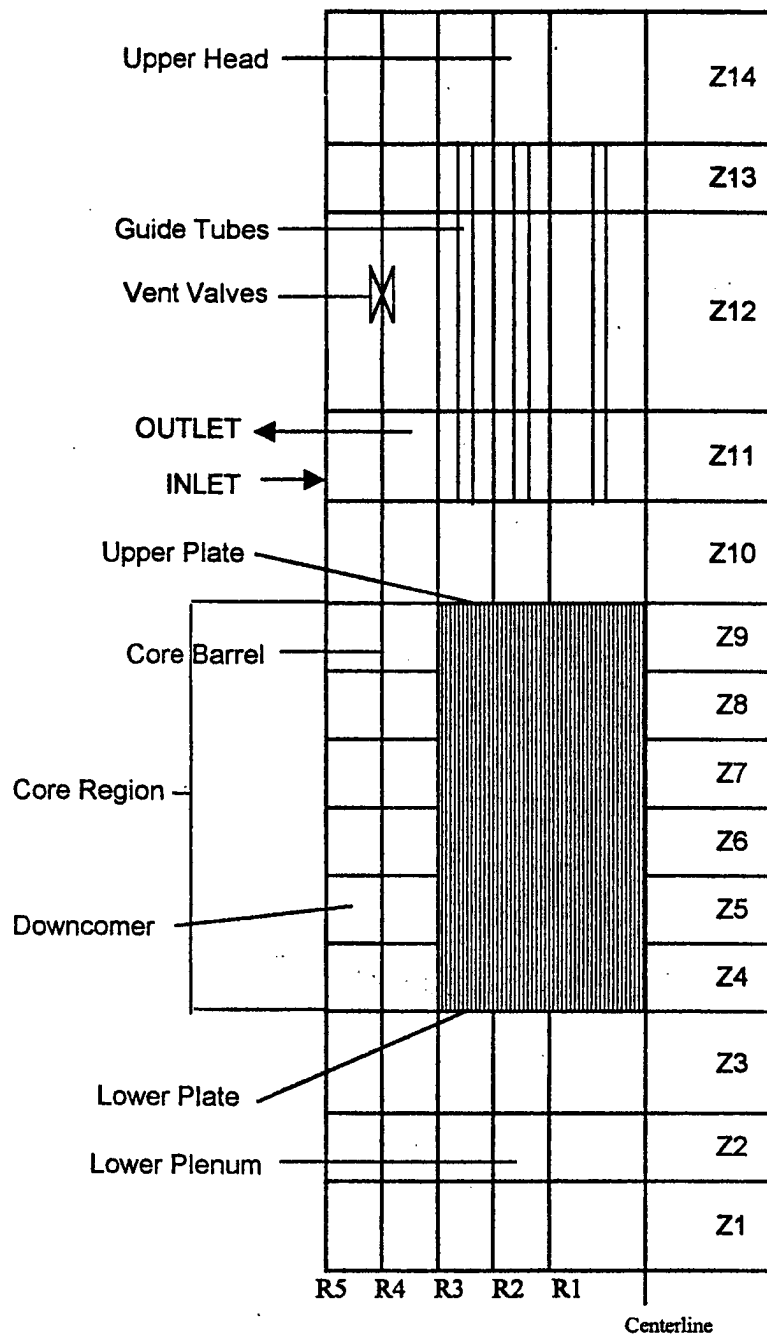


Figure 1.2. Side view of the TRAC-PF1 TMI-1 vessel component

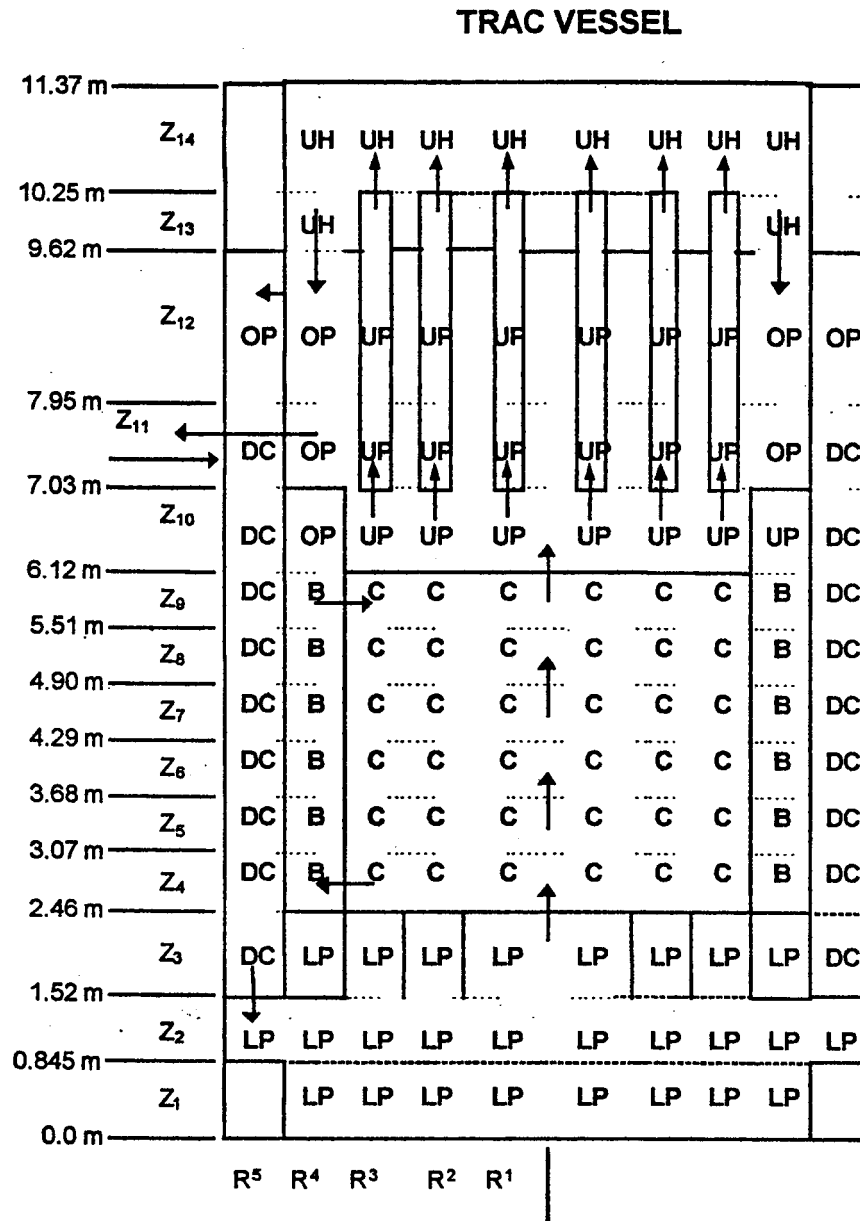


Figure 1.3. Radial and azimuthal nodalisation of TRAC-PF1 vessel model

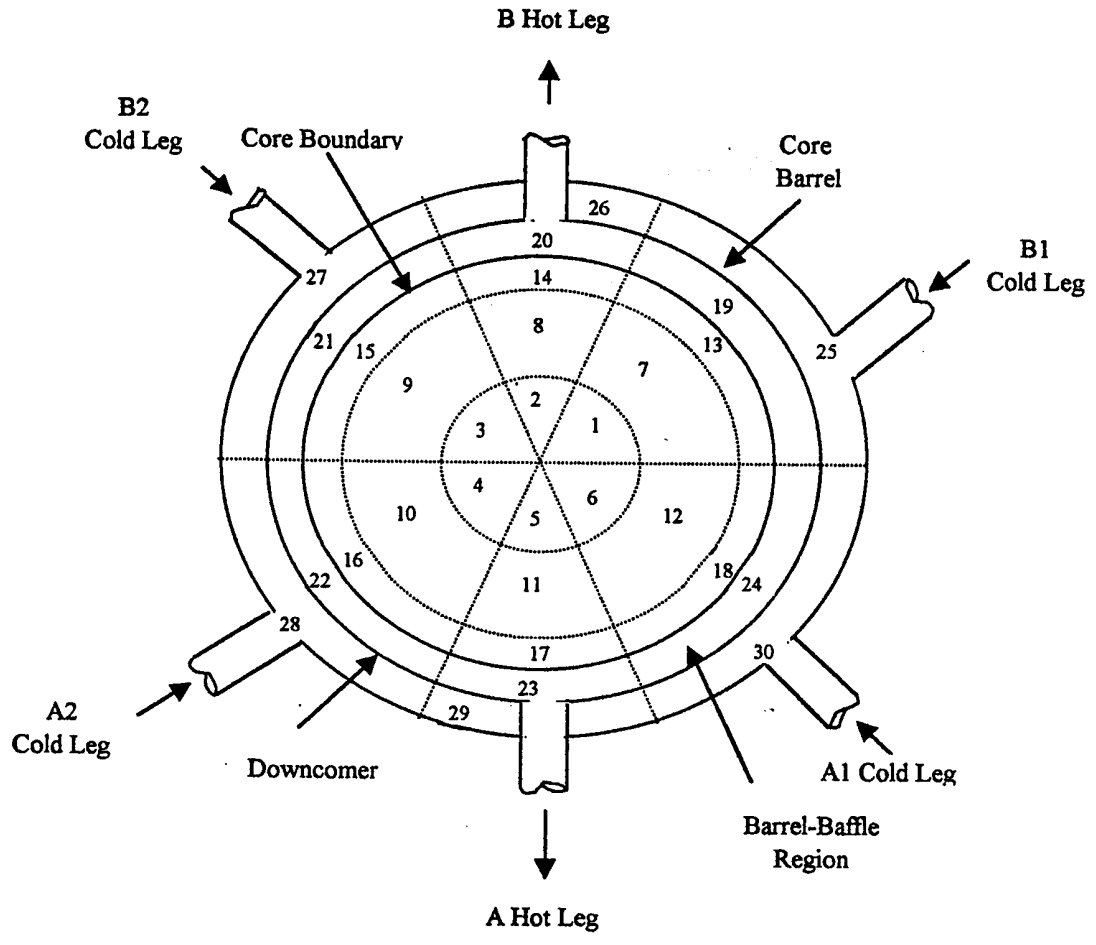


Figure 2.1 TMI-1 once-through steam generator model

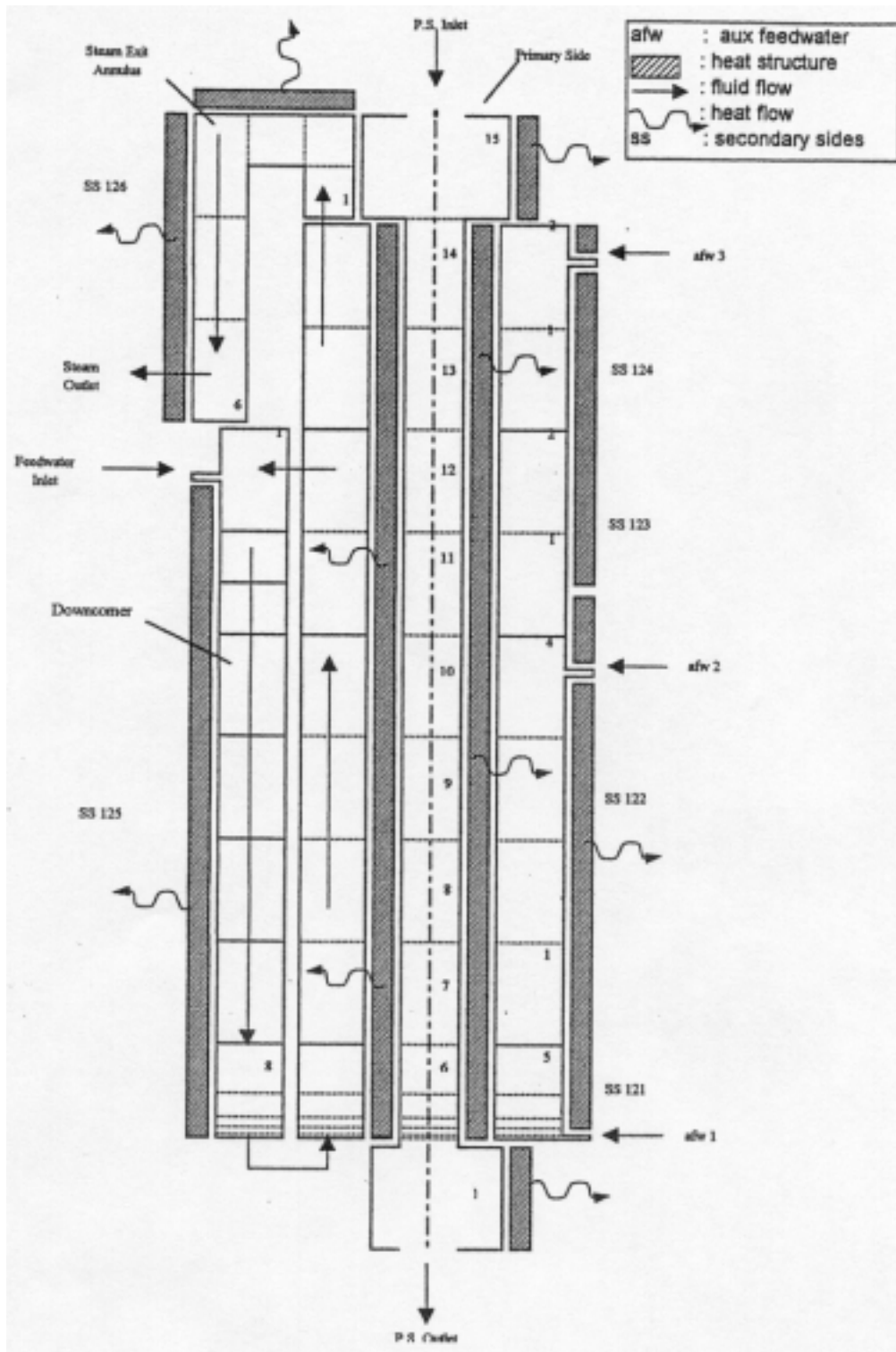
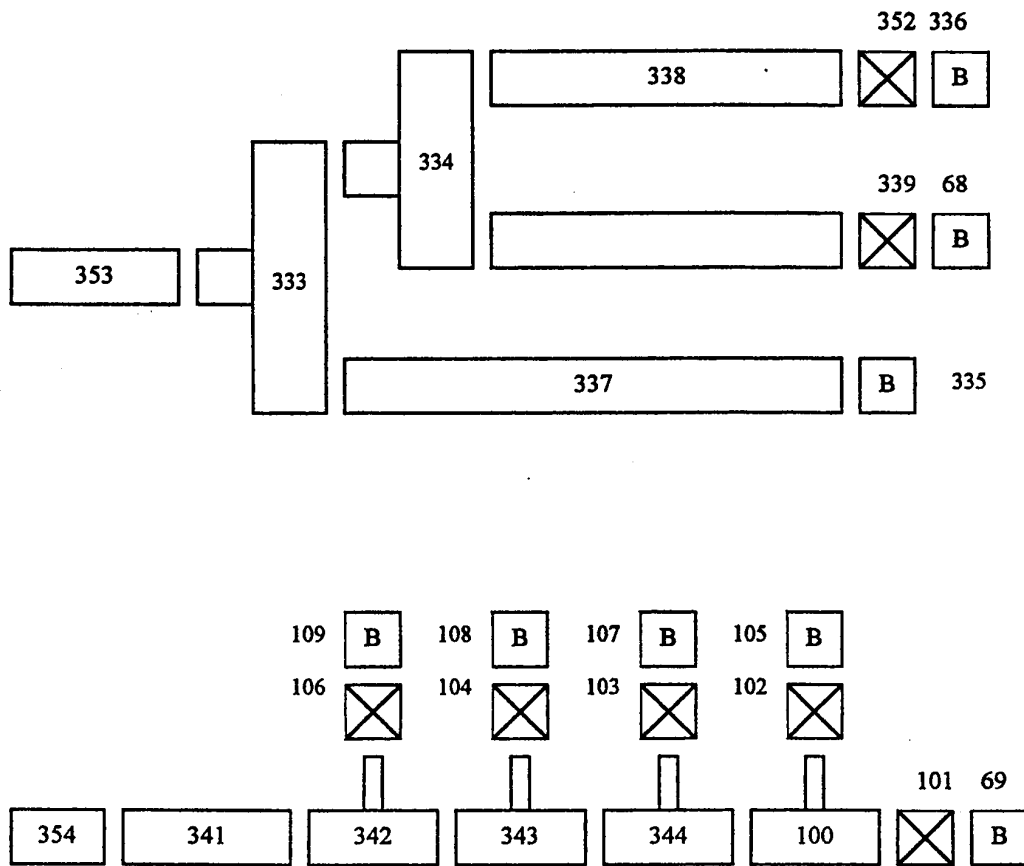


Figure 2.2. TRAC-PF1 TMI-1 steam line nodalisation

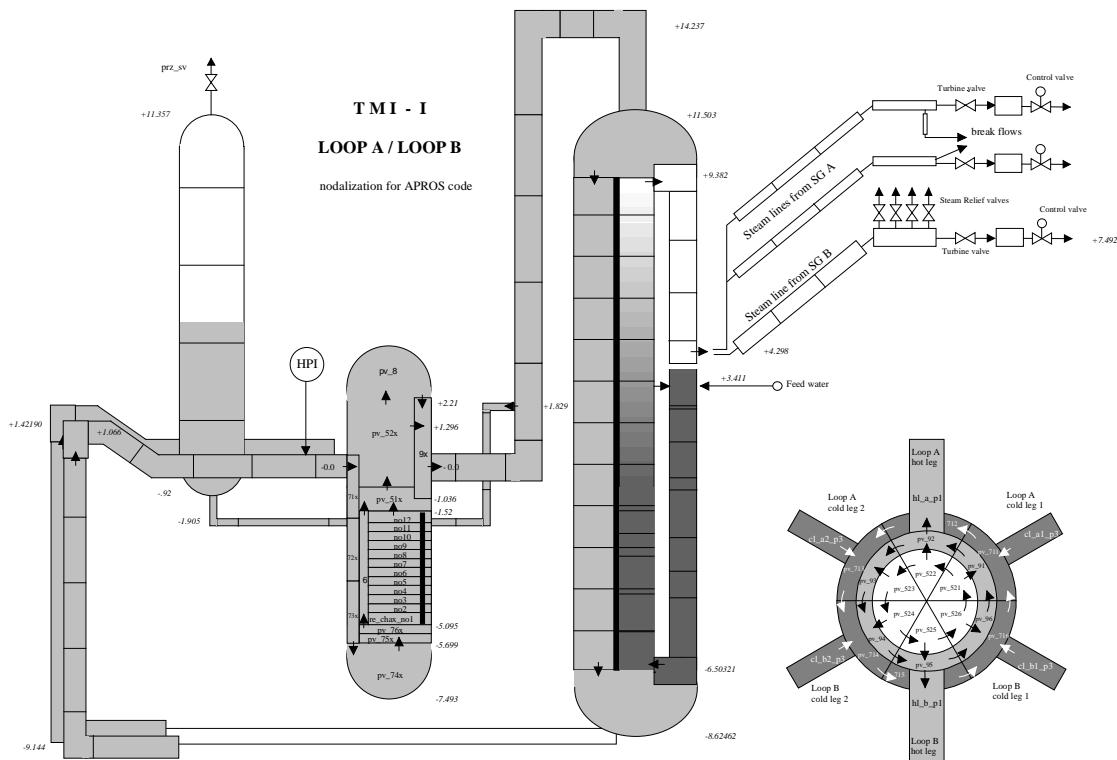


VTT-2
Finland (APROS code)

I. Primary system

1. Vessel thermal-hydraulic (T-H) model and nodalisation (1-D, 3-D and number T-H channels or cells) – how are channels/T-H cells chosen?

*One-dimensional nodalisation. Vessel is divided in six sectors.
Number of T-H cells is 139 (72 in the core and 67 in the vessel).
Nodalisation is based on information given on RETRAN and TRAC models.*

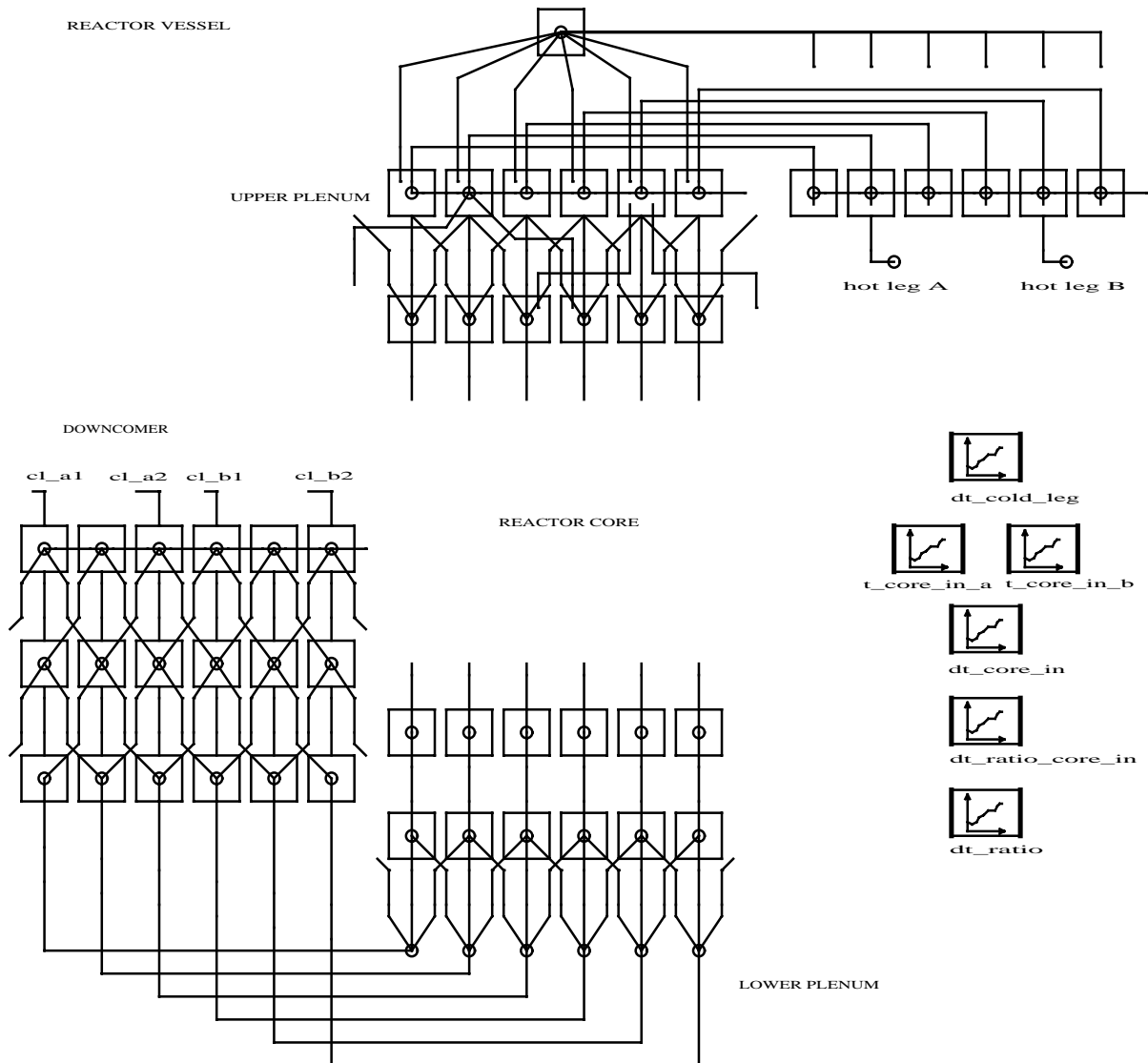


The nodalisation used in APROS is basically the same as with the SMABRE code. However, small differences exist, mainly because of the way the model is constructed in the codes.

2. Mixing model – how is the required mixing ratio implemented?

The vessel is modelled with six sectors all the way from the down-comer to outlet plenum (figure below). This creates an artificial two-dimensional model to simulate mixing of cold water from the broken loop and hot water from intact loop. The horizontal connections between the sectors are

described in the APROS model with “cross-flow” junctions. Flow areas and form loss factors are defined so that the temperature difference between broken and intact hot legs is about 50% of the temperature difference in cold legs. In the down-comer region the flow area of “cross-flow” junctions is 0.1 m^2 and form loss factor is 50. In the lower plenum the form loss factor is 35. Most of the mixing should occur in the upper plenum (80%), which is why the flow areas are large and form loss factors lower there (1.0 m^2 , 10 and 20). When simulating mixing with this kind of model the defined fixed mixing ratio was not followed. On the other hand, mixing depends on flow rate density differences, especially in the down-comer region (like in reality).



3. Upper plenum and upper head (of reactor vessel) paths (junctions) modelling?

In the upper plenum the adjacent channels are connected with “cross-flow” junctions like in the down-comer. In addition to this mixing with channels the hot and cold halves of the reactor are connected to allow required mixing. The upper head also takes part in mixing, since part of the flow in the model goes through the single node in upper head.

4. Radial and axial heat structure (fuel rod) nodalisation?

The core is divided in six sectors. Each sector is divided in 12 axial T-H and head structure nodes. In radial direction the fuel rod is divided in 10 heat structure nodes. Seven layers for fuel pellet, one for gas cap and one for cladding.

5. Relation used for Doppler temperature?

At each heat structure node the Doppler temperature is calculated as $0.3x$ (temperature at fuel pellet centre) + $0.7x$ (temperature at fuel pellet outer rim). When the core in APROS was divided into six sectors and each of the sectors into 12 axial nodes, this procedure produces 72 Doppler temperature values. The final Doppler temperature used in the feedback correlation is the (volume) average of the 72 individual values obtained.

II. Secondary system

1. Initial steam generator (SG) mass inventory?

26 015 kg.

2. SG down-comer nodalisation?

Five nodes. See figure of the nodalisation in Question I.1

3. Aspirator flow modelling?

The once-through steam generator is modelled as detailed as possible with given data, because it is an important contributor to the transient. The feedwater nozzles are modelled with the real flow area and diameter. Momentum flux was transferred in feedwater nozzle to take into account the velocity of feedwater spray in condensing steam in the top of down-comer (br6_mom_flux_used T). The hydraulic diameter of feedwater node (SG_A – inlet) was 4.78 mm to take in account characteristic dimension of the nozzle in condensation.

The aspirator junction, steam out-take from tube bundle to down-comer to preheat the feedwater, is modelled with the given flow area, 0.96 m^2 . To heat up 761 kg/s of feedwater to saturation requires 102 kg/s steam, which has to condense in the down-comer. The drawback is that during the steam line break, part of the feedwater goes through the aspirator junction directly into the middle of the tube bundle (see figure). The aspirator flow was modelled with a normal junction allowing reversal flow. It was not possible to judge the realism of the modelling, without knowing the actual geometry of the aspirator connection and the behaviour of the once-through steam generator in detail.

The once-through steam generator (model) was sensitive to aspirator flow and water level. Quite a lot of work was needed to adjust the model in the requested state (water inventory and steam superheat). Calculated temperature and void fraction profiles in steady state are plotted in the figures below. In the void fraction profile one can see the effect of steam out-take through the aspirator junction in Node 6 from the top. In the bottom of the steam generator water is close to saturation point (about 2°C sub-cooled) and in the top steam is almost 20°C superheated, as given in the specifications of the benchmark.

Figure 1. Broken steam generator feedwater and aspirator flow

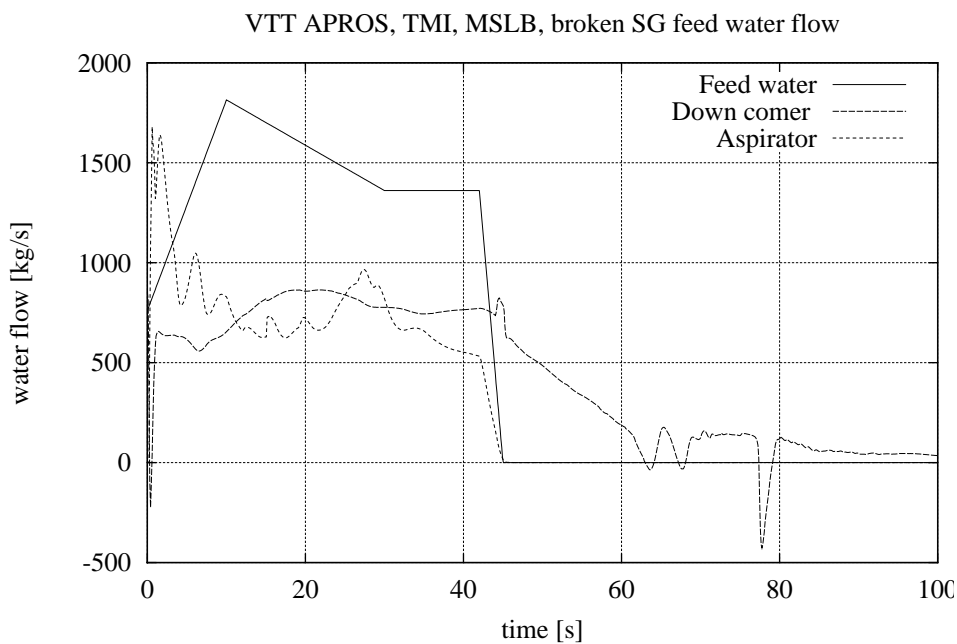


Figure 2. Calculated once-through steam generator temperature profile in steady state. Numbering of the nodes starts from inlet (top) of the steam generator and ends in the outlet (bottom).

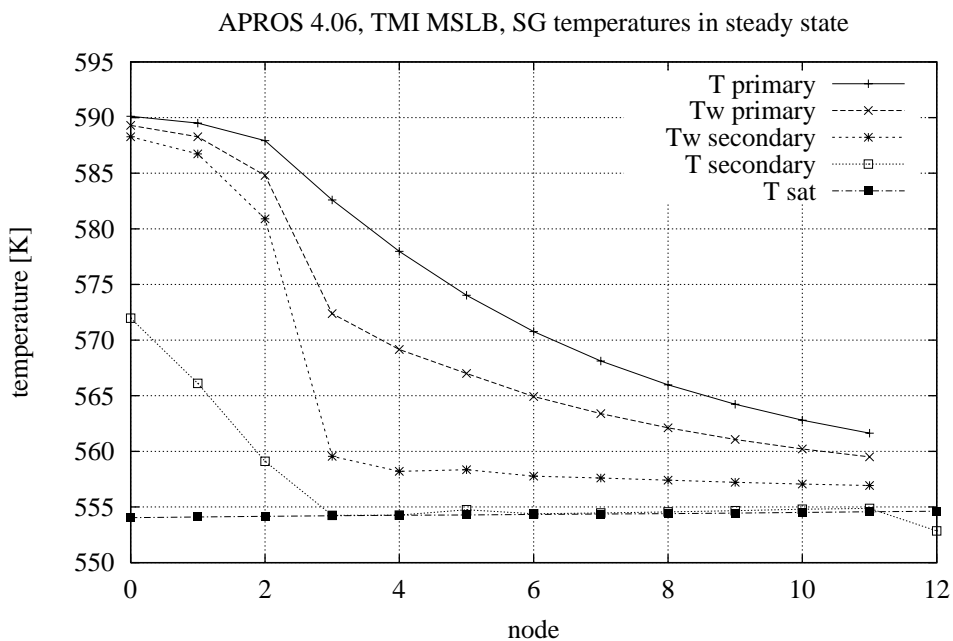
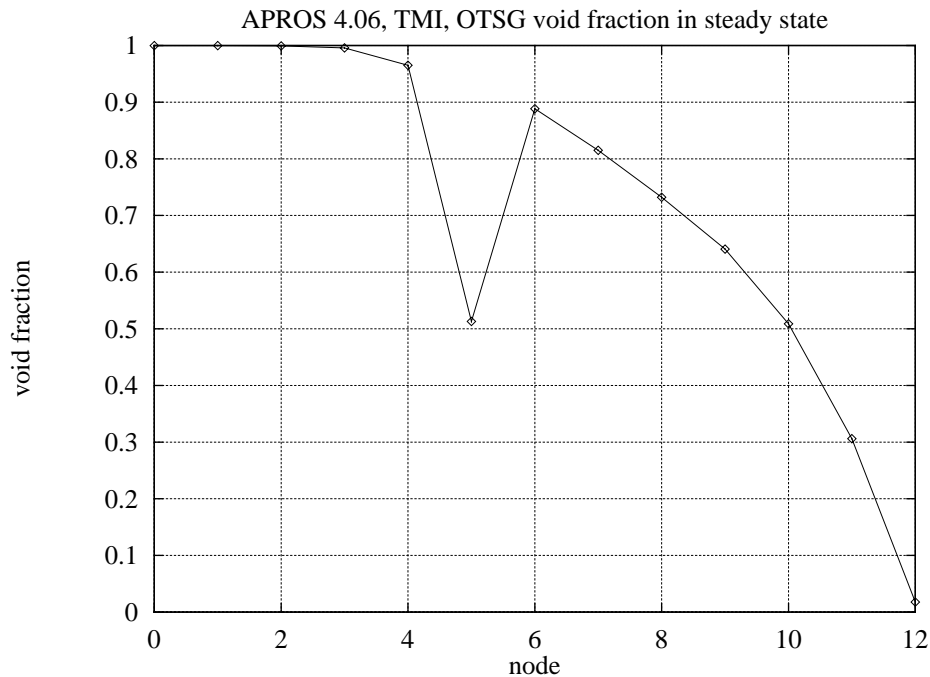


Figure 3. Calculated once-through steam generator void fraction profile in steady state



4. Steam line modelling?

Steam line A1: four nodes until the break (turbine valve).

Steam line A2: five nodes until the break.

Steam line B: four nodes until the turbine valve.

See picture of nodalisation in Question I.1.

5. Break flow modelling and critical flow model?

Main steam line:

- *Break area: 0.2462 m².*
- *Hydraulic diameter: 0.5599 m.*
- *Form loss coefficient: 1.0.*

Cross-connect line:

- *Break area: 0.0324 m².*
- *Hydraulic diameter: 0.2031 m.*
- *Form loss coefficient: 0.0 ! (error in modelling).*

Critical flow: "frozen" sound velocity model. Break flow velocity is limited to sound velocity of steam and liquid, weighted with void fraction.

6. Are you using the updated steam safety relief valves data (see Updated Specifications, April 1999, Table 5.4.2, p. 69)?

Yes.

7. Are you using the updated additional feedwater mass data (between the feedwater isolation valve and the broken SG) (see Updated Specifications, April 1999, Table 5.4.3, p. 69)?

Yes.

III. General

1. Deviations from the updated Final Specifications (April 1999, NEA/NSC/DOC(99)8)?

None as far as we know.

2. User assumptions?

Reverse flow allowed in SG aspirator junction.

3. Specific features of the codes used?

Six-equation thermal-hydraulic model. Normal point kinetics calculation for this exercise.